Jurassic–Early Cretaceous tectonic evolution of the North China Craton and Yanshanian intracontinental orogeny in East Asia: New insights from a general review of stratigraphy, structures, and magmatism

Huabiao Qiu, Wei Lin, Yan Chen, Michel Faure

Jurassic–Early Cretaceous tectonic evolution of the North China Craton and Yanshanian intracontinental orogeny in East Asia: new insights from a general review of stratigraphy, structures, and magmatism

Huabiao Qiu[1,2,3], Wei Lin[1*], Yan Chen[2], Michel Faure[2]

[1]State Key Laboratory of Lithospheric Evolution, Institute of Geology and Geophysics, Chinese Academy of Sciences/Innovation Academy for Earth Science, Chinese Academy of Sciences, Beijing100029, China

[2]Univ. Orléans, CNRS, BRGM, ISTO, UMR 7327, F-45071, Orléans, France

[3]Petroleum Exploration and Production Research Institute, SINOPEC, Beijing 100083, China

[*]Corresponding author: (linwei@mail.iggcas.ac.cn)

Abstract

The tectono-magmatic evolution of the North China Craton (NCC) plays a crucial role in understanding the Jurassic–Early Cretaceous (Yanshanian) intracontinental orogeny in East Asia. A holistic understanding of multi-phased deformation and magmatism in the NCC is greatly complicated by the sporadically distributed Mesozoic strata with significantly different stratigraphic associations in various zones. In this paper, we review the Jurassic–Early Cretaceous litho-stratigraphy with emphasis on unconformities to define a coherent chronostratigraphic framework of the entire NCC. Integrating available data concerning tectonic deformation, and geochemistry and fabric of igneous rocks into the well-established coherent chronostratigraphic framework, a four-stage tectonic evolutionary model of the NCC is proposed, providing new insights into the dynamics of the Yanshanian intracontinental orogeny in East Asia. The first stage concerns a N–S extension in the NCC during the Early–early Middle Jurassic (~200–170 Ma), expressed by the E–W striking brittle normal faults developed in the Lower–lower Middle Jurassic strata, and magmatism along the southern and northern margins of the NCC. It could be related to the post-orogenic extension after the deep continental subduction of the South China Block beneath the NCC. The second one is characterized by a N–S compression (i.e., Event A of the Yanshanian orogeny) in the late Middle Jurassic (~170–160 Ma), evidenced by the unconformity above the Lower–lower Middle Jurassic strata and the upper Middle Jurassic syn-tectonic deposition. The associated N–S directed thrusts and fault-related folds were mainly localized in the northern part of the NCC, possibly responding to the far-field compression related to the closure of the Mongol–Okhotsk Ocean. The third stage corresponds to a NW–SE compression (i.e., Event B of the Yanshanian orogeny) during the Late Jurassic–earliest Cretaceous (~160–135 Ma), illustrated by the NW–SE directed thrusts and the overprint of pre-existing N–S directed thrusts by the latter NW–SE directed thrusts. It was well recorded by the Upper Jurassic–lowermost Cretaceous syn-tectonic deposition and the unconformity above. This NW–SE compression in response to the flat slab subduction of the Paleo-Pacific Plate had influenced the entire NCC. However, the latest Middle–early Late Jurassic (~165–150 Ma) local NE–SW extension, recorded by ductile and brittle normal faults, magnetic lineation in granitic plutons, and magmatism that extended to Northeast China and its adjacent areas, also occurred in the northeastern part of the NCC. This could be related to tectonic transition from the N–S closure of

the Mongol–Okhotsk Ocean to the NNW-directed subduction of the Paleo-Pacific Plate. In the latest stage during the Early Cretaceous (~135–115 Ma), the large-scale crustal extension, characterized by metamorphic core complexes, magmatism, graben or half-graben basins, occurred in a vast area extending more than 4000 km, from Transbaikalia, through the NCC, to the South China Block. It could be the consequence of the lithospheric thinning and the formation of the wide rift due to the southeastward stress relaxation of the NW–SE convergent East Asian continent as the slab rollback of the Paleo-Pacific Plate. These results provide a notable example of polyphase intra-plate deformation and magmatism paradigm in response to intracontinental orogeny with variable plate-boundary geodynamics.

Keywords: Jurassic-Early Cretaceous, Stratigraphic Framework, Tectono-magmatic Process, North China Craton, Geodynamics of East Asia

1. Introduction

The NCC, one of the important continental blocks that form the East Asian continent (Davis et al., 2001), is separated from the Siberia Craton by the Central Asian Orogenic Belt in the north and from the South China Block (SCB) by the Qinling-Dabie-Sulu Orogenic belt in the south (Fig.1). After the Paleoproterozoic cratonization, the tectonic evolution of the NCC is related to two Phanerozoic orogenic cycles, including the Paleozoic–Triassic continental amalgamation with the Mongolian arc terranes and the SCB at block boundaries (Mattauer et al., 1985; Hacker et al., 2000; Windley et al. 2007; Xiao et al., 2003, 2015; Xu et al., 2013), and the Jurassic–Early Cretaceous intracontinental orogeny, referred to as "Yanshanian Movement" since about one century ago (Wong, 1927; Davis et al., 2001; Faure et al., 2012; Dong et al., 2015; Zhang et al., 2022). The welded Mongolian arc terranes-NCC-SCB continent formed after the Paleozoic–Triassic amalgamation in the periphery of the NCC (Fig.1). In the NCC, the Jurassic–Early Cretaceous intracontinental deformation, mainly characterized by the E–W to NE–SW striking, and some N–S striking fold-thrust belts, small-scale normal faults, and coeval magmatism, is widely exposed in the Yinshan-Yanshan belt, the Taihangshan belt, and the Ordos basin and its adjacent areas (Fig. 2; Davis et al., 2001, Faure et al., 2012; Dong et al., 2015; Zhang et al., 2022).

The "Yanshanian Movement", an orogenic terminology that characteristically refers to the Jurassic–Early Cretaceous intracontinental orogeny in the Chinese literature, was initially defined in the Yanshan belt in the west of Beijing by Wong (1927, 1929). During the past decades, considerable advances have been achieved in generating a wealth of data related to the stratigraphy, tectonic deformation, and magmatism in the NCC, aiding in a better understanding of the Yanshanian intracontinental orogeny. However, the stratigraphy and tectonic studies in different zones of the NCC, together with studies on igneous rocks, have not been integrated into a comprehensive study, resulting in a suite of incompatible models for individual zones or disciplines. This hinders the holistic understanding of the plate-scale tectono-magmatic process and the evaluation of geodynamic evolution models of the Yanshanian intracontinental orogeny. This is mainly reflected in the following aspects:

(1) The Yanshanian tectonic events were initially defined by two major unconformities below and above the volcanics of the Upper Jurassic Tiaojishan Formation (J_3t) resulting from deformation episodes in the Yanshan belt, i.e., Events A and B of the Yanshanian orogeny (Wong, 1927, 1929; Fig. 3). Nevertheless, the process of multi-phased deformation and magmatism is greatly complicated by the sporadically distributed Mesozoic strata with significantly different stratigraphic associations in various zones of the NCC, for instance, the corresponding contemporaneous volcanics are absent anywhere outside of the Yanshan belt (Fig. 3). The syn-tectonic strata were often neglected to constrain the deformation episodes in the holistically stratigraphic framework. A reliable chronostratigraphic framework in the Jurassic-Lower Cretaceous interval was never presented in detail through the North China-wide stratigraphic correlation (Fig. 2);

(2) The timing and kinematics of the widely distributed Jurassic–Early Cretaceous multi-phased deformation were rarely constrained within a coherent chronostratigraphic framework. The accurate deformation episodes were blurred by the incompatible isotopic geochronological results from different zones, hindering the holistic understanding of the deformation process of the NCC;

(3) The age and geochemistry of igneous rocks, and the fabric of syn-kinematic plutons provide key constraints on the Jurassic–Early Cretaceous tectonic setting and geodynamic mechanism of the NCC. However, the geochemistry and fabric results on the Jurassic–Early Cretaceous igneous rocks in the NCC have not been integrated into tectonic studies within the reliable chronostratigraphic framework, resulting in incompatible geodynamic models that are often restricted by a single discipline.

After its Paleozoic–Triassic amalgamation, the East Asian continent was bounded by the Mongol–Okhotsk Ocean (MOO) in the north, the Bangong–Nujiang Ocean (BNO) in the southwest, and the Paleo-Pacific Ocean (Izanagi) in the southeast. In the NCC, the Jurassic–Early Cretaceous tectono-magmatic evolutionary process with unified North China-wide timing and kinematic constraints in the various episodes is never established yet. The geodynamics of intraplate deformation in the NCC at large distances, 1,000 km or more, from the related plate boundaries remain enigmatic. Due to the different perspectives of models restricted by individual zones or disciplines, the Jurassic–Early Cretaceous intracontinental orogeny in the NCC was generally interpreted to be the consequence of: i) the north–south closure of the MOO (Yin and Nie, 1996); ii) the northwestward subduction of the Paleo-Pacific Plate (PPP; e.g., Zhu et al., 2011b; Wu et al., 2019; Hao et al., 2020); iii) the north–south interactions between the Eurasian intraplate deformation and the northwestward subduction of the PPP (Davis et al., 2001); or iv) multidirectional multi-plate convergence of the MOO, BNO, and PPP (e.g., Dong et al., 2015; Zhang et al., 2022). The NCC offers an ideal natural laboratory for polyphase intra-plate deformation and magmatism paradigm in response to the Jurassic-Early Cretaceous intracontinental orogeny with variable plate-boundary geodynamics. Intracontinental orogeny is usually sensitive to far-field stress reconfigurations at active plate boundaries (Silva et al., 2018). To understand the geodynamics of the Yanshanian intracontinental orogeny under multi-plate convergence in East Asia, it is necessary to have great insight of the tectono-magmatic process in the various episodes with accurate timing and kinematic constraints.

In this paper, we review available published data concerning Jurassic–Early Cretaceous litho-stratigraphy with emphasis on unconformities, tectonic deformation, and magmatism of the NCC. We combine results from multidisciplinary studies to develop a Jurassic–Early Cretaceous evolutionary model of the NCC that shed light on the geodynamics of the Yanshanian intracontinental orogeny in East Asia, with the following steps: (1) define a coherent chronostratigraphic framework of the entire NCC through a detailed North China-wide stratigraphic correlation by integrating previous litho-stratigraphy information and available isotopic geochronological data; (2) constrain the accurate deformation episodes within the established coherent chronostratigraphic framework; (3) integrate the geochemistry and fabric results on Jurassic–Early Cretaceous igneous rocks into the tectonic studies, presenting a clear tectono-magmatic process for the entire NCC; and (4) link the tectono-magmatic process to the

East Asian active plate boundaries to develop a logical geodynamic model for the Yanshanian intracontinental orogeny. This contribution provides a significant example of polyphase intra-plate deformation and magmatism responding to intracontinental orogeny with variable plate-boundary geodynamics.

2. Tectonic setting

After the cratonization through the Paleoproterozoic amalgamation of the Eastern, Intermediate (or Fuping), and Western blocks (Zhao et al., 2001; Faure et al., 2007; Li et al., 2012; Trap et al., 2012), the NCC was surrounded by the Paleo-Asian Ocean in the north (Windley et al. 2007; Xiao et al., 2003, 2015; Xu et al., 2013) and the eastern branches of the Paleo-Tethys Ocean in the south (Mattauer et al., 1985; Xu et al., 1986; Hacker et al., 2000). In the north of the NCC, the closure of the Paleo-Asian Ocean was characterized by the amalgamation of several microcontinental blocks in the Central Asian Orogenic Belt (e.g., the Erguna, Xing'an, Songnen, Jiamusi, and Khanka blocks; Liu et al., 2017; Zhou et al., 2018; Fig. 1), albeit the timing of the final closure of the Paleo-Asian Ocean remains still debated, i.e., Late Devonian (Xu et al., 2013; Zhao et al., 2013) or Late Permian–Early Triassic (Chen et al., 2000; Li, 2006; Jian et al., 2008; Lin et al., 2008; Xiao et al., 2003, 2015). In the south, the final amalgamation between the NCC and SCB occurred through multistage orogeny during the Paleozoic to Triassic, giving rise to a Late Triassic Dabie-Sulu high-pressure and ultrahigh-pressure (HP–UHP) orogenic belt (Fig. 1; e.g., Mattauer et al. 1985; Faure et al., 1999, 2003; Meng and Zhang, 1999; Hacker et al., 2000; Ratschbacher et al., 2003; Lin et al., 2005, 2009; Li et al., 2017, 2018).

During the Jurassic–Cretaceous, the welded East Asian continent was surrounded by the MOO, PPP, and BNO. The closure time of the MOO between the Siberian Craton and North China–Mongolian arc terranes remains controversial, e.g., the Early–Middle Jurassic (Zorin, 1999; Kravchinsky et al., 2002), the Late Jurassic–early Early Cretaceous (Cogné et al., 2005; Metelkin et al., 2010), or the Early Cretaceous (Enkin et al., 1992). Generally, it is acknowledged that the MOO closed progressively from west to east during the Jurassic–Early Cretaceous (Yin and Nie, 1996; Zorin, 1999; Kravchinsky et al., 2002; Metelkin et al., 2010; Dong et al., 2015). The suture extends from central Mongolia to the Okhotsk Sea (Tomurtogoo et al., 2005; Fig. 1). The onset of the PPP subduction in the southeast has been considered to occur in the Late Triassic (Sagong et al., 2005; Kim et al., 2015), or the Early Jurassic (Wu et al., 2007; Guo et al., 2015; Wang et al., 2019). It is well agreed that the influence of the Paleo-Pacific tectonic regime has extended to North and Northeast China since the Jurassic (e.g., Wu et al., 2007; Li et al., 2007a; Wang et al., 2019). The PPP subducted northwestward beneath the East Asian continent until the latest Mesozoic when the Izanagi-Pacific Ridge subducted (Lapierre et al., 1997). The BNO, extending for more than 2000 km from east to west in central Tibet, separates the Qiangtang terrane from the Lhasa terrane during the Mesozoic (Kapp et al., 2007; Zhu et al., 2016). The initial subduction has been considered to be either prior to the Early Jurassic (Guynn et al., 2006; Zhu et al., 2011a) or in the Middle Jurassic (Zhang et al., 2012; Li et al., 2016d). It has been widely accepted that a diachronous collision from east to west between the Qiangtang and Lhasa terranes occurred during the Middle Jurassic to Early Cretaceous (Guynn et al., 2006; Kapp et al., 2007; Zhu et al., 2016; Yan et al., 2016; Liu et al., 2018a). During the Cenozoic, the tectonic setting of the NCC was the consequence of the intracontinental deformation of the Eurasian plate and the subduction of the western Pacific plate.

3. Stratigraphic framework and unconformities

The Jurassic–Lower Cretaceous strata are well preserved in the Ordos basin and its adjacent areas, and scattered in a few isolated basins in the Yinshan-Yanshan belt (Fig. 2). Some residual Jurassic–Lower Cretaceous strata are concealed below the Cenozoic Bohai Bay and Hefei basins. The Jurassic–Lower Cretaceous strata unconformably or disconformably overlie the Triassic or older strata (Fig.3; Zhang et al., 2011, Meng et al., 2019). Integrating geochronological data, litho-stratigraphy, and syn-tectonic growth strata, we have carried out a detailed North China-wide stratigraphic correlation to develop a coherent chronostratigraphic framework for the Jurassic–Lower Cretaceous interval. It contains five tectonostratigraphic sequences, which are separated by two regional angular unconformities that are ascribed to Events A and B of the Yanshanian orogeny, as below: i) the Lower–lower Middle Jurassic sequence, ii) the upper Middle Jurassic sequence, iii) the lower Upper Jurassic volcanic sequence, iv) the Upper Jurassic–lowermost Cretaceous sequence, and v) the Lower Cretaceous sequence.

3.1 Lower–lower Middle Jurassic sequence

In the eastern NCC, the Lower–lower Middle Jurassic sequence is mainly scattered in the Yanshan belt (Fig. 2). The Xingshikou Formation, which was formerly considered to be of Early

Jurassic, has been recently assigned to Upper Triassic according to new geochronological and paleontological results (Yang et al., 2006; Chen et al., 2015; Meng et al., 2019). Thus, the Lower Jurassic strata consist of fluvial conglomerates and sandstones, and abundant volcanics (e.g., basalt, andesite, dacites, pyroclastic rocks, and tuffaceous sedimentary rocks) in the Nandaling Formation and its counterparts (Fig. 3, Tables 1 and S1). These strata are unconformable on the Triassic or older strata in the Western Hill of Beijing, and the Xiahuayuan, Luanping, and Beipiao basins, and absent in a vast area (Meng et al., 2019; Figs. 2 and 3). The volcanic rocks from the Nandaling Formation ($J_{1-2}n$) in the Western Hill yield a zircon age of 177–167 Ma (Zhao et al., 2006; He et al., 2017; Gao et al., 2018; Hao et al., 2019, 2020; Meng et al., 2019; Fig. 3, Tables 1 and S1). In the Luanping basin, the biotite $^{40}Ar/^{39}Ar$ age of a tuff sample from the Nandaling Formation ($J_{1-2}n$) is dated at 180 ± 1.8 Ma (Davis et al., 2001; Fig. 3, Tables 1 and S1). The tuff samples in the Xinglonggou Formation (J_1x) in the Beipiao basin are of Early Jurassic (188–176 Ma; Chen et al., 1997; Yang and Li, 2008; Fig. 3, Tables 1 and S1). In the above areas, the Lower Jurassic strata are conformably overlain by the lower Middle Jurassic coal-bearing unit, which mainly consists of basal conglomerates, sandstones, siltstones, mudstones, and coal measures (Meng et al., 2019; Fig. 3, Tables 1 and S1). It is characterized by fining- and deepening-upward depositional cycle from the Lower Jurassic fluvial deposits intercalated with volcanic rocks to the lower Middle Jurassic coal-bearing units in lacustrine and swamp facies (Fig. 3). In the Western Hill, the youngest detrital zircon ages from sandstones in the coal-bearing Yaopo Formation (J_2yp) are dated at ~175–174 Ma (Yang et al., 2006; Hao et al., 2019; Fig. 3, Tables 1 and S1). The youngest detrital zircon ages obtained from the coal-bearing Xiahuayuan Formation (J_2x) in the Xiahuayuan and Luanping basins are ~175–170 Ma (Li et al., 2016a; Lin et al., 2018; Hao et al., 2020). In the Beipiao basin in Western Liaoning, the ages of the coal-bearing Beipiao Formation (J_2b) are ~175–168 Ma (Meng et al., 2019; Fig. 3, Tables 1 and S1). The lower Middle Jurassic coal-bearing strata extend outward to a larger area (e.g., the Xiabancheng and Niuyingzi basins) where the lower Middle Jurassic Xiahuayuan (J_2x) or Guojiadian (J_2g) Formation overlies directly on the pre-Jurassic strata (Li et al., 2016a; Meng et al., 2019; Zhang et al., 2019; Fig. 3). The youngest detrital zircon ages obtained from the Guojiadian Formation (J_2g) are ~171–163 Ma (Cope, 2017; Zhang et al., 2019; Wu et al., 2021; Fig. 3, Tables 1 and S1).

In the western NCC, the Lower–lower Middle Jurassic sequence is mainly distributed in the Daqingshan in the Yinshan belt and the Ordos basin and its adjacent areas (Fig. 2). Similar to the eastern NCC, the Lower Jurassic strata were deposited scatteredly in local sags formed on the underlying unconformity (Yang et al., 2005). The Lower Jurassic strata mainly consist of alluvial and fluvial conglomerates and sandstones, whereas the contemporaneous volcanics are absent except for the Jiyuan region (Darby et al. 2001; Ritts et al. 2001; Gong et al., 2015; Li et al., 2015; Wang et al., 2017; Meng et al., 2019; Zhang et al., 2020; Fig. 3, Tables 1 and S1). In the Shiguai basin in Daqingshan, the Lower Jurassic Wudanggou Formation (J_1w), which changes into marginal alluvial conglomerates, and sandstones and shales in the shallow lacustrine and deltaic facies, is much thicker than its counterparts in the Ordos basin and adjacent area (Wang et al., 2017; Fig. 3, Tables 1 and S1). The syn-tectonic growth strata in the lowest Jurassic were developed in small-scaled grabens (Darby et al., 2001), where the ages of diverse palynoflora obtained from the Wudanggou Formation (J_1w) are ~200–183 Ma (Ritts et al. 2001; Wang et al., 2017; Fig. 3, Tables 1 and S1). The interbedded tuff layers in the Yongdingzhuan Formation (J_1y) in the Ningwu-Jingle and Yungang basins have zircon U-Pb ages of 179–171 Ma and 187.6±2 Ma, respectively (Li et al., 2014c; Zhang et al., 2020; Fig. 3, Tables 1 and S1). In the West Henan region, the Lower Jurassic Anyao Formation (J_1a) in the Jiyuan region contains abundant basic volcanic rocks, which are dated at 178.31 ± 3.77 Ma (Lu et al., 2004; Fig. 3, Tables 1 and S1). Similarly, the lower Middle Jurassic strata, conformably overlying the Lower Jurassic strata, change into conglomerates, sandstones, and mudstones intercalated with coal measures in fluvial, lacustrine, and swamp facies in the fining- and deepening-upward depositional cycle (Yang et al., 2005; Li et al., 2015; Wang et al., 2017; Meng et al., 2019; Fig. 3, Tables 1 and S1). This coal-bearing unit extends significantly outward to a vast area in the periphery of the Ordos basin and overlies directly on the underlying erosional surface (Yang et al., 2005; Meng et al., 2019; Fig. 3, Tables 1 and S1). The lower Middle Jurassic coal-bearing units as marker beds can be comparable from area to area in the NCC. The Zhaogou Formation (J_2zg) in the Shiguai basin has been dated by a palynoflora of the early Middle Jurassic age (Ge et al., 2010). In summary, the Lower–lower Middle Jurassic sequence (dated at ~200–170 Ma) is characterized by fining- and deepening-upward depositional cycle from the Lower Jurassic alluvial and fluvial deposits intercalated with volcanic rocks to the lower Middle Jurassic coal-bearing units in lacustrine and swamp facies. The Upper Jurassic volcanic rocks are mainly distributed in the northern and southern margins of the NCC (i.e., the Yanshan belt and the Jiyuan district).

3.2 Upper Middle Jurassic sequence

Event A of the Yanshanian orogeny, representing a regional contraction event, was initially defined by the unconformity beneath the volcanics of the Tiaojishan Formation (J_3t) in the Western Hill of Beijing (Figs. 2 and 3; Wong, 1929). Although the Tiaojishan Formation (J_3t) directly overlies all older strata in the Western Hill, the Tiaojishan Formation (J_3t) is in conformable contact with the underlying Longmen-Jiulongshan Formations (J_2l-J_2j) where the Longmen-Jiulongshan Formations (J_{2l}-J_{2j}) exist locally (Fig. 3; Li et al., 2014a; Hao et al., 2019, 2020). Drilling and exploratory trench data reveal that the conformable Longmen-Jiulongshan (J_2l-J_2j) and Tiaojishan (J_3t) Formations pinch out upwards by onlap against the underlying unconformity (Li et al., 2014a). However, the upper Middle Jurassic Longmen-Jiulongshan Formations (J_2l-J_2j) and their counterparts are absent in a vast area of the Yanshan belt (e.g., the Chicheng, Chengde, Xiabancheng, and Niuyingzi basins), where the Tiaojishan Formation (J_3t) overlies unconformably on the lower Middle Jurassic coal-bearing strata or pre-Jurassic strata (Fig. 3). Therefore, the unconformity representing Event A of the Yanshanian orogeny is located above the coal-bearing strata and older strata (Fig. 3; Li et al., 2014a; Liu et al., 2018b; Hao et al., 2019, 2020; Wu et al., 2021).

In the Yanshan belt, the upper Middle Jurassic Longmen-Jiulongshan Formations (J_2l-J_2j) and their counterparts (i.e., the Jiulongshan Formation in the Xiahuayuan and Luanping basins and the Haifanggou Formation in the Beipiao basin) comprise fluvial to alluvial conglomerates, and sandstones in the lower and deltaic to lacustrine sandstones and mudstones in the upper (Zhao et al. 2002; Liu et al., 2004; Shao and Zhang, 2014; Meng et al., 2019; Hao et al., 2020; Fig. 3, Tables 1 and S1). In the Western Hill, the youngest detrital zircon ages from sandstones in the Longmen Formation are focused on 168–164 Ma (Hao et al., 2019; Wu et al., 2021), whereas the sandstone and tuff samples yield the age of 161–154 Ma (Yang et al., 2006; Li et al., 2014a; Hao et al., 2019; Meng et al., 2019; Fig. 3, Tables 1 and S1). The ages of the Jiulongshan Formation (J_2j) in the Xiahuayuan and Luanping basins are concentrated on 163–156 Ma by dating the tuff and the youngest detrital zircons of sandstones (Chen et al., 2014; Lin et al., 2018; Meng et al., 2019; Hao et al., 2020; Fig. 3, Tables 1 and S1). In the Haifanggou Formation (J_2h) in the Beipiao basin, the tuff–interbed within the basal conglomerates is dated at 167–164 Ma, whereas the topmost tuffaceous breccia yields the eruption ages of 161.7±1.9 Ma (Zhang et al., 2005; Yang and Li, 2008; Chang et al., 2014; Huang, 2019; Hao et al., 2020; Fig. 3, Tables 1 and S1). The conglomerate-dominated lithological characteristics in the Longmen and Jiulongshan Formations (J_2l-J_2j) and their counterparts in the Yanshan belt, which have been considered as syn-tectonic deposition (Zhao et al., 2002, 2004), should be in response to Event A of the Yanshanian orogeny.

In the Yinshan belt, and the Ordos basin and its adjacent areas, the upper Middle Jurassic sequence, which mainly consists of fluvial to lacustrine conglomerates, sandstones, and mudstones, is comparable with those in the Yanshan belt (Zhang et al., 2008b; Li et al., 2014b; Li et al., 2016c; Wang et al., 2017; Fig. 3, Tables 1 and S1). This upper Middle Jurassic sequence unconformably overlies the underlying coal-bearing strata in the Yinshan belt, whereas it is disconformable on the latter ones in the Ordos basin and its adjacent areas (Yang et al., 2013; Wang et al., 2017; Li et al., 2014b; Zhang et al., 2020). The Changhangou Formation (J_2c) in the Shiguai basin, exhibiting a pronounced growth geometry, unconformably onlaps onto the underlying erosional surface in the coal-bearing strata (Wang et al., 2017). The tuff sample yields an age of 163.7 ± 1.0 Ma (Wang et al., 2017; Fig. 3, Tables 1 and S1). The upper Middle Jurassic Yungang Formation (J_2yg) in the Ningwu-Jingle and Yungang basins, exhibiting a typical wedge-like growth strata geometry, onlaps onto the limb of the fault-related folds (Chen et al., 2019; Zhang et al., 2020). The detrital zircons from the lower Yungang Formation in the Yungang and Ningwu-Jingle basins yield ages of 168–165 Ma (Chen et al., 2019; Zhang et al., 2020), and the age of the youngest detrital zircons obtained from the top of the Yungang Formation (J_2yg) in the Ningwu-Jingle basin is 160.7 ± 0.65 Ma (Li et al., 2015; Fig. 3, Tables 1 and S1). Although there is no obvious angular unconformity between the Yungang/Dongmengcun/Ma′ao Formations (J_2yg/J_2dm/J_2m) and the lower Middle Jurassic coal-bearing strata in the West Henan region, abrupt changes in the heavy mineralogy and sedimentary facies occurred in these strata (Fig.3; Li et al., 2014b; Zhang et al., 2020), probably indicating the existence of disconformity within these strata. Therefore, the unconformity (or disconformity) above the coal-bearing strata and the overlying upper Middle Jurassic syn-tectonic sequence (dated at ~170–160 Ma) in the entire NCC should be the response to Event A of the Yanshanian orogeny.

3.3 Upper Jurassic–lowermost Cretaceous sequence

3.3.1 Upper Jurassic volcanics

The upper Jurassic volcanics, assigned to the Tiaojishan (J_3t) or Lanqi (J_3l) Formation, are only distributed in the Yanshan belt and its adjacent areas (Fig. 2). As mentioned above, the upper Jurassic volcanics are in conformable contact with upper Middle Jurassic sequence, and unconformably overlie all older strata where the upper Middle Jurassic sequence is absent (Zhao et al., 2002; Liu et al., 2018b; Hao et al., 2019; Fig. 3, Tables 1 and S1). The volcanics in the Tiaojishan (J_3t) or Lanqi (J_3l) Formation comprise intermediate andesitic lavas, volcanic breccia, andesitic tuff, pyroclastics, and interbedded sedimentary rocks (Zhao et al., 2002; Hao et al., 2019; Fig. 3, Tables 1 and S1). The ages of the Tiaojishan Formation (J_3t) in the Western Hill range from 161 to 146 Ma (Li et al., 2001; Zhao et al., 2004; Yang et al., 2006; Yu et al., 2016; Hao et al., 2019; Fig. 3, Tables 1 and S1). The Tiaojishan Formation (J_3t) in the Hunyuan basin yields zircon ages of 152.77± 0.6 Ma (Li et al., 2015; Fig. 3, Tables 1 and S1). In the Xiahuayuan and Luanping basins, the volcanics in the Tiaojishan Formation (J_3t) are dated at ~164–153 Ma (Davis et al., 2001; Zhang et al., 2005, 2008a; Liu et al., 2006; Cope et al., 2007; Yu et al., 2016; Hao et al., 2020; Fig. 3, Tables 1 and S1). In the Chicheng basin, the andesite interlayers in the Tiaojishan Formation (J_3t) yield ages of 165–157 Ma, (Qi et al., 2015; Jiao et al., 2016; Lin et al., 2019; Fig. 3, Tables 1 and S1). In the Xiabancheng and Niuyingzi basins, the Tiaojishan Formation (J_3t) is of 164–153 Ma and the Lanqi Formation (J_3l) is of 159–158 Ma in age (Davis et al., 2001; Zhao et al., 2002, 2004; Cope et al., 2007; Liu et al., 2006; Li et al., 2016a; Wu et al., 2021; Fig. 3, Tables 1 and S1). In the Beipiao basin, the intermediate volcanic rocks in the Lanqi Formation (J_3l) yield ages of 166–153 Ma (Yang and Li, 2008; Zhang et al., 2008a; Wang et al., 2013b; Hao et al., 2020; Fig. 3, Tables 1 and S1). In summary, the volcanics in the Tiaojishan (J_3t) or Lanqi (J_3l) Formation in the Yanshan belt approximately range from 165 to 150 Ma in age.

3.3.2 Upper Jurassic–lowermost Cretaceous clastic rocks

In the Yanshan belt, the Upper Jurassic strata above the Tiaojishan Formation (J_3t) are absent in the Western Hill (Figs. 2 and 3). The unconformity, representing Event B of the Yanshanian orogeny, was initially defined above the volcanics of the Tiaojishan Formation (J_3t) in the Western Hill; Wong, 1929). As a matter of fact, the Tiaojishan Formation (J_3t) in the

Yanshan belt is conformably overlain by thick upper Jurassic–lowermost Cretaceous coarse clastic rocks of the Tuchengzi/Houcheng Formation (J_3-K_1tch/J_3-K_1h; Liu et al., 2018b; Fig. 3, Tables 1 and S1). Therefore, the unconformity representing Event B of the Yanshanian orogeny should be located above the Tuchengzi/Houcheng Formation (J_3-K_1tch/J_3-K_1h) in the Yanshan belt. The Tuchengzi/Houcheng Formation (J_3-K_1tch/J_3-K_1h), which consists of conglomerates, sandstones, and mudstones in the fluvial, alluvial to lacustrine facies, shares a similar lithology in different areas of the Yanshan belt (Fig. 3, Tables 1 and S1). The Upper Jurassic–lowermost Cretaceous Tuchengzi/Houcheng Formation (J_3-K_1tch/J_3-K_1h) in the Yanshan belt was constrained between 155 and 135 Ma (Swisher et al., 2002; Shao et al., 2003; Cope et al., 2007; Zhang et al., 2005, 2008a, 2009; Xu et al., 2012; Wang et al., 2013c; Li et al., 2015; Qi et al., 2015; Li et al., 2016a; Fu et al., 2018; Liu et al., 2018b; Lin et al., 2019; Fig. 3, Tables 1 and S1). The Tuchengzi Formation (J_3-K_1tch) contains several growth strata packages, onlapping or offlapping onto the limb of the fold-and-thrust belts in the Xiahuayuan and Chicheng basins (Liu et al., 2018b; Lin et al., 2019; Shi et al., 2019). Therefore, the syn-tectonic Tuchengzi/Houcheng Formation (J_3-K_1tch/J_3-K_1h) and the unconformity above in the Yanshan belt are thought to be in response to Event B of the Yanshanian orogeny (Zhao, 1990; Cope et al., 2007).

In the Yinshan belt, and the Ordos basin and its adjacent areas, the Upper Jurassic volcanics corresponding to the Tiaojishan Formation (J_3t) are absent (Fig. 3). The Upper Jurassic–lowermost Cretaceous clastic rocks share a similar lithology with the Yanshan belt. These Upper Jurassic–lowermost Cretaceous strata, which consist of fluvial, alluvial to lacustrine conglomerates, sandstones, and mudstones, are in unconformable contact with the underlying upper Middle Jurassic sequence (Zhang et al., 2008b; Li et al., 2014b, 2015; Wang et al., 2017; Meng et al., 2019; Zhang et al., 2020; Fig. 3, Tables 1 and S1). The Upper Jurassic Daqingshan Formation (J_3d) in the Shiguai basin exhibits typical growth strata geometry in the footwall of thrusts (Wang et al., 2017). In the Ordos basin, the Fenfanghe Formation (J_3f) also contains syn-tectonic growth strata in the western Ordos thrust and fold belt (Zhang et al., 2008b). The Upper Jurassic strata in the Yungang basin are absent (Li et al., 2014b, 2015; Zhang et al., 2020). In the Ningwu-Jingle basin, the Tianchihe Formation (J_3t) exhibits a typical growth strata geometry in the piggy-back basin (Chen et al., 2019). The tuffaceous micrite at the bottom of the Upper Jurassic Tianchihe Formation (J_3t) yields zircon ages of 160.6 ± 0.55 Ma (Li et al., 2014b; Fig. 3, Tables 1 and S1). Therefore, the Upper Jurassic-lowermost Cretaceous syn-tectonic sequence and the unconformity above in the entire NCC should be the response to Event B of the Yanshanian orogeny.

3.3 Lower Cretaceous sequence

In the NCC, the Lower Cretaceous is separated from the underlying Upper Jurassic–lowermost Cretaceous sequence by a regional angular unconformity representing Event B of the Yanshanian orogeny (Fig. 3). In the Yanshan belt, the Lower Cretaceous Zhangjiakou Formation (K_1zh) and the Donglingtai Formation (K_1d) comprise a series of siliceous volcanic rocks (e.g., rhyolitic tuff, rhyolite, andesite, quartz trachyte, and pyroclastics; Qi et al., 2015; Lin et al., 2018; Su et al., 2021; Tables 1 and S1). The Guyang Group (K_1g) in the Yinshan belt consists of fluvial to lacustrine conglomerates and sandstones with volcanic rocks (Gong et al., 2015; Tables 1 and S1). In the Yinshan-Yanshan belt, the Lower Cretaceous sequence, which fills a large number of normal or detachment fault-bounded grabens or half-grabens (Zhang et al., 2004a; Davis and Darby, 2010; Lin and Wei, 2018), has a lower age limit of 136–127 Ma (Niu et al., 2003, 2004; Zhao et al., 2004; Yuan et al., 2005; Zhang et al., 2005; Davis and Darby, 2010; Tables 1 and S1). The Lower Cretaceous sequence in the Ordos basin and its adjacent areas (e.g., Zhidan Group (K_1z), and the Zuoyun Formation (K_1zy) in the Ningwu-jingle and Yungang basins) changes into the fluvial conglomerates to sandstones (Zhang et al., 2011; Li et al., 2014b, 2016c; Zhang et al., 2020). In the Yungang basin, the andesite at the base of the Zuoyun Formation (K_1zy) yields a zircon U–Pb age of 130.1 ± 0.8 Ma (Li et al., 2016c; Tables 1 and S1).

4. Regional deformation

In the NCC, the Jurassic–Early Cretaceous intracontinental deformation, mainly characterized by the supracrustal non-metamorphic structures, such as brittle thrust and normal faults, is well exposed in the Yanshan belt (including the northern Taihangshan belt), the Yinshan belt, and the periphery of the Ordos basin (Fig. 2; Davis et al., 2001; Zhang et al., 2011; Dong et al., 2015). The well-preserved Jurassic–Lower Cretaceous strata in the Yanshan belt, the Yinshan belt, and the Ordos basin and its adjacent areas could provide age constraints on the Jurassic–Early Cretaceous brittle deformation. In this paper, the regional deformation in the Yanshan belt, the Yinshan belt, and the periphery of the Ordos basin is summarized within the chronostratigraphic framework as below.

4.1 Yanshan belt

4.1.1 Inherited fold-thrust structures

In the NCC, the pre-Jurassic deformation is inferred to correlate the tectonic events at block boundaries, i.e., the closure of the Paleo-Asian Ocean or the collision between the NCC and SCB. The related deformation includes the Middle–Late Triassic E–W striking south-verging Shangyi-Chicheng ductile shear zone, the Fengning-Longhua ductile shear zone, the Damiao-Niangniangmiao ductile shear zone, the Malanyu anticline, and the Jixian thrust in the Yanshan belt (Fig. 4; Wang et al., 2013a), and the Late Triassic south-verging fold-thrusts in the southern West Qinling (Meng and Zhang, 1999; Meng et al., 2019). Several pre-Jurassic ENE striking brittle fold-thrusts in the central Yanshan belt were reworked during the Jurassic–Early Cretaceous (e.g., the Mengjiazhuang thrust, the Jiyuqing thrust, the Liudaohe thrust in the south Chengde basin; Table 2, Fig. 4). The footwalls of these ENE striking fold-thrusts contain the vertically stacked Cambrian–Ordovician, Permian–Triassic, and Middle Jurassic strata, whereas these strata are absent in the hanging walls (Fig. 4b; Li et al., 2016a). The preserved Middle Jurassic strata concern the Xiahuayuan Formation (J_2x; Meng et al., 2019), suggesting the pre-J_2x activity of these thrusts. In these thrusts, the Late Jurassic Tiaojishan Formation (J_3t), unconformably overlying on the tightly folded underlying strata, is only involved in the eastward trending open folding. This suggests that the southward thrusting and tight folding occurred during the period of post-J_2x to pre-J_3t (Fig. 4b; Li et al., 2016a). The locally distributed Longmen-Jiulongshan Formations (J_2l-J_2j) and their counterparts should be syn-tectonic deposits in the flexural basins and/or piggy-back basins, in response to the thrusting related to Event A of the Yanshanian orogeny. The open refolding occurred in the Tiaojishan Formation (J_3t) and Tuchengzi Formation (J_3-K_1tch). The Early Cretaceous Zhangjiakou Formation (K_1zh), bounded by the Chengde normal fault, overlies these refolded strata (Fig. 4b; Li et al., 2016a). Considering the syn-tectonic deposition of the Tuchengzi Formation (J_3-K_1tch), this open refolded event should be in response to Event B of the Yanshanian orogeny during the period of post-J_3t to pre-K_1zh.

4.1.2 Event A of the Yanshanian orogeny-related deformation

In the central Yanshan belt, the Mesoproterozoic strata in the hanging wall of the E-striking Duanshuwa-Jianbaoshan thrust thrust southward onto the Middle Jurassic Xiahuayuan Formation

(J_2x) and the underlying Paleozoic or Proterozoic rocks (Table 2, Fig. 4; Li et al., 2016a). The Duanshuwa-Jianbaoshan thrust and several neighboring E-striking thrusts (e.g., the Xinglong thrust, the Qingshuihu fault, the Zhujiagou fault, and the Miyun-Xifengkou fault and its NE striking branch faults) are unconformably overlain by the Late Jurassic Tiaojishan volcanic rocks (J_3t) or intruded by the Siganding and Wangpingshi plutons, and mafic dykes at the ages of 162 and 157 Ma, respectively (Chen, 1998; Zeng et al., 2021). It suggests that these thrusts should be the response to Event A of the Yanshanian orogeny during the period of post-J_2x to pre-J_3t. In the eastern Yanshan belt, the Guojiadian Formation (J_2g) in the footwall is involved in the southeastward thrusting Yangzhangzi-Wafangdian fault, which is intruded by the 160.2 Ma rhyolitic porphyry (Zhang et al., 2002). This phenomenon suggests that this fault was active during the period of post-J_2g to pre-J_3l, responding to Event A of the Yanshanian orogeny (Zhang et al., 2002).

4.1.3 Event B of the Yanshanian orogeny-related deformation

In the central Yanshan belt, the Mesoproterozoic strata in the hanging walls of several E–NE striking thrusts (e.g., the Dayingzi thrust, the Shanggu-Pingquan thrust, the Gubeikou-Pingquan fault, and the Chengde thrust) thrust on the Tuchengzi Formation (J_3-K_1tch) (Table 2, Fig. 4; Davis et al., 2001; Li et al., 2016a). These thrusts are unconformably overlain by the Early Cretaceous Zhangjiakou Formation (K_1zh) or intruded by the Early Cretaceous plutons (i.e., 132 Ma Wulingshan pluton, 130 Ma Shouwangfe pluton, the 113 Ma Jiashan pluton, the 111 Ma Guozhangzi pluton, and the 129 Ma Qiancengbei pluton; Table 2, Fig. 4; Davis et al., 2001; Li et al., 2016a). Considering that the Tuchengzi/Houcheng Formation (J_3-K_1tch/J_3-K_1h) in the Yanshan belt was of the syn-tectonic deposits with a growth strata geometry in the footwalls or hanging walls of thrusts (Liu et al., 2018b; Lin et al., 2019; Shi et al., 2019), these structural relationships suggest that these thrusts are related to Event B of the Yanshanian orogeny during the period of post-J_3t to pre-K_1zh (the same below). Meanwhile, the Sihetang ductile shear zone was considered to form in the north of the Yunmengshan pluton during this period, in view of the 145 Ma syn-tectonic Yunmengshan pluton (Table 2, Fig. 4; Davis et al., 2001; Zhu et al., 2015).

The E-striking Gubeikou-Pingquan fault extends westward along the Shangyi-Chicheng ductile shear zone in the western Yanshan belt (Fig. 4; Lin et al., 2020; Yang et al., 2021). Several NE-striking thrusts are developed in the south of the Gubeikou-Pingquan fault (e.g., the

Qianjiadian thrust, the Shaliangzi thrust, and the Tanghekou thrust). The first two faults thrust southeastward and the latter one thrusts northwestward (Table 2, Fig. 4; Lin et al., 2020). To the south, a series of nearly NE-striking thrusts are developed in the Western Hill, the Xiahuayuan basin, and the Shangyi basin (e.g., the Nandazhai-Babaoshan thrust, the Xiahuayuan thrust, and the Banshen-Shuiquangou thrust; Table 2, Fig. 4). These faults thrust northwestward, indicated by the NW–SE directional fault-slip data (Table 2, Fig. 4; Zhang et al., 2006; Lin et al., 2020; Yang et al., 2021). All these NE-striking thrusts displace the Meso- and Neo-Proterozoic strata southeastward or northwestward over the Tuchengzi Formation (J_3-K_1tch)/Houcheng Formation (J_3-K_1h) or the Tiaojishan Formation (J_3t) where the J_3-K_1tch is absent in the Western Hill, and unconformably overlain by the Early Cretaceous Zhangjiakou Formation/Donglingtai Formation (K_1zh/K_1d; Zhang et al., 2006; Lin et al., 2020; Yang et al., 2021). It suggests that these NE striking thrusts are related to Event B of the Yanshanian orogeny during the period of post-J_3t to pre-K_1zh/K_1d. The E-striking Gubeikou-Pingquan fault and Miyun-Xifengkou fault are considered to have experienced a dextral strike-slip displacement (Zhang et al., 2004a; Faure et al., 2012). The E- and WNW-striking secondary faults of the Gubeikou-Pingquan fault have a dominant strike-slip or transpressional displacement with dextral or dextral oblique thrusting striations (Lin et al., 2020). The paleostress field was a NW–SE compression, inferred from the fault-slip data (e.g., striations) from secondary faults and adjacent NE-striking thrusts (Lin et al., 2020; Yang et al., 2021). The Upper Jurassic Houcheng Formation (J_3-K_1h) is involved in the dextral Gubeikou-Pingquan fault, unconformably overlain by the Lower Cretaceous Zhangjiakou Formation (Lin et al., 2020). It suggests that the Gubeikou-Pingquan fault experienced a dextral strike-slip or transpressional reactivation related to Event B of the Yanshanian orogeny during the period of post-J_3t and pre-K, which is coeval with the thrusts in the western Yanshan belt.

The eastern Yanshan belt is mainly characterized by NE-striking thrusts (e.g., the Nangongyingzi-Beipiao fault) that displace the Mesoproterozoic–Neoproterozoic or Paleozoic sediments in the hanging walls southeastward or northwestward over the Upper Jurassic Tuchengzi Formation (J_3-K_1tch) of the footwalls (Table 2, Fig. 4; Zhang et al., 2002). Most of these thrusts are unconformably overlain by the Lower Cretaceous Zhangjiakou Formation/Yixian Formation (K_1zh/K_1y; Zhang et al., 2002). The structural relationship suggests that these thrusts were mainly active during the period of post-J_3l and pre-K_1y (Event B of the Yanshanian orogeny). The NE-striking Jianchang-Chaoyang fault (also namely Nantianmen fault) displaces the Archaean crystalline basement over the Lower Cretaceous and underlying strata (Su et al., 2020). The Tuchengzi Formation (J_3-K_1tch) and underlying strata below an angular unconformity are involved in the relatively tight fault-related folds, while the overlying Lower Cretaceous strata are slightly deformed. It suggests that this fault was active during the period of post-J_3l to pre-K_1y and then reactivated post-K_1y. Fault-slip data show that this fault firstly thrusts southeastward under a NW–SE compression and then is reactivated as a reverse sinistral fault accommodating with a NNW–SSE compression (Su et al., 2020).

4.1.4 Three-stage extensional deformation

In the eastern NCC, the three-stage extensional deformation occurred within the Yanshan belt during the Jurassic–Early Cretaceous. The first extensional episode was documented in the Niuyingzi basin where the Zhuzhangzi fault was originally a normal fault bounding the Guojiadian Formation (J_2g) during the early Middle Jurassic (Fig. 2; Davis et al., 2009). During the second extensional episode, a detachment ductile shear zone with a top-to-the-NE shear sense was initially formed during the ~156–150 Ma NE–SW extension before the nucleation of the Early Cretaceous Kalaqin metamorphic core complex (MCC; Fig. 2; Lin et al., 2014). This early Late Jurassic extension is also suggested by the brittle normal faults bounding the volcanics of the Tiaojishan Formation (J_3t) in the Chengde basin and the Diao'e and Houcheng sub-basins of the Chicheng basin (Figs. 2 and 4; Davis et al., 2001; Qi et al., 2015; Lin et al., 2018). The well-known third NW-SE extensional episode was well recorded by the Early Cretaceous MCCs (e.g., the Yiwulüshan, Kalaqin, and Yunmengshan MCCs within a time span of 131–114 Ma) and the graben or half-graben basins (Fig. 4; Wang et al., 2001; Lin et al. 2013a, 2013b, 2014; Lin and Wei, 2018).

4.2 Yinshan belt

4.2.1 Two-stage contractional deformation

In the Yinshan belt, the E–W striking high-angle basement-involved thrusts are widely distributed in western Daqingshan. Numerous E–W striking thrusts cut the Lower Jurassic Wudanggou Formation (J_1w) and underlying Archean crystalline basement through Paleozoic strata in the south of the Shiguai basin (Table 2, Fig. 5; Gong et al., 2015; Wang et al., 2017). The Hetangou-Dongerba thrust, bounding the Shiguai basin, displaces the Permian and underlying strata over the Jurassic coal-bearing Wudanggou (J_1w) and Zhaogou (J_2zg) Formations (Table 2,

Fig. 5; Wang et al., 2017). The syn-tectonic Changhangou (J_2c) growth strata with a clear onlap geometry were deposited ahead of the front of this thrust. A cross-cutting relationship of superimposed striations shows that the N–S striations were overprinted by the NW–SE ones, documenting an early N–S compression and a later NW–SE compression. To the north, the Beilinshan thrust cuts the Changhangou (J_2c) growth strata, presenting the NW–SE striations with the absence of the N–S ones (Table 2, Fig. 5; Wang et al., 2017). The Daqingshan Formation (J_3d), exhibiting a growth strata geometry, onlaps onto a north-verging blind thrust in its central segment or directly onlaps onto the front of this thrust elsewhere (Wang et al., 2017). To the east, this thrust is truncated by the detachment fault of the Hohhot MCC in Louhuashan (Fig. 5). All the structural relationships suggest that most of the E-striking thrusts occurred during the period of post-J_2zg to pre-J_3d under a N–S compression related to Event A of the Yanshanian orogeny. Afterward, these E-striking thrusts were reactivated or nucleated during the period of post-J_2c to pre-K_1g under a NW–SE compression related to Event B of the Yanshanian orogeny. In the north, two NW-striking dextral strike-slip faults, which cut the Daqingshan Formation (J_3d) and truncated by the Early Cretaceous Hohhot detachment fault, should be active during this NW–SE compression (Fig. 5; Gong et al., 2015).

The high-angle thrusts in western Daqingshan gradually change eastward into a low-angle and thin-skinned geometry (Wang et al., 2017). In eastern Daqingshan, the low-angle Daqingshan thrust was exhumed by the Early Cretaceous Hohhot detachment fault (Table 2, Fig. 5). The allochthonous Proterozoic strata have been thrust northwestward from the SE atop the autochthonous conglomerates of the Daqingshan Formation (J_3d), illustrated by the S–C fabrics defined by marble lenses and a shear foliation (Gong et al., 2015). It suggests that the low-angle thrusts in eastern Daqingshan nucleated during the period of post-J_2c to pre-K_1g under a NW–SE compression.

Besides, in Langshan, a steeply dipping NE-striking thrust fault juxtaposes the Archean crystalline basement against a variety of footwall units, most of which are Lower Cretaceous and undifferentiated Jurassic strata (Fig. 2; Darby and Ritts, 2007). The Lower Cretaceous strata are in unconformable contact with the Jurassic ones. The striations on thrust fault planes and axial planes of related folds suggest that a Late Jurassic to Early Cretaceous NNW–SSE compression occurred in Langshan (Darby and Ritts, 2007).

4.2.2 Two-stage extensional deformation

In the Yinshan belt, a series of small-scale normal faults, bounding syn-tectonic growth strata in small-scale grabens, cut the Wudanggou Formation (J_1w) and the unconformity below or develop in the weakly folded Zhaogou Formation (J_2zg) in the Shiguai basin (Fig. 5; Darby et al. 2001; Ritts et al. 2001; Wang et al. 2017). The fault-slip data suggest that these normal faults nucleated during the Early–early Middle Jurassic N–S extension. Stratigraphic and sedimentological analyses also suggested that the Shiguai basin was an E–W striking Early–early Middle Jurassic half-graben, which is inverted during the later contraction (Darby et al. 2001). The Early Cretaceous extensional deformation in the Yinshan belt mainly includes the Hohhot MCC and related detachment faults (Fig. 5; Davis and Darby, 2010). The south-dipping Hohhot detachment fault shows the top-to-the-SE shearing under the NW–SE extension during 127–119 Ma. In addition, the Early Cretaceous extension, presented by brittle normal faults, also occurred in Langshan (Fig. 2; Darby and Ritts, 2007).

4.3 Periphery of the Ordos Basin

4.3.1 Event B of the Yanshanian orogeny-dominated deformation

The intracratonic Ordos basin is surrounded by the Cenozoic Hetao and Fenwei Grabens in the north and south, respectively (Fig. 2). The Jurassic–Early Cretaceous deformation is well documented in the western and eastern margins. In the Western Ordos fold-thrust belt, the Jurassic and underlying strata are involved in a series of eastward thrusting faults and unconformably overlain by the Cretaceous strata, revealed by seismic reflection data (Figs. 2 and 6, Table 2). Northward, a nearly N-striking fold-thrust belt in Zhuozishan juxtaposes the Lower Paleozoic and underlying strata against a vertical to overturned Upper Jurassic Fenfanghe Formation (J_3f) in the east (Figs. 7a and 7b, Table 2; Darby and Ritts, 2002; Li et al., 2022). A large number of striations on the fault plane are oriented in the NW–SE direction (Li et al., 2022). These folded strata involved in the west-dipping thrust faults are unconformably overlain by the Cretaceous strata in the east of Zhuozishan (Fig. 7a). Considering the syn-tectonic growth strata of the Fenfanghe Formation (J_3f) in the east of Zhuozishan (Zhang et al., 2008b), the fold-thrust belt in the western Ordos margin should be active during the period of post-J_2a to pre-K_1z under the NW–SE compression related to Event B of the Yanshanian orogeny.

Further west, a series of thrusts and folds in the northern Helanshan fold-thrust belt (e.g., the Chaqigou-Tatagou and Dashuigoumen-Dawukou faults) displace northwestward the Carboniferous–Permian strata over the Triassic strata in the east (Table 2, Fig. 7c; Darby and Ritts, 2002; Huang, et al., 2015; Yang and Dong, 2018; Li et al., 2022). In the west, the Lower Paleozoic strata thrust southeastward onto the Middle Jurassic Anding Formation (J_2a) in the hanging wall of the Xiaosongshan fault. In the southern Helanshan fold-thrust belt, the Devonian strata thrust southeastward onto the tightly folded Jurassic Fenfanghe Formation (J_3f) and underlying strata along the Dazhanchang fault (Fig. 7d, Table 2; Yang and Dong, 2020). The Dazhanchang fault and related folds are unconformably overlain in the thrust front by the Lower Cretaceous. All fault-slip vectors of these thrusts and folds are consistent in the NW–SE direction (Huang, et al., 2015; Yang and Dong, 2018, 2020; Li et al., 2022), indicating that a NW–SE compression related to Event B of the Yanshanian orogeny occurred in the Helanshan fold-thrust belt during the period of post-J_2a to pre-K_1z. Besides, the syn-tectonic growth strata in the Middle Jurassic Zhiluo Formation (J_2z) and Anding Formation (J_2a) have been identified in the east of the Dazhanchang fault (Fig. 7e; Cheng et al., 2022). A reversal of paleocurrent directions from west-directed to east-directed occurred in the Zhuozi Shan during the Early–Middle Jurassic (Darby and Ritts, 2002). Despite the lack of discovery of syn-sedimentary structures, these phenomena should be the response to Event A of the Yanshanian orogeny during the late Middle Jurassic.

In the east of the Ordos basin, the Ningwu-Jingle basin is a NE-striking synclinal basin, locally confined by the NE-striking thrust faults (e.g., the Chunjing thrust, the Mafangzhen thrust, and the Dujiacun thrust; Table 2, Fig. 8a; Chen et al., 2019). The Lower–Middle Jurassic Yongdingzhuang (J_1y) and Datong (J_2d) Formations and underlying strata are involved in the NE-striking fold deformation. Two sets of vertically stacked growth strata (i.e., the Yungang Formation (J_2yg) and the Tianchihe Formation (J_3tc)) were deposited in the synclinal core (Fig. 8; Chen et al., 2019). The NE-striking Yungang basin is bounded by the SE-dipping thrust faults in the southeast (e.g., the northwestward thrusting Kouquan thrust and Emaokou fault). The syn-tectonic growth strata in the Yungang Formation (J_2yg) were deposited in the thrust front and unconformably overlain by the Lower Cretaceous strata in the north (Zhang et al., 2020). The fault-slip vectors in the Yungang basin are consistent in the NW–SE direction, suggesting that these NE-striking thrusts were active under a NW–SE compression (Zhang et al., 2020). Considering the simultaneity with the Fenfanghe Formation (J_3f) in the Ordos basin and the Daqingshan

Formation (J_3d) in the Yinshan belt, the growth strata in the Tianchihe Formation (J_3tc) should be deposited during the Late Jurassic–earliest Cretaceous NW–SE compression related to Event B of the Yanshanian orogeny. The growth strata in the Yungang (J_2yg), coeval with the Zhiluo (J_2z) and Anding (J_2a) Formations in the Ordos basin and the Changhangou Formation (J_2c) in the Yinshan belt, should be in response to the late Middle Jurassic N–S compression related to Event A of the Yanshanian orogeny.

4.3.2 Two-stage extensional deformation

The Early–early Middle Jurassic extensional normal faults were widely distributed in the Ordos basin and its adjacent areas (Fig. 2). In the central and northeastern Ordos basin, the NNE–SSW or nearly N–S extensional normal faults, indicated by the NNE–SSW fault-slip vectors, were identified in the Upper Triassic–Lower Jurassic strata (Zhang et al., 2011). In the Yungang and neighboring Guangling basins, the normal faults, which cut the basal conglomerates in the lower Lower Jurassic, are covered by the upper Lower Jurassic strata (Li et al., 2015). In the Qingshuihe basin, east of the southern Ordos basin, the E–W to WNW–ESE-striking normal faults cut the Paleozoic to Middle Jurassic strata (Zhang et al., 2011). In the southern NCC, the syn-sedimentary normal faults and soft-sediment deformation also occurred in the Lower Jurassic Anyao Formation (Meng et al., 2019). The Early–early Middle Jurassic extensional deformation is characterized by the small-scale N–S extensional brittle normal faults. Besides, the Early Cretaceous NW–SE extension is widely identified in the Ordos basin and its adjacent areas, mainly expressed by small-scale brittle normal faults (Zhang et al., 2011).

5. Magmatism

5.1 Petrological and geochemical characteristics of magmatic rocks

The Jurassic magmatism that occurred in the eastern NCC can be divided into two stages (Fig. 9), i.e., Early–early Middle Jurassic (191–167 Ma), and Late Jurassic (~166–142 Ma with a peak at 164–152 Ma). The Early Cretaceous (135–115 Ma) magmatism is distributed throughout the NCC (Fig. 9). The Early–early Middle Jurassic (191–170 Ma) intrusive rocks, composed of granite, monzogranites, monzonite, and syenite, are mainly distributed in the Yanshan belt, the southern Yanbian area, the Liaodong peninsula, and sporadically in western Shandong as well as northern Jiangsu (e.g., Zhang et al., 2014; Wu et al., 2019; and references therein; Fig. 2). These granitoids, belonging to metaluminous, high-K calc-alkaline or shoshonitic, and I-type granites, are mainly distributed in the southern and northern margins of the eastern NCC (Fig. 2). The Early–early Middle Jurassic intrusive rocks (191–170 Ma) show typical characteristics of adakite-like primary magmas derived from partial melting of the ancient lower crust. The εNd(t) and εHf(t) values, from low negative to low positive, suggest the interaction of various lower to upper crust, lithospheric mantle, and asthenospheric mantle sources (Lan et al., 2012; Zhang et al., 2014). In the Western Hill, the Nandaling basalts, basaltic andesites, and dacites (188–176 Ma) present low initial $^{87}Sr/^{86}Sr$ ratios and variable negative εNd(t) values, originating from upwelling of asthenosphere and decompressional melting of the early subduction-metasomatized continental lithospheric mantle (Guo et al., 2007; Wang et al., 2007; Fig. 2). The Xinglonggou andesites and dacites in Western Liaoning (177–167 Ma) are high-Mg# adakites with arc-like isotopic compositions, deriving from a subducted-oceanic slab (Yang and Li, 2008; Fig. 2).

The Late Jurassic (164–152 Ma) intrusive rocks, including granitoids and gabbro-pyroxenite complexes, are mainly distributed in the eastern NCC, e.g., the Yanshan belt, the northern Taihangshan, the southern Yanbian area, the Liaodong peninsula, the Jiaodong peninsula, and the Bengbu area (Fig. 2; e.g., Zhang, 2007; Zhang et al., 2014; Wu et al., 2019; and references therein). The granitoids, consisting of granite, monzodiorite, syenite, diorite, and mozonite, are mainly calc-alkaline and I-type with minor A-type and S-type granites. These rocks have adakite-like geochemical signatures and ancient crust-derived isotopic characteristics. The intermediate–mafic intrusive complexes, possessing slightly to moderately enriched isotopic compositions, were derived from the partial melting of subcontinental lithospheric mantle metasomatized by earlier subduction slab-derived fluids (Zhang et al., 2004b; Zhang, 2007; Zhang et al., 2010). The contemporaneous Tiaojishan volcanic rocks and their counterparts (i.e., Lanqi Formation and Houcheng Formation) are mainly distributed in the Yanshan belt and its adjacent areas. The eruption ages are variable from Western Liaoning (166–153 Ma), through Chengde-Luanping (162–153 Ma) and Western Hill-Xuanhua-Yuxian (158–142 Ma; Guo et al., 2022). They are andesite, dacite, trachyandesite, and volumetrically minor basalt and rhyolite (Zhang et al., 2014). Late Jurassic volcanic rocks, mainly calc-alkaline and intermediate-felsic, share highly coherent petrological, geochemical and unradiogenic Hf isotope features similar to those of volcanic rocks from modern continental arcs in a subduction-related setting (Wu et al., 2005, 2008; Guo et al., 2022). These volcanic rocks are mainly derived from the partial melting of the lower crust through magma underplating at the crust-mantle boundary (Yang and Li, 2008).

The Early Cretaceous (135–115 Ma) magmatism, representing a giant igneous event (Wu et al., 2005), is extensively distributed in the northern and southern margins of the NCC as well as the interior of the eastern NCC (Zhang et al., 2004b; Zhang et al., 2014; Wu et al., 2019). The Early Cretaceous intrusive rocks include dolerite, gabbro, diorite, granodiorite, I- and A-type granite, and syenite, whereas the volcanic rocks are mainly basalt, rhyolite, rhyolitic tuff, trachyte, and trachyandesite. Unlike Jurassic granitoids, these Early Cretaceous granitoids are not adakitic but commonly alkaline (Zhang et al., 2014; Wu et al., 2019). The temporal and spatial distribution of mafic magmatism suggests that the variably enriched Mesozoic lithospheric mantle existed beneath the NCC during the Early Cretaceous (Zhang, 2007; Zhang et al., 2010). The Early Cretaceous igneous rocks are derived from multiple sources, i.e., depleted mantle, enriched lithospheric mantle, ancient lower crust, and juvenile crust, suggesting the intensive mantle-crust interaction in the NCC during the Early Cretaceous time (Yang et al. 2004; Zhang et al., 2014; Wu et al., 2019).

5.2 Fabrics of granitic plutons

The fabrics of granitic plutons have been used for their potential to record the tectonic regime (i.e., compressional, extensional, and strike-slip) coeval with granite emplacement (e.g., Paterson et al., 1989; Bouchez and Gleizes, 1995). The study of anisotropy of magnetic susceptibility (AMS) is an effective and practical way to reveal the structural elements of apparently isotropic to weakly deformed granitic plutons (e.g., Archanjo et al., 1994; Bouchez et al., 1997). In the NCC, numerous granitic plutons have been targeted to understand the Jurassic–Early Cretaceous tectonic regime through the AMS study.

5.2.1 New fabric data of Jurassic plutons

In the NCC, fabric studies have been rarely performed on the Jurassic granitic plutons in the Yanshan belt. In this study, we selected the granitic Jianchang-Jiumen plutons in the eastern Yanshan belt to provide Jurassic regional tectonic information through an AMS study (Fig. 4). The Jianchang-Jiumen plutons, extending ~50 km along a NE–SW long axis (Fig. 10), are the representative Jurassic plutons in North China. Both the Jiumen and Jianchang plutons appear isotropic without observable planar and linear fabrics at outcrops. They consist of an Early Jurassic pale-red monzogranite (194–176 Ma) in the Jiumen pluton and a Late Jurassic light gray monzogranite (161–153 Ma) in the Jianchang one (Wu et al., 2006; Cui, 2015). New SIMS zircon U-Pb dating of four samples (JJ39 in the Jiumen pluton, and JJ24, JJ30, and JJ42 in the Jianchang one) yields the ages of 189.9 ± 2.7 Ma, 158.6 ± 2.5 Ma, 157.4 ±2.3 Ma, 157.4 ±2.3 Ma, respectively (cf. Text S1 in supplementary materials for details; Figs. 10 and 11).

The Jianchang-Jiumen plutons intrude into the undeformed Archaean granite and unmetamorphosed Neoproterozoic–Paleozoic sedimentary rocks (Fig. 10). To the north, these Neoproterozoic–Paleozoic sedimentary strata are folded prior to pluton emplacement, as suggested by the undeformed Late Triassic granitic stock intruded into the core of the Yangjiazhangzi syncline (Fig. 10). The outward dipping bedding in the country rocks is subparallel to the pluton border (Fig. 10). It suggests that the Jianchang-Jiumen plutons intruded into the pre-existing anticline and were constructed by magma inflation and pushing aside the country rocks (cf. Text S2 in supplementary materials for details). Microscopically, quartz grains are anhedral and undeformed without signs of undulose extinction or weak dynamic recrystallization with some small subgrains at the border of coarse grains with undulose extinction. The other rock-forming minerals are all euhedral without any deformation. Thus, the fabrics in the Jianchang-Jiumen plutons are magmatic or submagmatic, acquired during, or just after, the crystallization of the magma without significant solid-state deformation (cf. Text S2 in supplementary materials for details). Magnetic mineralogy investigations suggest that the magnetic fabrics of the Jianchang-Jiumen plutons are dominated by pseudo-single domain magnetite, implying that the principal axis of the magnetic fabrics can be correlated to the petro-fabrics of studied samples (e.g., Hargraves et al., 1991; Tarling and Hrouda, 1993; cf. Text S3 in supplementary materials for details). At the map scale, both magnetic foliation and lineation in the Early Jurassic Jiumen pluton are highly scattered with variable dips (Fig. 12). This may be due to an overprint by the intrusion of the Late Jurassic Jianchang pluton near its bottom where the remnant of the Jiumen pluton are scattered within the Jianchang pluton (Fig. 10). Nevertheless, in the Jianchang pluton, the margin-parallel magnetic foliations mainly present moderately to highly outward dipping around its northwestern part and subparallel striking to the southeastern margin of the pluton (Fig. 12a). The margin-parallel outward dipping magnetic foliations around the northwest define a dome-like roof beneath the Jiumen pluton (Fig. 12a). The magnetic lineations display gentle to moderate NE–SW plunging throughout the pluton (mean at 60°/20°; Fig. 12b). Without any regional strain, the magmatic lineation that reflects the magma flow within the pluton would have variable orientations and plunges depending on magma convection (e.g., Paterson, 1989). These NE–SW plunging magnetic lineations may provide a record of the early Late Jurassic NE–SW regional extension.

5.2.2 Fabrics of Jurassic granitic plutons

The Early Jurassic regional tectonic information is still not available from the fabrics of the granitic plutons due to overprinting of the fabrics in the Jiumen pluton by the later intrusion of the Jianchang pluton. Nevertheless, considerable effort has been devoted to the fabric study on numerous Late Jurassic plutons in the Yanshan belt and Jiaodong peninsula (Table 3; Lin et al., 2021). Similar to the Jianchang pluton, several contemporaneous granitic plutons are mainly composed of isotropic granite without observable planar and linear fabrics at outcrops (e.g., Siganding pluton, Luanjiahe pluton, and Wendeng pluton; Table 3). Several Late Jurassic plutons have been greatly overprinted by the NW–SE directed detachment faulting of the Early Cretaceous MCCs (e.g., the Yiwulüshan, Linglong, and Queshan plutons; Wang, 2013; Lin et al., 2013a, 2013b; Meng and Lin, 2021; Lin et al., 2021). The syn-tectonic Kunyushan pluton exhibits the margin-parallel gneissic to mylonitic foliation with a locally NE–SW subhorizontal mineral and stretching lineation in its northern margin (Meng and Lin, 2021). The AMS measurement suggests that the syn-emplacement fabrics of these Late Jurassic plutons possess mainly margin-parallel or concentric magnetic foliation patterns, exhibiting a dome-like geometry (Lin et al., 2021; Table 3). The lineations in the plutons exhibit variable orientations and plunges without any correlation with the regional strain (e.g., Paterson, 1989). Together with NE–SW striking mineral and stretching lineations in the ductile shear zone in the northern margin of the Kuyushan pluton, the consistent NE–SW magnetic lineations in several plutons (e.g., the Jianchang, Siganding, Kuyushan, Luanjiahe, and Wendeng plutons) were considered to have recorded the early Late Jurassic NE–SW regional extension in the northeastern part of the NCC (Lin et al., 2021; Table 3).

5.2.3 Fabrics of the Early Cretaceous granitic plutons

During the Early Cretaceous, MCCs are well developed in the NCC (Lin and Wei, 2018 and references therein). Within the Yunmengshan MCC, the fabrics of the Early Cretaceous

Yunmengshan pluton were overprinted by the NW–SE directed Shuiyu detachment faulting (Wang, 2013). The syn-tectonic Gudaoling, Yinmawanshan, Congjia, and Guojialing plutons emplaced into the core of the South Liaoning and Linglong MCCs in the Liaodong and Jiaodong Peninsulas (Charles et al., 2011; 2012). The fabrics of these Early Cretaceous plutons within the core of the MCCs are consistent with the mylonitic ones in the ductile shear zones. The magnetic, mineral and stretching lineations record the Early Cretaceous NW–SE regional extension (Lin et al., 2021; Table 3). Besides, numerous Early Cretaceous granitic plutons without observable planar and linear fabrics at outcrops are distributed in the NCC. The AMS measurement suggests that these isotropic granitic plutons present almost margin-parallel or concentric magnetic foliation patterns with a dome-like geometry (Lin et al., 2021; Table 3). Most of these isotropic plutons, exhibiting highly scattered magnetic lineations, were not influenced by the regional strain. However, the consistency of the NW–SE magnetic lineations in the Wang'anzhen and Aishan plutons suggests that they record the Early Cretaceous NW–SE regional extension (Lin et al., 2021; Table 3).

6. Discussion

A general review and synthesis of available data concerning strata and unconformities, tectonic deformation, and magmatism enable us to establish a detailed Jurassic–Early Cretaceous tectonostratigraphic framework of the NCC (Fig. 13). Integrating all structural elements with associated kinematics, and geochemistry and fabric data of igneous rocks into a coherent tectonostratigraphic framework, we propose a four-stage tectonic evolutionary model to delineate the process of Jurassic–Early Cretaceous (Yanshanian) intracontinental orogeny in the NCC (Figs. 14–16). Accordingly, the geodynamic relationships of the episodic intracontinental deformation with variable plate subduction/collision settings at different active boundaries in East Asia are discussed. The results provide a significant example of polyphase intra-plate deformation and magmtism paradigm in response to intracontinental orogeny with variable plate-boundary dynamics.

6.1 The Early–early Middle Jurassic (~200-170 Ma): N-S extension related to the post-orogenic extension between the North China Craton and the South China Block

In the NCC, an ongoing debate concerns the Early–early Middle Jurassic tectonic setting. The Late Triassic–Early Jurassic compressional setting has been proposed to account for the unconformity between the Triassic and Lower Jurassic strata. The Xingshikou conglomerate was considered to represent the Lower Jurassic syn-tectonic molasse in a flexural basin (Zhao, 1990; Liu et al., 2007; Liu et al., 2012; Li et al., 2016a). However, the Xingshikou Formation, which has been assigned to Upper Triassic, is in disconformable contact with the overlying Lower Jurassic strata (Yang et al., 2006; Meng et al., 2014, 2019). Sedimentary studies argue that the NCC was under a Late Triassic–early Middle Jurassic extensional tectonic setting, in view of the fining- and deepening-upward depositional associations containing abundant volcanic rocks (Meng et al., 2014, 2019). The Lower–lower Middle Jurassic coal-bearing strata (~200–170 Ma) contain abundant mafic volcanic rocks in the Nandaling and Xinglonggou Formations ($J_{1-2}n/J_1x$) in the Yanshan belt and the Anyao Formation (J_1a) in the Jiyuan region (Fig. 13). Moreover, numerous E–W striking brittle normal faults with N–S oriented striations on the fault plane in the Yinshan belt as well as the Ordos basin and its adjacent areas (Fig. 14a; Darby et al., 2001; Ritts et al., 2001; Li et al., 2004, 2015; Zhang et al., 2011). Therefore, it is reasonable to infer that the NCC was under a N–S regional extension during the period of the Early–early Middle Jurassic (~200-170 Ma), giving rise to rift basins that are filled with coal-bearing strata containing mafic volcanic rocks.

To the north of the NCC, the closure of the Paleo-Asian Ocean occurred in the late Devonian (Xu et al., 2013; Zhao et al., 2013) or the late Permian to Early Triassic (Chen et al., 2000; Jan et al., 2008; Li, 2006; Lin et al., 2008; Xiao et al., 2003, 2015). In the south, the deep continental subduction between the NCC and SCB occurred during the Triassic, giving rise to the Late Triassic Dabie-Sulu HP–UHP orogenic belt (e.g., Mattauer et al. 1985; Faure et al., 1999, 2003; Hacker et al., 2000; Ratschbacher et al., 2003; Lin et al., 2005, 2009; Li et al., 2017; Fig. 1). The onset of subduction of the PPP was considered to occur in the Early Jurassic at least, as evidenced by the occurrence of the Early Jurassic calc-alkaline igneous rocks and accretionary complexes in the East Asian continental margin (e.g., in Northeast China and Korean Peninsula; Wu et al., 2007; Guo et al., 2015; Tang et al., 2018; Wang et al., 2019; Li et al., 2020). It was proposed that the NCC was under an Early Jurassic WNW-directed initial PPP subduction-related or back-arc extensional setting, generating the Early Jurassic adakite-like igneous rocks (Wu et al. 2005, 2019; Zhu et al., 2018; Hao et al., 2020). However, the E–W striking bimodal volcanic zone (~250 km long and ~40 km wide, ages at ~190–165 Ma) with voluminous rhyolitic and basaltic rocks is only distributed in the Nanling Range of the SCB interior (He et al., 2010; Yu et al., 2010; Fig. 15a). The basalt–gabbro–syenite–granite rock suite, not metasomatized by the subduction-related fluids, was considered to occur in a post-orogenic extensional setting in the SCB interior (Li et al., 2007b; Li et al., 2021). Furthermore, both the Early–early Middle Jurassic volcanics and granitoids are mainly distributed in the southern and northern margins of the NCC (Zhang, 2007; Fig. 14a). Together with the widely distributed N–S extensional normal faults, we suggest that the N–S extension in the NCC is more likely to be related to the post-orogenic extension after the deep continental subduction of the SCB beneath the NCC (Fig. 15a). The initial high-angle subduction of the PPP, if there was, could not influence the NCC interior. The Early Jurassic adakite-like rocks were likely related to the pre-existing subducted paleo-oceanic slab (Guo et al., 2007; Wang et al., 2007; Yang and Li, 2008).

6.2 The late Middle Jurassic–earliest Cretaceous (~170–135 Ma): two-stage compression with a latest Middle–early Late Jurassic (~165–150 Ma) local extension

Albeit a consensus suggests that the NCC experienced a compression-dominated episode during the Middle Jurassic–earliest Cretaceous (Davis et al., 2001; Zhang et al., 2014; Dong et al., 2015; Li et al., 2016), a clear tectonic process has not been established yet. One group of researchers considers that the NCC underwent a tectonic process characterized by alternating contractional and extensional deformation during the Middle Jurassic–earliest Cretaceous (e.g., Davis et al., 2001, 2009; Zhang et al., 2011; Faure et al., 2012; Wang et al., 2017). Alternatively, another group proposes that the NCC experienced multi-directed compressions under the East Asian multi-plate convergent tectonic system during this Middle Jurassic–earliest Cretaceous period (e.g., Dong et al., 2015; Zhang et al., 2022). The extensional episode has been not considered by the latter. Integrating all structural elements and associated kinematics into a well-established tectonostratigraphic framework, we present a clear tectono-magmatic process during the late Middle Jurassic–earliest Cretaceous (~170–135 Ma), characterized by a two-stage compression with the latest Middle–early Late Jurassic (~165–150 Ma) local extension, and related dynamic origins.

6.2.1. The late Middle Jurassic (~170–160 Ma): N–S compression in response to the far-field compression related to the closure of the Mongol–Okhotsk Ocean

The late Middle Jurassic N–S compressional event (i.e., Event A of Yanshanian orogeny) is well recorded by the unconformity above the coal-bearing strata and the upper Middle Jurassic syn-tectonic conglomerates and sandstones (Fig. 13). The N–S directed fold-thrusts were mainly localized in the northern NCC (Fig. 14b), e.g., the E–ENE striking fold-thrust belts in the Yinshan–Yanshan belt. The syn-tectonic Longmen and Jiulongshan Formations (J_2l-J_2j) and their counterparts could locally fill into the flexural basins and/or piggy-back basins in the front or back of the fold-thrusts (Figs. 4–8). The duration of Event A of Yanshanian orogeny has been constrained to the period of post-Yaopo Formation (J_2yp) and its counterparts, to the depositional period of the syn-tectonic Longmen and Jiulongshan Formations (J_2l-J_2j) and their counterparts, i.e., ~170–160 Ma (Fig. 13). In the SCB, the contemporaneous late Middle Jurassic compressional deformation was absent, presenting that the Middle to Late Triassic NW- or NWW- striking intracontinental compressional deformation was overprinted by the Late Jurassic NE- striking thrusts and fault-related folds (Chu et al., 2012a, 2012b, 2018, 2019; Li et al., 2016b, 2021). To the north of the NCC, it is generally accepted that the MOO closed progressively from west to east during the Jurassic–Early Cretaceous (Zorin, 1999; Kravchinsky et al., 2002; Metelkin et al., 2010). Although the WNW-directed subduction of the PPP has been considered to be responsible for Event A of the Yanshanian orogeny (e.g., Zhu et al., 2018; Hao et al., 2020), it is incompatible with the N–S directed fold-thrusts developed in the northern NCC. Therefore, the far-field compression related to the closure of the MOO can be considered as the best explanation for this N–S compression during Event A of the Yanshanian orogeny in the northern NCC (Fig. 15b).

6.2.2. The Late Jurassic–earliest Cretaceous (~160–135 Ma): large-scale NW–SE compression in response to the flat slab subduction of the Paleo-Pacific Plate

The Late Jurassic–earliest Cretaceous mainly NW–SE compressional event (i.e., Event B of the Yanshanian orogeny) is well illustrated by the syn-tectonic deposition (the Tuchengzi Formation and its counterparts) and the unconformity above them (Fig. 13). The NW–SE directed fold-thrust belts are developed throughout the NCC (Fig. 14d). In the Yanshan belt, numerous NE- to NNE- striking faults and fault-related folds have formed to accommodate a NW–SE shortening (Davis et al., 2001; Zhang et al., 2002; Li et al., 2016a; Liu et al., 2020; Su et al., 2020). The pre-existing E-striking late Middle Jurassic Gubeikou-Pingquan fault and Miyun-Xifengkou fault in the Yanshan belt are considered to have experienced dextral strike-slip displacement due to this oblique NW–SE compression (Faure et al., 2012; Lin et al., 2019). In western Daqingshan, and the Ningwu-Jingle and Yungang basins, the late Middle Jurassic high-angle N–S directed thrusts were overprinted by the younger NW–SE directed thrusts indicated by the superimposed N–S and NW–SE trending striations, and the vertically superimposed syn-tectonic conglomerates (e.g., the Changhangou (J_2c) and Daqingshan (J_3d) Formations, and the Yungang (J_2yg) and Tianchihe Formations (J_3tc); Wang et al., 2017; Chen et al., 2019; Figs. 13 and 14d). Large-scale low-angle thin-skinned thrusts recorded a NW–SE compression in eastern Daqingshan (Gong et al., 2015; Fig.14d). Furthermore, the contemporaneous NW–SE directed thrusts were widely developed in western Ordos, Helanshan, Zhuozishan, and Langshan (Darby and Ritts, 2002; Huang, et al., 2015; Yang and Dong, 2018; Li et al., 2022). The NW–SE compression had influenced the western margin of the NCC, indicated by the NW–SE striking fault-slip vectors in Helanshan (Huang, et al., 2015; Yang and Dong, 2018, 2020; Li et al., 2022). In the front or back of these fold-thrusts, the syn-tectonic Tuchengzi Formation (J_3-K_1tch) and its counterparts could fill into the flexural basins and/or piggy-back basins (Figs. 4–8). The duration of Event B of the Yanshanian orogeny has also been well constrained to the period of the depositional period of the syn-tectonic Tuchengzi Formation (J_3-K_1tch) and its counterparts, to pre-Zhangjiakou Formation (K_1zh) and its counterparts (Fig. 13; ~160–135 Ma in the western NCC and ~155–135 Ma in the eastern NCC). Besides, as a Late Triassic syn-orogenic transform fault, the Tan-Lu fault reactivated as a thoroughgoing sinistral strike-slip fault and offset the NCC during the earliest Cretaceous (143–137 Ma; Zhu et al., 2018). The Late Triassic Xingcheng-Taili ductile shear zone adjacent to the Tan-Lu fault reactivated during the Late Jurassic–earliest Cretaceous (~152–139 Ma; Liang et al., 2015, 2022). During the Late Jurassic, the NNW-directed low-angle flat slab subduction of the PPP occurred in the eastern margin of the NCC (Wu et al., 2019). Considering the widely distributed NE striking thrusts and fault-related folds in the SCB under this Late Jurassic–earliest Cretaceous NW–SE compression (Lin et al., 2000, 2008; Li et al., 2016b; Li et al., 2021), this large-scale NW–SE compression in the NCC could be a consequence of the flat slab subduction of the PPP beneath the East Asian continent (Fig. 15d). Due to the contemporaneous south-directed Sihetang ductile zone locally developed in the Yanshan belt (Davis et al., 2001; Zhu et al., 2015), it was also proposed that the united action, imposed by far-field compression related to the closure of the MOO and the PPP subduction, controlled Event B of the Yanshanian orogeny (Zhu et al., 2018). We suggest that the large-scale NW–SE compression dominated by the flat slab subduction of the PPP had significantly influenced the entire NCC, according to the widely developed NW–SE directed fold-thrust belts throughout the NCC (Fig. 15d).

6.2.3. The latest Middle–early Late Jurassic (~165–150 Ma): local NE–SW extension related to tectonic transition from the N–S closure of the Mongol–Okhotsk Ocean to the NNW-directed subduction of Paleo-Pacific Plate

Generally, in the western NCC, the late Middle Jurassic (~170–160 Ma) N–S compression related to the closure of the MOO was immediately followed by the Late Jurassic–earliest Cretaceous (~160–135 Ma) NW–SE compression in response to the subduction of the PPP (Figs. 13 and 15). It is characterized by two sequences of superimposed syn-tectonic conglomerates (e.g., the Changhangou (J_2c) and Daqingshan (J_3d) Formations, and the Yungang (J_2yg) and Tianchihe Formations (J_3tc); Figs. 3 and 13). However, in the eastern NCC, the early Late Jurassic (~164–152 Ma) volcanic and pyroclastic rocks (Tiaojishan/Lanqi Formation (J_3t/J_3l) and coeval intrusive rocks are distributed in the northern Taihangshan, the Yanshan belt, the southern Yanbian area, the Liaodong peninsula, the Jiaodong peninsula, and the Bengbu area (Figs. 2 and 14c). These rocks are mainly adakites derived from partial melting of the low crust and the subcontinental lithospheric mantle metasomatized by earlier subduction slab-derived fluids (Zhang et al., 2004b; Zhang, 2007; Zhang et al., 2010). The brittle normal faults are widely distributed in the volcanic strata in the Yanshan belt where part of these normal faults bound the small-scale rift basin (Davis et al., 2001, 2009; Qi et al., 2015; Lin et al., 2018; Fig. 14c). A top-to-the-NE detachment ductile shear zone was initially formed during Late Jurassic (~156–150 Ma) NE–SW extension before the nucleation of the Early Cretaceous Kalaqin MCC (Lin et al., 2014; Fig. 14c). By the fabric studies of granitic plutons, the consistent NE–SW trending magnetic lineations also recorded the early Late Jurassic NE–SW extension in the northeast part of the NCC (e.g., the Jianchang, Siganding, Kuyushan, Luanjiahe, and Wendeng plutons; Table 3, Fig. 14c). However, the latest Middle–early Late Jurassic (~165–150 Ma) NE–SW extension and magmatism only occurred in the northeastern part of the NCC. The contemporaneous magmatism extended from the northeastern part of the NCC to Northeast China and its adjacent areas. A suite of Late Jurassic igneous rocks (~161–156 Ma) was also developed in the Erguna and Great Xing’an Ranges far away from the continental margins, e.g., eastern NE China, Russian Far East, Japan, and Korea Peninsula (Zhang et al., 2022; Fig. 15c). The Late Jurassic extension and magmatism mainly occurred in the transition zone between the Paleo-Pacific domain and the Mongol–Okhotsk domain. In the SCB, Late Jurassic roughly N–S extension, and contemporaneous granites and bimodal volcanic rocks only distributed in the Nanling tectonic belt and its adjacent areas were considered to be related to slab tearing of the NNW-directed subducted PPP (Shu et al., 2007; Li et al., 2021; Fig. 15c). The NNW-directed low-angle flat slab subduction of the PPP could have gradually influenced the NCC interior during the latest Middle–early Late Jurassic. It has been proposed that the NCC was in a back-arc extensional setting related to the PPP subduction during the Late Jurassic (Zhu et al., 2018). Given the widely large-scale NW–SE compression in the western NCC, we suggest that this latest Middle–early Late Jurassic local NE–SW extension in the northeast part of the NCC, probably extending to Northeast China, should be related to the tectonic transition from the closure of the MOO to the PPP subduction (Fig. 15c).

6.3 The Early Cretaceous (135–115 Ma): large-scale NW–SE extension related to the slab rollback of the Paleo-Pacific Plate

The Early Cretaceous large-scale crustal extension is one of the most pronounced characteristics in East Asia, expressed by MCCs, magmatism, graben or half-graben basins in a vast area extending more than 4000 km, from Transbaikalia, through the NCC, to the SCB (Wang et al., 2011; Li et al., 2014b; Zhang et al., 2014, Wang et al., 2011; Lin and Wei, 2018; Fig.16). The MCCs and syn-tectonic magmatic domes in East Asia with consistent NW–SE extensional direction occurred during a relatively narrow time span (131–118 Ma), e.g., the Hohhot, Yunmengshan, Kalaqin, Yiwulüshan, Xiuyan, South Liaoning, Linglong, Queshan, Jiaonan and Xiaoqinling MCCs in the NCC (e.g., Wang et al., 2011; Lin and Wei, 2018; Fig. 16). Coeval with the MCCs and extensional basins, a vast plutonic-volcanic flare-up occurred (e.g., Zhang et al., 2014; Wu et al., 2019; Fig. 16). The Early Cretaceous magmatic rocks, ranging in age from 135 to 115 Ma with a peak at ca. 132–125 Ma, were derived from multiple sources, e.g., depleted mantle, enriched lithospheric mantle, ancient lower crust, and juvenile crust (Yang et al. 2004; Wu et al., 2019). The consistent NW–SE trending magnetic lineations in numerous granitic plutons also recorded the Early Cretaceous NW–SE extension (Table 3). Multi-plate convergence (i.e., the closure of the MOO, the subduction of the PPP, and the closure of the BNO) occurred in the East

Asia continent during the Jurassic to the Early Cretaceous (Dong et al., 2015; Fig. 16). The large-scale NW–SE compression related to the NNW-directed flat slab subduction of the PPP had influenced the north of the NCC during the earliest Cretaceous (Fig. 15d). In the southeast, as the slab rollback of the PPP during the Early Cretaceous, it triggered lithospheric removal or delamination, and thinning of the NCC (Liu et al., 2016; Lin and Wei, 2018; Wu et al., 2019). Meanwhile, the wide rift could have occurred due to the southeastward stress relaxation of the NW–SE convergent East Asian continent (Fig. 16). It resulted in the formation of the MCCs and graben or half-graben basins (Wang et al., 2011; Lin and Wei, 2018), extensive magmatism with extremely variable rock types and chemical compositions (Wu et al., 2005), and replacement of the thick (~200 km) Archean lithospheric mantle beneath the eastern NCC to a thin (< 80 km) juvenile one (Wu et al., 2019).

7 Conclusions

Synthesizing available data concerning strata and unconformities, tectonic deformation, and magmatism, a clear four-stage tectonic evolution of the NCC during the Jurassic-Early Cretaceous is proposed, providing new insights into the Yanshanian intracontinental orogeny in East Asia, from which we draw four main conclusions.

1. The N–S extension related to the post-orogenic extension after the deep continent subduction of the SCB beneath the NCC, characterized by the E–W striking brittle normal faults in the Lower–lower Middle Jurassic strata, and the magmatism along the southern and northern margins of the NCC, occurred during the Early–early Middle Jurassic (~200–170 Ma);

2. Two-stage compression, corresponding to Events A and B of the Yanshanian orogeny, was well evidenced by the unconformity above the Lower–lower Middle Jurassic strata and the upper Middle Jurassic syn-tectonic deposition, and the Upper Jurassic–lowermost Cretaceous syn-tectonic deposition and the unconformity above, respectively. These syn-tectonic deposits could be deposited in the flexural basins and/or piggy-back basins in the front or back of the fold-thrusts. The late Middle Jurassic (~170–160 Ma) N–S compression (i.e., Event A of the Yanshanian orogeny) occurred in the northern NCC in response to the far-field compression related to the closure of the MOO. The Late Jurassic–earliest Cretaceous (~160–135 Ma) NW–SE compression (i.e., Event B of the Yanshanian orogeny) in response to the flat slab subduction of the PPP had affected the entire NCC;

3. The latest Middle–early Late Jurassic (~165–150 Ma) local NE–SW extension, characterized by ductile and brittle normal faults and magnetic lineations in granitic plutons, and magmatism that extended to Northeast China and its adjacent areas, occurred in the northeastern part of the NCC. It could be related to the tectonic transition from the N–S closure of the MOO to the NNW-directed PPP subduction;

4. The Early Cretaceous (~135–115 Ma) large-scale NW–SE crustal extension in East Asia should be a consequence of the lithospheric removal or delamination and thinning, and the formation of the wide rift due to the southeastward stress relaxation of the NW–SE convergent East Asian continent as the slab rollback of the PPP.

Our study shows a new example of polyphase intra-plate deformation and magmtism paradigm in response to intracontinental orogeny with variable plate-boundary dynamics.

Acknowledgments

This work has been financially supported by the National Natural Science Foundation of China (91855212, 91755205, and 41472193). Dr. Zhiheng Ren, Dr. Lingtong Meng, and Dr. Jipei Zeng are acknowledged for their help in the field work. Prof. Franz Neubauer and two anonymous reviewers together with the editor Tim Kusky are thanked very much for their constructive comments and suggestions, which lead to a significant improvement of our manuscript.

References

Archanjo, C. J., Launeau, P., Bouchez, J. L., 1994. Magnetic fabrics vs. magnetite and biotite shape fabrics of the magnetite-bearing granite pluton of Gameleiras (Northeast Brazil). Physics of the Earth and Planetary Interiors 89(1–2), 63–75. https://doi.org/10.1016/0031- 9201(94)02997-P

BGMNM (Bureau of Geology and Mineral Resources of the Nei Mongol Autonomous Region), 1983. Geological map of the Nei Mongol Autonomous Region, People's Republic of China (Tumute Youqi sheet): Nei Mongol Geological Bureau, scale 1:200 000.

BGMH (Bureau of Geology and Mineral Resources of Hebei Province BGMH), 1989. Regional geology of Hebei Province. In: Beijing Municipality and Tianjin Municipality (in Chinese). Geological Publishing House, Beijing.

BGML (Bureau of Geology and Mineral Resources of Liaoning Province BGML), 1989. The Geological Report of the People's Republic of China Ministry of Geology and Mineral Resources, Part One, Regional Geology, No. Fourteenth, Regional Geology of Liaoning Province (in Chinese). Geological Publishing House, Beijing.

Bouchez, J.L., Gleizes, G., 1995. Two-stage deformation of the Mount-Louis-Andorra granite pluton (Variscan Pyrenees) inferred from magnetic susceptibility anisotropy. Journal of the Geological Society 152 (4), 669–679. https://doi.org/10.1144/gsjgs.152.4.0669

Bouchez, J.L., Hutton, D., Stephens, W.E., 1997. Granite is Never Isotropic: An Introduction to AMS Studies of Granitic Rocks. Granite: From Segregation of Melt to Emplacement Fabrics, pp. 95–112. Paris: Springer Science and Business Media. https://doi.org/10.1007/978-94-017-1717-5_6

Chang, S.C., Zhang, H., Hemming, S.R., Mesko, G.T., Fang, Y., 2014. $^{40}Ar/^{39}Ar$ age constraints on the Haifanggou and Lanqi Formations: When did the first flowers bloom, in Jourdan, F., Mark, D.F., and Verati, C., eds., Advances in $^{40}Ar/^{39}Ar$ Dating: From Archaeology to Planetary Sciences: Geological Society of London, Special Publications 378, 277–284, https://doi .org/10.1144/SP378.1

Charles, N., Gumiaux, C., Augier, R., Chen, Y., Zhu, R.X., Lin, W, 2011. Metamorphic core complexes vs. synkinematic plutons in continental extension setting: Insights from key structures (Shandong Province, eastern China). Journal of Asian Earth Science 40, 261–278.

Charles, N., Gumiaux, C., Augier, R., Chen, Y., Faure, M., Lin, W., Zhu, R.X., 2012. Metamorphic core complex dynamics and structural development: Field evidences from the Liaodong Peninsula (China, East Asia). Tectonophysics 560-561, 22–50

Chen, A., 1998. Geometric and kinematic evolution of basement-cored structures: intraplate orogenesis within the Yanshan orogen, northern China. Tectonophysics 292(1), 17-42. https://doi.org/10.1016/S0040-1951(98)00062-6

Chen, B., Jahn, B. M., Wilde, S., Xu, B., 2000. Two contrasting Paleozoic magmatic belts in northern Inner Mongolia, China: Petrogenesis and tectonic implications. Tectonophysics 328(1), 157–182. https://doi.org/10.1016/S0040-1951(00)00182-7

Chen, H.Y., Zhang, Y.Q., Zhang, J.D., Fan, Y.G., Peng, Q.P., Lian, Q., Sun, L.P., Yu, L., 2014. LA-ICP-MS zircon U-Pb age and geochemical characteristics of tuff of Jiulongshan Formation from Chengde Basin, northern Hebei (in Chinese with English abstract). Geological Bulletin of China 33, 7, 966–973.

Chen, H.Y., Zhang, Y.Q., Liu, B.B., Peng, Q.P., 2015. Sedimentary characteristics and stratigraphic age of Xingshikou Formation in Chengde Basin of Northern Hebei (in Chinese with English Abstract). Geological Survey of China 2, 31–34.

Chen, X., Jiangyu, L.I., Dong, S., Shi, W., Bai, Y., Zhang, Y., Ding, W., 2019. Tectonic deformation of Jurassic Ningwu-Jingle basin and its implication for the beginning of Yanshanian orogeny in central North China Craton. Geotectonica et Metallogenia 43(3), 389-408.

Chen, Y.X., Chen, W.J., Zhou, X.H., Li, Z.J., Liang, H.D., Li, Q., Xu, K., Fan, Q.C., Zhang, G.H., Wang, F., Wang, Y., Zhou, S.Q., Chen, S.H., Hu, B., Wang, Q.J., 1997. Liaoxi and Adjacent Mesozoic Volcanic Rocks: Chronology, Geochemistry and Tectonic Settings (in Chinese with English abstract): Beijing, China, The Seismological Press.

Cheng, Y., Gao, R., Lu, Z., Li, W., Su, H., Han, R., Chen, H., 2022. Meso-Cenozoic Tectonic Evolution of the Kexueshan Basin, Northwestern Ordos, China: Evidence from Paleo-Tectonic Stress Fields Analyses. Frontiers in Earth Science 10, 1-19.

Chu, Y., Faure, M., Lin, W., Wang, Q., 2012a. Early Mesozoic tectonics of the South China block: Insights from the Xuefengshan intracontinental orogen. Journal of Asian Earth Sciences 61, 199–220.

Chu, Y., Faure, M., Lin, W., Wang, Q., Ji, W., 2012b. Tectonics of the Middle Triassic intracontinental Xuefengshan Belt, South China: New insights from structural and chronological constraints on the basal décollement zone. International Journal of Earth Sciences 101(8), 2125–2150.

Chu, Y., Lin, W., 2018. Strain analysis of the Xuefengshan Belt, South China: From internal strain variation to formation of the orogenic curvature. Journal of Structural Geology 116, 131–145.

Chu, Y., Lin, W., Faure, M., Xue, Z., Ji, W., Feng, Z., 2019. Cretaceous episodic extension in the South China Block, East Asia: Evidence from the Yuechengling Massif of central South China. Tectonics 38. https://doi.org/10.1029/2019TC005516

Cogné, J.P., Kravchinsky, V.A., Halim, N., Hankard, F., 2005. Late Jurassic–Early Cretaceous closure of the Mongol–Okhotsk Ocean demonstrated by new Mesozoic palaeomagnetic results from the Trans-Baikal area (SE Siberia). Geophysical Journal International 163, 813–832.

Cope, T.D., 2003. Sedimentary Evolution of the Yanshan Fold-Thrust Belt, Northeast China. Ph. D Dissertation, Stanford University, pp. 1–230.

Cope, T., 2017. Phanerozoic magmatic tempos of North China. Earth and Planetary Science Letters 468, 1–10.

Cope, T.D., Shultz, M.R., Graham, S.A., 2007. Detrital record of Mesozoic shortening in the Yanshan belt, NE China: testing structural interpretations with basin analysis. Basin Research 19(2), 253-272.

Cui, F. H., 2015. Petrogenesis of Mesozoic granitoids and crustal evolution in Xingcheng area, western Liaoning Province. Ph. D Thesis, Jilin University, pp. 1-152.

Darby, B.J., Davis, G.A., Zheng, Y.D., 2001. Structural evolution of the southwestern Daqing Shan, Yinshan belt, Inner Mongolia, China, in Hendrix, M.S., & Davis, G.A., eds., Paleozoic and Mesozoic tectonic evolution of central Asia: From continental assembly to intracontinental deformation, Boulder, Colorado. Geological Society of America Memoir 194, 199–214.

Darby, B. J., Ritts, B. D., 2002. Mesozoic contractional deformation in the middle of the Asian tectonic collage: the intraplate Western Ordos fold–thrust belt, China. Earth and Planetary Science Letters 205(1-2), 13–24. https://doi.org/10.1016/s0012-821x(02)01026-9

Darby, B. J., Ritts, B. D., 2007. Mesozoic structural architecture of the Lang Shan, North-Central China: Intraplate contraction, extension, and synorogenic sedimentation. Journal of Structural Geology 29(12), 2006–2016. https://doi.org/10.1016/j.jsg.2007.06.011

Davis, G.A., Darby, B.J., 2010. Early Cretaceous overprinting of the Mesozoic Daqing Shan fold-and-thrust belt by the Hohhot metamorphic core complex, Inner Mongolia, China. Geoscience Frontiers 1(1), 1-20.

Davis, G. A., Meng, J. F., Cao, W. R., 2009. Triassic and Jurassic tectonics in the eastern Yanshan belt, North China: insights from the controversial Dengzhangzi Formation and its neighboring units. Earth Science Frontiers 16 (3), 69–86. https://doi.org/10.1016/S1872-5791(08)60090-1

Davis, G. A., Zheng, Y. D., Wang, C., 2001. Mesozoic tectonic evolution of the Yanshan fold and thrust belt, with emphasis on Hebei and Liaoning provinces, northern China. In: Hendrix, M.S., Davis, G.A. (Eds.), Paleozoic and Mesozoic tectonic evolution of central Asia: From continental assembly to intracontinental deformation, Boulder, Colorado. Geological Society of America Memoir 194, 171–197.

Dong, S., Zhang, Y., Zhang, F., Cui, J., Chen, X., Zhang, S., Miao, L., Li, J., Shi, W., Li, Z., Huang, S., Li, H., 2015. Late Jurassic–Early Cretaceous continental convergence and intracontinental orogenesis in East Asia: a synthesis of the Yanshan revolution. Journal of Asian Earth Sciences 114, 750–770. https://doi.org/10.1016/j.jseaes.2015.08.011

Enkin, R.J., Yang, Z., Chen, Y, Courtillot, V., 1992. Paleomagnetic constraints on the geodynamic history of the major blocks of China from the Permian to the present. Journal of Geophysical Research Solid Earth 97(B10), 13953–13989.

Faure, M., Lin, W., Chen, Y., 2012. Is the Jurassic (Yanshanian) intraplate tectonics of North China due to westward indentation of the NCC? Terra Nova 24 (6), 456–466. https://doi.org/10.1111/ter.12002

Faure, M., Lin, W., Scharer, U., Shu, L., Sun, Y., Arnaud, N., 2003. Continental subduction and exhumation of UHP rocks. Structural and geochronological insights from the Dabieshan (East China). Lithos 70(3), 213-241.

Faure, M., Lin, W., Shu, L., Sun, Y., Scharer, U., 1999. Tectonics of the Dabieshan (eastern China) and possible exhumation mechanism of ultra high-pressure rocks. Terra Nova 11(6), 251-258.

Faure, M., Trap, P., Lin, W., Monié, P., Bruguier, O., 2007. Polyorogenic evolution of the Paleoproterozoic Trans-North China Belt, new insights from the in Lüliangshan-Hengshan-Wutaishan and Fuping massifs. Episodes Journal of International Geoscience, Seoul National University 30 (2), 95–106.

Feng, Q., 2021. Structural characteristics and evolution, and hydrocarbon occurrence of the south-central segment of the western Ordos Basin (in Chinese with English abstract). Dissertation for Master Degree. Xi’an: Northwest University. 1–87.

Fu, Z. B., Zhao, Y., Liu, J. L., Zhang, S. H., Gao, H. L., 2018. Revisiting of the Yanshanian basins in western and northern Beijing, North China. Journal of Asian Earth Sciences 163, 90–107. https://doi.org/10.1016/j.jseaes.2018.05.016

Gao, H-L., Zhao, Y., Ye, H., Zhang, S-H., Liu, J., Wang, G-C., 2018. Dating Jurassic volcanic rocks in the Western Hills of Beijing, North China: implications for the initiation of the Yanshanian tectonism and subsequent thermal events. Journal of Asian Earth Sciences 161, 164-177. https://doi.org/10.1016/j.jseaes. 2018.05.008

Ge, Y.H., Sun, C.L., Wang, Y.F., 2010. The flora from Zhaogou Formation in Shiguai basin, Inner Mongolia and the geological age (in Chinese with English abstract). Global Geology 29, 175–182.

Gong, W., Hu, J., Chen, H., Li, Z., Qu, H., Yang, Y., 2015. Late Mesozoic tectonic evolution and kinematic mechanisms in the Daqing shan at the northern margin of the North China Craton. Journal of Asian Earth Sciences 114, 103-114. http://dx.doi.org/10.1016/j.jseaes.2015.07.016

Guo, F., Li, H.X., Fan, W.M., Li, J.Y., Zhao, L., Huang, M.W., Xu W.L., 2015. Early Jurassic subduction of the Paleo-Pacific Ocean in NE China: Petrologic and geochemical evidence from the Tumen mafic intrusive complex. Lithos 244–245, 46–60.

Guo, F., Fan, W.M., Li, X.Y., Li, C.W., 2007. Geochemistry of Mesozoic mafic volcanic rocks from the Yanshan belt in the northern margin of North China Block: relations with post-collisional lithospheric extension. In: Zhai, M., Windley, B.F., Kusky, T.M., Meng, Q. (Eds.), Mesozoic Sub-continental Lithospheric Thinning Under Eastern Asia. Geological Society, London, Special Publications 280, pp. 101–130.

Guo, J.F., Ma, Q., Xu, Y.G., Zheng, J.P., Zhou, Z.Y., Ma, L., Bai, X.J., 2022. Migration of Middle-Late Jurassic volcanism across the northern North China Craton in response to subduction of Paleo-Pacifc Plate. Tectonophysics 833, 229338. https://doi.org/10.1016/j.tecto.2022.229338

Guynn, J.H., Kapp, P., Pullen, A., Gehrels, G., Heizler, M., Ding, L., 2006. Tibetan basement rocks near Amdo reveal “missing” Mesozoic tectonism along the Bangong suture, central Tibet. Geology 34, 505–508.

Hacker, B.R., Ratschbacher, L., Webb, L., McWilliams, M.O., Ireland, T., Calvert, A., Dong, S., Wenk, H., Chateigner, D., 2000. Exhumation of ultrahigh-pressure continental crust in east central

China: Late Triassic-Early Jurassic tectonic unroofing. Journal of Geophysical Research: Solid Earth 105 (B6), 13339–13364. https://doi.org/10.1029/2000JB900039

Hao, W., Zhu, G., Zhu, R., 2019. Timing of the Yanshan Movement: evidence from the Jingxi Basin in the Yanshan fold-and-thrust belt, eastern China. International Journal of Earth Sciences 108(6), 1961-1978.

Hao, W., Zhu, R., Zhu, G., 2020. Jurassic tectonics of the eastern North China Craton: Response to initial subduction of the Paleo-Pacific Plate. Geological Society of America Bulletin 133(1-2), 19-36.

Hargraves, R. B., Johnson, D., Chan, C. Y., 1991. Distribution anisotropy: the cause of AMS in igneous rocks? Geophysical Research Letters 18(12), 2193–2196. https://doi.org/10.1029/91GL01777

He, Z.Y., Xu, X.S., Niu, Y.L., 2010. Petrogenesis and tectonic signifcance of a Mesozoic granite–syenite–gabbro association from inland South China. Lithos 119, 621–641.

He, X.F., Santosh, M., Ganguly, S., 2017. Mesozoic felsic volcanic rocks from the North China craton: Intraplate magmatism associated with craton destruction: Geological Society of America Bulletin, 129(7–8), 947–969. https://doi.org/10.1130/B31607.1

Huang, D.Y., 2019. Jurassic integrative stratigraphy and timescale of China. Science China Earth Sciences 62, 01, 227–259. https://doi.org/10.1007/s11430-017-9268-7

Huang, X., Shi, W., Chen, P., Li, H., 2015. Superposed deformation in the Helanshan Structural Belt: Implications for Mesozoic intracontinental deformation of the North China Plate. Journal of Asian Earth Sciences, 114, 140–154. https://doi.org/10.1016/j.jseaes.2015.05.027

Ji, W.B., Faure, M., Lin, W., Chen, Y., Chu Y., Xue Z.H., 2018. Multiple emplacement and exhumation history of the Late Mesozoic Dayunshan–Mufushan batholith in southeast China and its tectonic significance: 1. Structural analysis and geochronological constraints. Journal of Geophysical Research: Solid Earth 123, 689–710. https://doi.org/10.1002/2017JB014597

Jian, P., Liu, D., Kröner, A., Windley, B. F., Shi, Y., Zhang, F., Shi, G., et al., 2008. Time scale of an Early to Mid-Paleozoic orogenic cycle of the long-lived Central Asian Orogenic Belt, Inner Mongolia of China: implications for continental growth. Lithos 101, 233–259. https://doi.org/10.1016/j.lithos.2007.07.005

Jiao, R.C., He, J.R., Wang, R.R., W, Q.Q., Hui, G.J., 2016. LA–ICP–MS U-Pb dating of zircons from Tuchengzi Formation in Qianjiadian of North Beijing and its significance (in Chinese with English abstract). Geology in China 43 (5), 1750–1760.

Kapp, P., DeCelles, P.G., Gehrels, G.E., Heizler, M., Ding, L., 2007. Geological records of the Lhasa-Qiangtang and Indo-Asian collisions in the Nima area of central Tibet. Geological Society of America Bulletin 119, 917–933.

Kim, S.W., Kwon, S., Ko, K., Yi, K., Cho, D.L., Kee, W.S., Kim, B.C., 2015. Geochronological and geochemical implications of Early to Middle Jurassic continental adakitic arc magmatism in the Korean Peninsula. Lithos 227, 225–240.

Kravchinsky, V.A., Cogné, J.P., Harbert, W.P., Kuzmin, M.I., 2002. Evolution of the Mongol–Okhotsk Ocean as constrained by new palaeomagnetic data from the Mongol–Okhotsk suture zone, Siberia. Geophysical Journal International 148, 34–57.

Lan, T.G., Fan, H.R., Santosh, M., Hu, F.F., Yang, K.F., Yang, Y.H., Liu, Y.S., 2012. Early Jurassic high-K calc-alkaline and shoshonitic rocks from the Tongshi intrusive complex, eastern North China Craton: implication for crust–mantle interaction and post-collisional magmatism. Lithos 140–141, 183–199.

Lapierre, H., Jahn, B.M., Charvetc, J., Yu, Y.W., 1997. Mesozoic felsic arc magmatism and continental olivine tholeiites in Zhejiang Province and their relationship with the tectonic activity in southeastern China. Tectonophysics 274, 321-338.

Li, C., Wang, Z., Lü, Q., Tan, Y., Li, L., Tao, T., 2021. Mesozoic tectonic evolution of the eastern South China Block: A review on the synthesis of the regional deformation and magmatism. Ore Geology Reviews 131(4), 104028.

Li, C., Zhang, C., Cope, T. D., Lin, Y., 2016a. Out-of-sequence thrusting in polycyclic thrust belts: an example from the Mesozoic Yanshan belt, North China Craton. Tectonics 35, 2082–2116. https://doi.org/10.1002/2016TC004187

Li, H., Zhang, H., Qu, H., Cai, X., Wang, M., 2014a. Initiation, the First Stage of the Yanshan (Yenshan) in Western Hills. Constraints from Zircon U–Pb Movement Dating (in Chinese with English abstract). Geological Review 60(5), 1026-1042.

Li, J., Dong, S., Zhang, Y., Zhao, G., Johnston, S. T., Cui, J., Xin, Y., 2016b. New insights into Phanerozoic tectonics of South China: part 1, polyphase deformation in the Jiuling and Lianyunshan domains of the central Jiangnan orogen. Journal of Geophysical Research Solid Earth 121(4), 3048-3080. https://doi.org/10.1002/2015JB012778

Li, J. Y., 2006. Permian geodynamic setting of Northeast China and adjacent regions: closure of the Paleo-Asian Ocean and subduction of the Paleo-Pacific Plate. Journal of Asian Earth Sciences 26(3), 207–224. https://doi.org/10.1016/j.jseaes.2005.09.001

Li, M.J., Zheng, M.L., Cao, C.C., 2004. Evolution of superposed Jurassic and Cretaceous basins in Beishan-Alxa area (in Chinese with English abstract). Oil and Gas Geology 25(1), 54-57.

Li, S. Z., Kusky, T. M., Zhao, G., Wu, F., Liu, J. Z., Sun, M., Wang, L., 2007a. Mesozoic tectonics in the Eastern Block of the North China Craton: implications for subduction of the Pacific plate beneath the Eurasian plate. Geological Society London Special Publications 280(1), 171-188.

Li, S.Z., Jahn, B.M., Zhao, S.J., Dai, L.M., Li, X.Y., Suo, Y.H., Guo, L.L., Wang, Y.M., Liu, X.C., Lan, H.Y., Zhou, Z.Z., Zheng, Q.L., Wang, P.C., 2017. Triassic southeastward subduction of North China Craton to South China Block: insights from new geological, geophysical and geochemical data. Earth-Science Reviews 166, 270-285.

Li, S.Z., Zhao, G.C., Santosh, M., Liu, X., Dai, L.M., Suo, Y.H., Tam, P.Y., Song, M.C., Wang, P.C., 2012. Paleoproterozoic structural evolution of the southern segment of the Jiao-Liao-Ji Belt, North China Craton. Precambrian Research 200-203, 59-73. https://doi.org/10.1016/j.precamres.2012.01.007

Li, S.Z., Zhao, S.J., Liu, X., Cao, H.H., Yu, S., Li, X.Y., Somerville, I., Yu, S.Y., Suo, Y.H., 2018. Closure of the Proto-Tethys Ocean and Early Paleozoic amalgamation of microcontinental blocks in East Asia. Earth-Science Reviews 186, 37-75.

Li, S.M., Zhu, D.C., Wang, Q., Zhao, Z.D., Zhang, L.L., Liu, S.A., Chang, Q.S., Lu, Y.H., Dai, J.G., Zheng, Y.C., 2016d. Slab-derived adakites and subslab asthenosphere-derived OIB-type rocks at 156 ± 2 Ma from the north of Gerze, central Tibet: records of the Bangong-Nujiang oceanic ridge subduction during the Late Jurassic. Lithos 262, 456–469

Li, W., Jiang, D., Dong, Y., Zheng, Z., Zhao, J., Kang, W., Zhang, L., 2022. Mesozoic contractional deformation in central East Asia: Constraints from deformation and sedimentary record of the Helanshan fold and thrust belt, North China Craton. Gondwana Research 107, 235-255. https://doi.org/10.1016/j.gr.2022.03.011

Li, W.P., Lu, F.X., Li, X.H., Zhou, Y.Q., Sun, S.P., Li, J.Z., Zhang, D.G., 2001. Geochemical features and origin of volcanic rocks of Tiaojishan Formation in Western Hills of Beijing (in Chinese with English abstract). Acta Petrologica Et Mineralogica 20 (2), 123–133.

Li, X.H., Li, W.X., Li, Z.X., 2007b. On the genetic classifcation and tectonic implications of the Early Yanshanian granitoids in the Nanling Range, South China. Chinese Science Bulletin 52 (14), 1873–1885.

Li, Y., Xu, W. L., Zhu, R. X., Wang, F., Ge, W. C., Sorokin, A. A., 2019. Late Jurassic to early Early Cretaceous tectonic nature on the NE Asian continental margin: Constraints from Mesozoic accretionary complexes. Earth-Science Reviews 103042. https://doi.org/10.1016/j.earscirev.2019.103042

Li, Z. H., Dong, S. W., Qu, H. J., 2014b. Timing of the initiation of the Jurassic Yanshan movement on the North China Craton: evidence from sedimentary cycles, heavy minerals, geochemistry, and zircon U–Pb geochronology. International Geology Review 56(3), 288-312. https://doi.org/10.1080/00206814.2013.855013

Li, Z.H., Feng, S.B., Yuan, X.Q., Qu, H.J., 2014c. Chronology and its significance of the Lower Jurassic tuff in Ordos Basin and its periphery (in Chinese with English abstract). Oil and gas geology 35, 729-741.

Li, Z. H., Qu, H. J., Gong, W. B., 2015. Late Mesozoic basin development and tectonic setting of the northern North China Craton. Journal of Asian Earth Sciences 114, 115-139. https://doi.org/10.1016/j.jseaes.2015.05.029

Li, Z.H., Qu, H.J., Yang, Y.H., Gong, W.B., 2016c. Late Mesozoic sedimentary-volcanic filling record in Yungang basin and its tectonic implications (in Chinese with English abstract). Geology in China 43, 1481-1494.

Liang, C., Liu, Y., Neubauer, F., Jin, W., Zeng, Z., Genser, J., et al., 2015. Structural characteristics and LA–ICP-MS U–Pb zircon geochronology of the deformed granitic rocks from the Mesozoic Xingcheng-Taili ductile shear zone in the North China Craton. Tectonophysics 650, 80–103. https://doi.org/10.1016/j.tecto.2014.05.010

Liang, C., Neubauer, F., Liu, Y., Heberer, B., Genser, J., Dunkl, I., et al., 2022. Diachronous onset and polyphase cooling of the Taili-Yiwulüshan metamorphic core complex corridor, NE China, and its relationships to the formation of adjacent extensional basins. Gondwana Research https://doi.org/10.1016/j.gr.2020.09.004

Lin, C.F., Liu, S.F., Zhuang, Q.T., Steel, R.J., 2018. Sedimentation of Jurassic fan-delta wedges in the Xiahuayuan Basin reflecting thrust-fault movements of the western Yanshan fold-and-thrust belt, China. Sedimentary Geology 368, 24–43. https://doi.org/10.1016/j.sedgeo.2018.03.005.

Lin, C., Liu, S., Shi, X., Zhuang, Q., 2019. Late Jurassic-Early Cretaceous deformation in the western Yanshan fold-thrust belt: Insights from syn-tectonic sedimentation in the Chicheng basin, North China. Tectonics 38. https://doi.org/10.1029/2018TC005402

Lin, S. Z., Zhu, G., Zhao, T., Song, L., Liu, B., 2014. Structural characteristics and formation mechanism of the Kalaqin metamorphic core complex in the Yanshan area, China. Chinese Science Bulletin 59, 3174–3189, https://doi.org/10.1360/N972014-00100

Lin, W., Charles, N., Chen, K., Chen, Y., Faure, M., Wu, L., Wang, F., 2013a. Late Mesozoic compressional to extensional tectonics in theYiwulüshan massif, NE China and its bearing on the evolution of the Yinshan–Yanshan orogenic belt part II: Anisotropy of magnetic susceptibility and gravity modeling. Gondwana Research 23(1), 78–94. https://doi.org/10.1016/j.gr.2012.02.012

Lin, W., Faure, M., Chen, Y., Ji, W.B., Wang, F., Wu, L., Charles, N., Wang, J., Wang, Q.C., 2013b. Late Mesozoic compressional to extensional tectonics in the Yiwulüshan massif, NE China and its bearing on the evolution of the Yinshan-Yanshan orogenic belt. Part I: Structural analyses and geochronological constraints. Gondwana Research 23, 54–77. https://doi.org/10.1016/j.gr.2012.02.013.

Lin, W., Faure M., Monie´, P. Schäerer, U. Zhang L., Sun Y., 2000. Tectonics of SE China: New insights from the Lushan massif (Jiangxi Province). Tectonics 19, 852–871. https://doi.org/10.1029/2000TC900009.

Lin, W., Faure, M., Nomade, S., Shang, Q., Renne, P. R., 2008. Permian–Triassic amalgamation of Asia: insights from Northeast China sutures and their place in the final collision of North China and Siberia. Comptes Rendus Geoscience 340(2-3), 190-201.

Lin, W., Shi, Y. H., Wang, Q. C., 2009. Exhumation tectonics of the HP-UHP orogenic belt in Eastern China: new structural–petrological insights from the Tongcheng massif, Eastern Dabieshan. Lithos 109, 285–303.

Lin, W., Wang, Q. C., Faure, M., Arnaud, N., 2005. Tectonic evolution of Dabie orogen: in the view from polyphase deformation of the Beihuaiyang metamorphic zone. Science China Series D 48(7), 886-899.

Lin, W., Wang, Q. C., Chen, K., 2008. Phanerozoic tectonic of South China block: New insights from the polyphase deformation in the Yunkai massif. Tectonics 27, TC6004, https://doi.org/10.1029/2007TC002207.

Lin, W., Wei, W., 2020. Late Mesozoic extensional tectonics in the North China Craton and its adjacent regions: a review and synthesis. International Geology Review 1–29. https://doi.org/10.1080/00206814.2018.1477073

Lin, W., Zeng, J., Meng, L., Qiu, H., Wei, W., Ren, Z., Chu, Y., et al. Extensional tectonics and North China Craton destruction: Insights from the magnetic susceptibility anisotropy (AMS) of granite and metamorphic core complex. Science China Earth Science. 64, 1557–1589 (2021). https://doi.org/10.1007/s11430-020-9754-1

Lin, Y., Zhang, C., Li, C., Deng, H., 2020. From dextral contraction to sinistral extension of intracontinental transform structures in the Yanshan and northern Taihang Mountain belts during Early Cretaceous: Implications to the destruction of the North China Craton. Journal of Asian Earth Sciences 189, 104139. https://doi.org/10.1016/j.jseaes.2019.104139

Liu, B., Neubauer, F., Liang, C., Liu, J., Li, W., 2020. Geological control of the eastern Great Wall: Mountain-basin relationships in the eastern North China Craton. Gondwana Research 102(1–2), 60–76. https://doi.org/10.1016/10.1016/j.gr.2020.06.023

Liu, D.L., Shi, R.D., Ding, L., Zou, H.B., 2018a. Late cretaceous transition from subduction to collision along the Bangong-Nujiang Tethys: New volcanic constraints from central Tibet. Lithos 296, 452–470

Liu, L., Xu, X., Xia, Y., 2016. Asynchronizing paleo-Pacific slab rollback beneath SE China: Insights from the episodic Late Mesozoic volcanism. Gondwana Research 37, 397-407, https://doi.org/10.1016/j.gr.2015.09.009.

Liu, J., Zhao, Y., Liu, X.M., 2006. Age of the Tiaojishan Formation volcanics in the Chengde Basin, northern Hebei province (in Chinese with English abstract). Acta Petrologica Sinica 22, 2617–2630.

Liu, J., Zhao, Y., Liu, X., Wang, Y., Liu, X., 2012. Rapid exhumation of basement rocks along the northern margin of the North China craton in the early Jurassic: Evidence from the Xiabancheng Basin, Yanshan Tectonic Belt. Basin Research 24(5), 544-558. https://doi.org/10.1111/j.1365-2117.2011.00538.x

Liu, S.F., Li, Z., Zhang, J.F., 2004. Mesozoic basin evolution and tectonic mechanism in Yanshan, China. Science China Earth Sciences 47, 24–38

Liu, S. F., Lin, C. F., Liu, X. B., Zhuang, Q. T., 2018b. Syn-tectonic sedimentation and its linkage to fold-thrusting in the region of Zhangjiakou, North Hebei, China. Science China Earth Sciences 61(6), 681-710. https://doi.org/10.1007/s11430-017-9175-3

Liu, S.F., Zhang, J.F., Hong, S.Y., Ritts, B.D., 2007. Early Mesozoic basin development and its response to thrusting in the Yanshan fold and thrust belt, China. International Geology Review 49 (11), 1025–1049.

Liu, Y.J., Li, W.M., Feng, Z.Q., Wen, Q.B., Neubauer, F., Liang, C.Y., 2017. A review of the Paleozoic tectonics in the eastern part of Central Asian Orogenic Belt. Gondwana Research 43, 123–148. https://doi.org/10.1016/j.gr.2016.03.013

Lu, F.X., Wang, C.Y., Zheng, J.P., Zhang, R.S., 2004. Lithospheric composition and structure beneath the northern margin of the Qinling orogenic belt. Science China Series D 47, 13–22.

Mattauer, M., Matte, P., Malavieille, J., Tapponnier, P., Maluski, H., Qin, X.Z., Lu, Y.L., Tang, Y.Q., 1985. Tectonics of the Qinling belt: build-up and evolution of eastern Asia. Nature 317 (6037), 496–500. https://doi.org/10.1038/317496a0

Meng, L., Lin, W., 2021. Episodic Crustal Extension and Contraction Characterizing the Late Mesozoic Tectonics of East China: Evidence From the Jiaodong Peninsula, East China. Tectonics 40, e2020TC006318. https://doi.org/10.1029/2020TC006318

Meng, Q.R., Wei, H.H., Wu, G.L., Duan, L., 2014. Early Mesozoic tectonic settings of the northern North China Craton. Tectonophysics 611 (1), 155–166. https://doi.org/10.1016/j.tecto.2013.11.015

Meng, Q. R., Wu, G. L., Fan, L. G., Wei, H. H., 2019. Tectonic evolution of early Mesozoic sedimentary basins in the North China Craton. Earth-Science Reviews 190, 416–438. https://doi.org/10.1016/j.earscirev.2018.12.003

Meng, Q. R., Zhang, G. W., 1999. Timing of collision of the North and South China blocks: controversy and reconciliation. Geology 27 (2), 123–126. https://doi.org/10.1130/0091-7613(1999)027<0123:TOCOTN>2.3.CO;2

Metelkin, D.V., Vernikovsky, V.A., Kazansky, A.Y., Wingate, M.T.D., 2010. Late Mesozoic tectonics of Central Asia based on paleomagnetic evidence. Gondwana Research 18, 400–419.

Niu, B.G., He, Z.J., Song, B., Ren, J., 2003. SHRIMP dating of volcanic rocks of the Zhangjiakou Formation and its significance (in Chinese with English abstract). Geological Bulletin China 22 (2), 140–141.

Niu, B.G., He, Z.J., Song, B., Ren, J., Xiao, L., 2004. SHRIMP geochronology of volcanics of the Zhangjiakou and Yixan Formation, northern Hebei Province, with a discussion on the age of the Xing'anling Group of the Great Hinggan Mountain and volcanic strata of the southeastern coastal area of China. Acta Geological Sinica (English Edition) 78 (6), 1214–1228.

Paterson, S.R., Vernon, R.H., Tobisch, O.T., 1989. A review of criteria for the identification of magmatic and tectonic foliations in granitoids. Journal of Structural Geology 11 (3), 349–363.

Qi, G. W., Zhang, J. J., Wang, M., 2015. Mesozoic tectonic setting of rift basins in eastern North China and implications for destruction of the North China Craton. Journal of Asian Earth Sciences 111, 414-427. https://doi.org/10.1016/j.jseaes.2015.06.022

Qiu, H., Lin, W., Chen, Y., Faure, M., Meng, L., Ren, Z., Zeng, J., Hou, Q., 2021. Magma chamber-related transition from magmatic to solid-state fabrics within the Late Triassic granitic Dushan pluton (North China). Geophysical Journal International 227, 759-775. https://doi.org/10.1093/gji/ggab252

Qiu, H., Lin, W., Faure, M., Chen, Y., Meng, L., Zeng, J., Ren, Z., Li, Q., 2020. Late Triassic extensional tectonics in the northern North China Craton, insights from a multidisciplinary study of the Wangtufang pluton. Journal of Asian Earth Sciences 200, 104462. 10.1016/j.jseaes.2020.104462

Ratschbacher, L., Hacker, B. R., Calvert, A., Webb, L. E., Hu, J., 2003. Tectonics of the Qinling (Central China): tectonostratigraphy, geochronology, and deformation history. Tectonophysics 1-53.

Ritts, B. D., Darby, B. J., Cope, T., 2001. Early Jurassic extensional basin formation in the Daqing Shan segment of the Yinshan belt, northern North China Craton, Inner Mongolia. Tectonophysics 339(3-4), 239-258. https://doi.org/10.1016/S0040-1951(01)00115-9

Sagong, H., Kwon, S.T., Ree, J.H., 2005. Mesozoic episodic magmatism in South Korea and its tectonic implication. Tectonics, 24(5), TC5002.1-TC5002.18.

Shao, J.A., Zhang, J.H., 2014. The early mesozoic continental crust reformation in Yanshan area-giving discussion to Indosinian movement. Earth Science Frontiers 21, 302–309 (in Chinese with English abstract)

Shao, J.A., Meng, Q.R., Wei, H.Q., Zhang, L.Q., Wang, P.Y., 2003. Nature and tectonic environment of Late Jurassic volcanic-sedimentary basins in northern Hebei Province (in Chinese with English abstract). Geological Bulletin of China 22(10), 751–761.

Shi, X., Liu, S., Lin, C., 2019. Growth structures and growth strata of the Qianjiadian Basin in the western Yanshan fold and thrust belt, North China. Science China Earth Sciences 62, 1092–1109, https://doi.org/10.1007/s11430-018-9345-6

Shu, L.S., Zhou, X.M., Deng, P., Zhu, W.B., 2007. Mesozoic-Cenozoic basin features and evolution of South China. Acta Geologica Sinica. 81 (4), 573–586.

Silva, D., Piazolo, S., Daczko, N. R., Houseman, G., Raimondo, T., Evans, L., 2018. Intracontinental orogeny enhanced by far-field extension and local weak crust. Tectonics 37, 4421–4443. https://doi.org/10.1029/2018TC005106

Su, N., Zhu, G., Liu, C., Zhang, S., Li, Y., Yin, H., Wu, X., 2020. Alternation of back-arc extension and compression in an overriding plate: evidence from Cretaceous structures in the western Liaoning region, eastern China. International Journal of Earth Sciences 109(2), 707-727.

Su, N., Zhu, G., Wu, X., Yin, H., Lu, Y., Zhang, S., 2021. Back-arc tectonic tempos: Records from Jurassic–Cretaceous basins in the eastern North China Craton. Gondwana Research 90, 241-257.

Swisher, C.C., Wang, X.L., Zhou, Z.H., Wang, Y.Q., Jin, F., Zhang, J.Y., Xu, X., Zhang, F.C., 2002. Further support for a Cretaceous age for the feathered dinosaur beds of Liaoning, China: new ^{40}Ar/^{39}Ar dating of the Yixian and Tuchengzi formations. Chinese Science Bulletin 47(2),135–138.

Tang, J., Xu, W., Wang, F., Ge, W., 2018. Subduction history of the Paleo-Pacific slab beneath Eurasian continent: Mesozoic-Paleogene magmatic records in Northeast Asia. Science China Earth Sciences 61(5), 527–559. https://doi.org/10.1016/10.1007/s11430-017-9174-1

Tomurtogoo, O., Windley, B.F., Kröner, A., Badarch, G., Liu, D.Y., 2005. Zircon age and occurrence of the Adaatsag ophiolite and Muron shear zone, central Mongolia: constraints on the evolution of the Mongol–Okhotsk Ocean, suture and orogen. Journal of the Geological Society 162, 125–134.

Trap, P., Faure, M., Lin, W., Le Breton, N., Monié, P., 2012. Paleoproterozoic tectonic evolution of the Trans-North China Orogen: toward a comprehensive model. Precambrian Research 222, 191–211. https://doi.org/10.1016/j.precamres.2011.09.008

Tarling, D. H., Hrouda, F., 1993. Magnetic Anisotropy of Rocks. London, U. K.: Chapman and Hall.

Wang, F., Xu, W.L., Xing, K.C., Wang, Y.N., Zhang, H.H., Wu, W., Sun, C.Y., Ge, W.C., 2019. Final closure of the Paleo–Asian Ocean and Onset of Subduction of Paleo–Pacific Ocean: Constraints from Early Mesozoic magmatism in Central southern Jilin Province, NE China. Journal of Geophysical Research: Solid Earth 124, 2601–2622.

Wang, L.L., Hu, D.Y., Zhang, L.J., Zheng, S.L., He, H.Y., Deng, C.L., Wang, X.L., Zhou, Z.H., Zhu, R.X., 2013b. SIMS U-Pb zircon age of Jurassic sediments in Linglongta, Jianchang, western Liaoning: constraint on the age of the oldest feathered dinosaurs (in Chinese with English abstract) Chinese Science Bulletin, 58, 1346–1353.

Wang, J., 2013. Late Mesozoic extensional structure in the northern North China Craton and its geodynamic implications (in Chinese with English abstract). Dissertation for Doctoral Degree. Beijing: Institute of Geology and Geophysics, Chinese Academy of Sciences, 1–181.

Wang, S.E., Gao, L.Z., Wan, X.Q., Song, B., 2013c. Ages of the Tuchengzi Formation in western Liaoning-northern Hebei area in correlation with those of international strata. Geological Bulletin of China 32(11), 1673–1690.

Wang, Y., Dong, S., Shi, W., Chen, X., Jia, L., 2017. The Jurassic structural evolution of the western Daqingshan area, eastern Yinshan belt, North China. International Geology Review 1-23. https://doi.org/10.1080/00206814.2017.1300784

Wang, Y., Zhou, L., Zhao, L., 2013a. Cratonic reactivation and orogeny: an example from the northern margin of the North China Craton. Gondwana Research 24 (3–4), 1203–1222. https://doi.org/10.1016/j.gr.2013.02.011.

Wang, T., Zheng, Y., Zhang, J., Zeng, L., Donskaya, T., Guo, L., Li, J., 2011. Pattern and kinematic polarity of late Mesozoic extension in continental NE Asia: Perspectives from metamorphic core complexes. Tectonics 30(6), TC6007, https://doi.org/10.1029/2011TC002896.

Wang, Z., Zhao, Y., Zou, H., Li, W., Liu, X., Wu, H., Xu, G., Zhang, S., 2007. The early Jurassic Nandaling flood basalts in the Yanshan belt, North China craton: the origin and geodynamic implications. Lithos 96, 543–566.

Windley, B.F., Alexeiev, D., Xiao, W., Kröner, A., Badarch, G., 2007. Tectonic models for accretion of the Central Asian Orogenic Belt. Journal of the Geological Society 164 (1), 31–47. https://doi.org/10.1144/0016-76492006-022

Wong W. H., 1927. Crustal movements and igneous activities in Eastern China since Mesozoic time. Bulletin of Geological Society of China 6, 9-37.

Wong, W. H., 1929. The Mesozoic orogenic movement in eastern China. Bulletin of Geological Society of China 8, 33–44.

Wu, G.L., Meng, Q.R., Zhu, R.X., Fan, L.G., Zhu, J.C., 2021. Middle Jurassic orogeny in the northern North China Block. Tectonophysics 801, 228713.

Wu, F.Y., Yang, J.H., Wilde, S.A., Zhang, X.O., 2005. Geochronology, petrogenesis and tectonic implications of Jurassic granites in the Liaodong Peninsula, NE China. Chemical Geology 221, 127–156.

Wu, F.Y., Xu, Y.G., Gao, S., Zheng, J.P., 2008. Lithospheric thinning and destruction of the North China Craton (in Chinese with English abstract). Acta Petrologica Sinica 24, 1145–1174.

Wu, F. Y., Yang, J. H., Lo, C. H., Wilde, S. A., Sun, D. Y., Jahn, B. M., 2007. The Heilongjiang Group: A Jurassic accretionary complex in the Jiamusi Massif at the western Pacific margin of northeastern China. Island Arc 16(1), 156–172. https://doi.org/10.1111/j.1440-1738.2007.00564.x

Wu, F. Y., Yang, J. H., Xu, Y. G., Wilde, S. A., Walker, R. J., 2019. Destruction of the North China Craton in the Mesozoic. Annual Review of Earth and Planetary Sciences 47(1), 73–95. https://doi.org/10.1146/annurev-earth-053018-060342

Wu, F. Y., Yang, J. H., Zhang, Y. B., Liu, X. M., 2006. Emplacement ages of the Mesozoic granites in southeastern part of the Western Liaoning Province. Acta Petrologica Sinica 22(2), 315–325.

Wu, F.Y., Zhao, G.C., Sun, D.Y., Wilde, S.A., Zhang, J.H., 2007. The Hulan Group: its role in the evolution of the Central Asian Orogenic Belt of NE China. Journal of Asian Earth Sciences 30, 542–556.

Xiao, W. J., Windley, B., Hao, J., Zhai, M. G., 2003. Accretion leading to collision and the Permian Solonker suture, Inner Mongolia, China: termination of the Central Asian Orogenic Belt. Tectonics 22, 1069–1089. http://doi.org/10.1029/ 2002TC001484

Xiao, W., Windley, B.F., Sun, S., Li, J., Huang, B., Han, C., Yuan, C., Sun, M., Chen, H., 2015. A tale of amalgamation of three Permo-Triassic collage systems in Central Asia: oroclines, sutures, and terminal accretion. Annual Review of Earth and Planetary Sciences 43 (1), 477–501. https://doi.org/10.1146/annurev-earth-060614-105254

Xu, B., Charvet, J., Chen, Y., Zhao, P., Shi, G., 2013. Middle Paleozoic convergent orogenic belts in western Inner Mongolia (China): framework, kinematics, geochronology and implications for tectonic evolution of the Central Asian Orogenic Belt. Gondwana Research 23 (4), 1342–1364. https://doi.org/10.1016/j.gr.2012.05.015

Xu, Z., Lu, Y., Tang, Y., Mattauer, M., Matte, P., Malavieille, J., Tapponnier, P., Maluski, H., 1986. Deformation characteristics and Tectonic evolution of the eastern Qinling orogenic belt. Acta Geologica Sinica 60(3), 23–35. https://doi.org/10.1111/j.1755-6724.1986.mp60003003.x

Xu, H., Liu, Y.Q., Kuang, H.W., Jiang, X.J., Nan, P., 2012. U-Pb SHRIMP age for the Tuchengzi Formation, northern China, and its implications for biotic evolution during the Jurassic-Cretaceous transition. Paleoworld 21, 222–234.

Yan, M., Zhang, D., Fang, X., Ren, H., Zhang, W., Zan, J., Song, C., Zhang, T., 2016. Paleomagnetic data bearing on the Mesozoic deformation of the Qiangtang Block: implications for the evolution of the Paleo-and Meso-Tethys. Gondwana Research 39, 292–316

Yang, Q., Shi, W., Hou, G., Zhang, Y., Zhao, Y., 2021. Late Mesozoic Intracontinental Deformation in the Northern Margin of the North China Craton: A Case Study From the Shangyi Basin, Northwestern Hebei Province, China. Frontiers in Earth Science 9, 1-26.

Yang, J.H., Wu, F.Y., Shao, J.A., Wilde, S.A., Xie, L.W., Liu, X.M., 2006. Constraints on the timing of uplift of the Yanshan Fold and Thrust Belt, North China. Earth and Planetary Science Letters 246, 336–352

Yang, J. H., Wu, F. Y., Chung, S. L., Wilde, S. A., Chu, M. F., 2004. Multiple sources for the origin of granites: geochemical and Nd/Sr isotopic evidence from the Gudaoling granite and its mafic enclaves, Northeast China. Geochimica Et Cosmochimica Acta 68(21), 4469-4483.

Yang, M., Liang, L., Jin, Z., Qu, X., Zhou, D., 2013. Segmentation and inversion of the Hangjinqi fault zone, the northern Ordos basin (North China). Journal of Asian Earth Sciences 70–71, 64–78.

Yang, W., Li, S.G., 2008. Geochronology and geochemistry of the Mesozoic volcanic rocks in western Liaoning: implications for lithospheric thinning of the North China craton. Lithos 102, 88–117.

Yang, X., Dong, Y., 2018. Mesozoic and Cenozoic multiple deformations in the Helanshan Tectonic Belt, Northern China. Gondwana Research 60, 34–53. https://doi.org/10.1016/j.gr.2018.03.020

Yang, X., Dong, Y., 2020. Multiple phases of deformation in the Southern Helanshan Tectonic Belt, Northern China. Journal of Asian Earth Sciences 104497. https://doi.org/10.1016/j.jseaes.2020.104497

Yang, Y., Li, W., Ma, L., 2005. Tectonic and stratigraphic controls of hydrocarbon systems in the Ordos Basin: a multicycle cratonic basin in central China. AAPG Bulletin 89(2), 255-269.

Yin, A., Nie, S., 1996. A Phanerozoic palinspastic reconstruction of China and its neighboring regions. In: Yin, A., & Harrison, T.A. (Eds.), The Tectonic Evolution of Asia. Cambridge University Press, New York, pp. 442–485.

Yu, H.F., Zhang, Z.C., Shuai, G.W., Chen, Y., Tang, W.H., 2016. SHRIMP and LA–ICP–MS U-Pb ages and geological significance of the volcanic rocks in the Tiaojishan Formation in Ming Tombs area–Western Hills, Beijing (in Chinese with English abstract). Geological Review 4, 807–826.

Yu, X.Q., Wu, G.G., Zhao, X., Gao, J.F., Di, Y.J., Zheng, Y., Dai, Y.P., Li, C.L., Qiu, J.T., 2010. The Early Jurassic tectono-magmatic events in southern Jiangxi and northern Guangdong provinces, SE China: constraints from the SHRIMP zircon U-Pb dating. Journal of Asian Earth Sciences 39, 408–422.

Yuan, H.L., Liu, X.M., Liu, Y.S., Gao, S., Ling, W.L., 2005. U-Pb zircon geochronology and geochemistry of Late Mesozoic volcanic rocks in Western Hills, Beijing. Science China 35(9), 821–836.

Zeng, J., Wei, W., Lin, W., Meng, L., Qiu, H., Chu, Y., Ren, Z., Wang, Y., Feng, Z., Li, Q., Ling, X., 2021. The Late Jurassic extensional event in the Yanshan fold and thrust belt (North China): New insights from an integrated study of structural geology, geophysics, and geochemistry of the Siganding granitic pluton. Journal of Asian Earth Sciences 211, 104708. https://doi.org/10.1016/j.jseaes.2021.104708

Zhang, A., Liu, S., Lin, C., Zhang, B., 2019. Timing of deposition in the Dengzhangzi and Guojiadian Basins of the Yanshan fold-thrust belt, North China. International Geology Review 9, 1-22.

Zhang, C., Wang, G., Wu, Z., Zhang, L., Sun, W., 2002. Thrust tectonics in the eastern segment of the intraplate Yanshan orogenic belt, western Liaoning province, North China (in Chinese with English abstract). Acta Geologica Sinica 76(1), 64-76.

Zhang, C. H., Wu, G. G., Xu, D. B., Wang, G. H., Sun, W. H., 2004a. Mesozoic tectonic framework of the intraplate and evolution in the central segment Yanshan orogenic belt (in Chinese with English abstract). Geological Bulletin of China 23(9–10), 864-875.

Zhang, C.H., Zhang, Y., Li, H.L., Wu, G.G., Wang, G.H., Xu, D.B., Xiao, W.F., Dai, L., 2006. Late Mesozoic thrust tectonics framework in the western part of the Yanshan orogenic belt and the Western Hills of Beijing: characteristics and significance (in Chinese with English abstract). Earth Science Frontiers 13(2), 165-183.

Zhang, H., Yuan, H.L., Hu, Z.C., Liu, X.M., Diwu, C.R., 2005. U-Pb zircon dating of the Mesozoic volcanic strata in Luanping of north Hebei and its significance (in Chinese with English abstract): Earth Science-Journal of China University of Geoscience, 30, 6, 07–720.

Zhang, H., Wang, M.X., Liu, X.M., 2008a. Constraints on the upper boundary age of the Tiaojishan Formation volcanic rocks in West Liaoning-North Hebei by LA–ICP–MS dating. Science Bulletin 53(22), 3574–3584

Zhang, H., Wei, Z.L., Liu, X.M., Li, D., 2009. Constraints on the age of the Tuchengzi Formation by LA–ICP–MS dating in northern Hebei–western Liaoning, China. Science China Earth Sciences 52 (4), 461–470.

Zhang, H.-F., 2007. Temporal and spatial distribution of Mesozoic mafic magmatism in the North China Craton and implications for secular lithospheric evolution. Geological Society, London, Special Publications 280(1), 35–54. https://doi.org/10.1144/sp280.2

Zhang, H.F., Sun, M., Zhou, M.F., Fan, W.M., Zhou, X.H., Zhai, M.G., 2004b. Highly heterogeneous late Mesozoic lithospheric mantle beneath the North China Craton: evidence from Sr–Nd–Pb isotopic systematics of mafic igneous rocks. Geological Magazine 141, 55–62.

Zhang, K.J., Zhang, Y.X., Tang, X.C., Xia, B., 2012. Late Mesozoic tectonic evolution and growth of the Tibetan plateau prior to the Indo-Asian collision. Earth-Sciences Reviews 114, 236–249.

Zhang, S. H., Zhao, Y., Davis, G. A., Ye, H., Wu, F., 2014. Temporal and spatial variations of Mesozoic magmatism and deformation in the North China Craton: implications for lithospheric thinning and decratonization. Earth-Science Reviews 131(4), 49–87. https://doi.org/10.1016/j.earscirev.2013.12.004

Zhang, X., Zhang, H., Jiang, N., Wilde, S. A., 2010. Contrasting Middle Jurassic and Early Cretaceous mafic intrusive rocks from western Liaoning, North China craton: petrogenesis and tectonic implications. Geological Magazine 147(06), 844–859. https://doi.org/10.1017/s0016756810000373

Zhang, Y., Dong, S., Zhao, Y., Zhang, T., 2008b. Jurassic tectonics of North China: a synthetic view. Acta Geologica Sinica-English Edition 82(2), 310-326.

Zhang, Y., Shi, W., Dong, S., 2011. Changes of Late Mesozoic tectonic regimes around the Ordos Basin (North China) and their geodynamic implications. Acta Geologica Sinica 85(6), 1254-1276.

Zhang, Y., Qiu, E., Dong, S., Li, J., Shi, W., 2022. Late Mesozoic intracontinental deformation and magmatism in North and NE China in response to multi-plate convergence in NE Asia: An overview and new view. Tectonophysics 835, 229377, https://doi.org/10.1016/j.tecto.2022.229377

Zhang, Y., Shi, W., Dong, S., Wang, T., Yang, Q., 2020. Jurassic intracontinental deformation of the central North China Plate: Insights from syn-tectonic sedimentation, structural geology, and U-Pb geochronology of the Yungang Basin, North China. Tectonophysics 778, 228371.

Zhao, G., Wilde, S. A., Cawood, P. A., Sun, M., 2001. Archean blocks and their boundaries in the North China Craton: lithological, geochemical, structural and P-T, path constraints and tectonic evolution. Precambrian Research 107(1), 45–73. https://doi.org/10.1016/S0301-9268(00)00154-6

Zhao, P., Chen, Y., Xu, B., Faure, M., Shi, G., Choulet, F., 2013. Did the Paleo-Asian Ocean between NCC and Mongolia Block exist during the late Paleozoic? first paleomagnetic evidence from central-eastern Inner Mongolia, China. Journal of Geophysical Research: Solid Earth 118 (5), 1873–1894. https://doi.org/10.1002/jgrb.50198

Zhao, Y., 1990. The Mesozoic orogenesis and tectonic evolution of the Yanshan area (in Chinese with English abstract). Geology Review 36 (1), 1–13.

Zhao, Y., Cui, S.Q., Guo, T., Xu, G., 2002. Evolution of a Jurassic basin of the Western Hills, Beijing, North China and its tectonic implications (in Chinese with English abstract). Geological Bulletin of China 21, 211–217.

Zhao, Y., Zhang, S.H., Xu, G., Yang, Z.Y., Hu, J.M., 2004. The Jurassic major tectonic events of the Yanshanian intraplate deformation belt (in Chinese with English abstract). Geological Bulletin of China 23 (9–10), 854–863.

Zhao, Y., Song, B., Zhang, S.H., Liu, J., 2006. Geochronology of the inherited zircons from Jurassic Nandaling basalt of the Western Hills of Beijing, North China: Its implications (in Chinese with English abstract). Earth Science Frontiers 2006, 13(2), 184-190.

Zhou, J.B., Wilde, S.A., Zhao, G.C., Han, J., 2018. Nature and assembly of microcontinental blocks within the Paleo-Asian Ocean. Earth-Science Reviews 186, 76–93. https://doi.org/10.1016/j.earscirev.2017.01.012

Zhu, D.C., Zhao, Z.D., Niu, Y.L., Mo, X.X., Chung, S.L., Hou, Z.Q., Wang, L.Q., Wu, F.Y., 2011a. The Lhasa Terrane: Record of a microcontinent and its histories of drift and growth. Earth and Planetary Science Letters 301, 241–255

Zhu, D.C., Li, S.M., Cawood, P.A., Wang, Q., Zhao, Z.D., Liu, S.A., Wang, L.Q., 2016. Assembly of the Lhasa and Qiangtang terranes in central Tibet by divergent double subduction. Lithos 245, 7–17.

Zhu, G., Chen, Y., Jiang, D., Lin, S., 2015. Rapid change from compression to extension in the North China Craton during the Early Cretaceous: Evidence from the Yunmengshan metamorphic core complex. Tectonophysics 656, 91–110. https://doi.org/10.1016/j.tecto.2015.06.009

Zhu, G., Jiang, D., Zhang, B., Chen, Y., 2011b. Destruction of the eastern North China Craton in a back-arc setting: evidence from crustal deformation kinematics. Gondwana Research 22(1), 86-103. https://doi.org/10.1016/j.gr.2011.08.005

Zhu, G., Liu, C., Gu, C., Zhang, S., Li, Y., Su, N., Xiao, S., 2018. Oceanic plate subduction history in the western Pacific Ocean: Constraint from late Mesozoic evolution of the Tan-Lu Fault Zone. Science China Earth Sciences 61(4), 386–405. https://doi.org/10.1007/s11430-017-9136-4

Zorin, Yu.A., 1999. Geodynamics of the western part of the Mongolia–Okhotsk collisional belt, Trans-Baikal region (Russia) and Mongolia. Tectonophysics 306, 33–56.

Figures

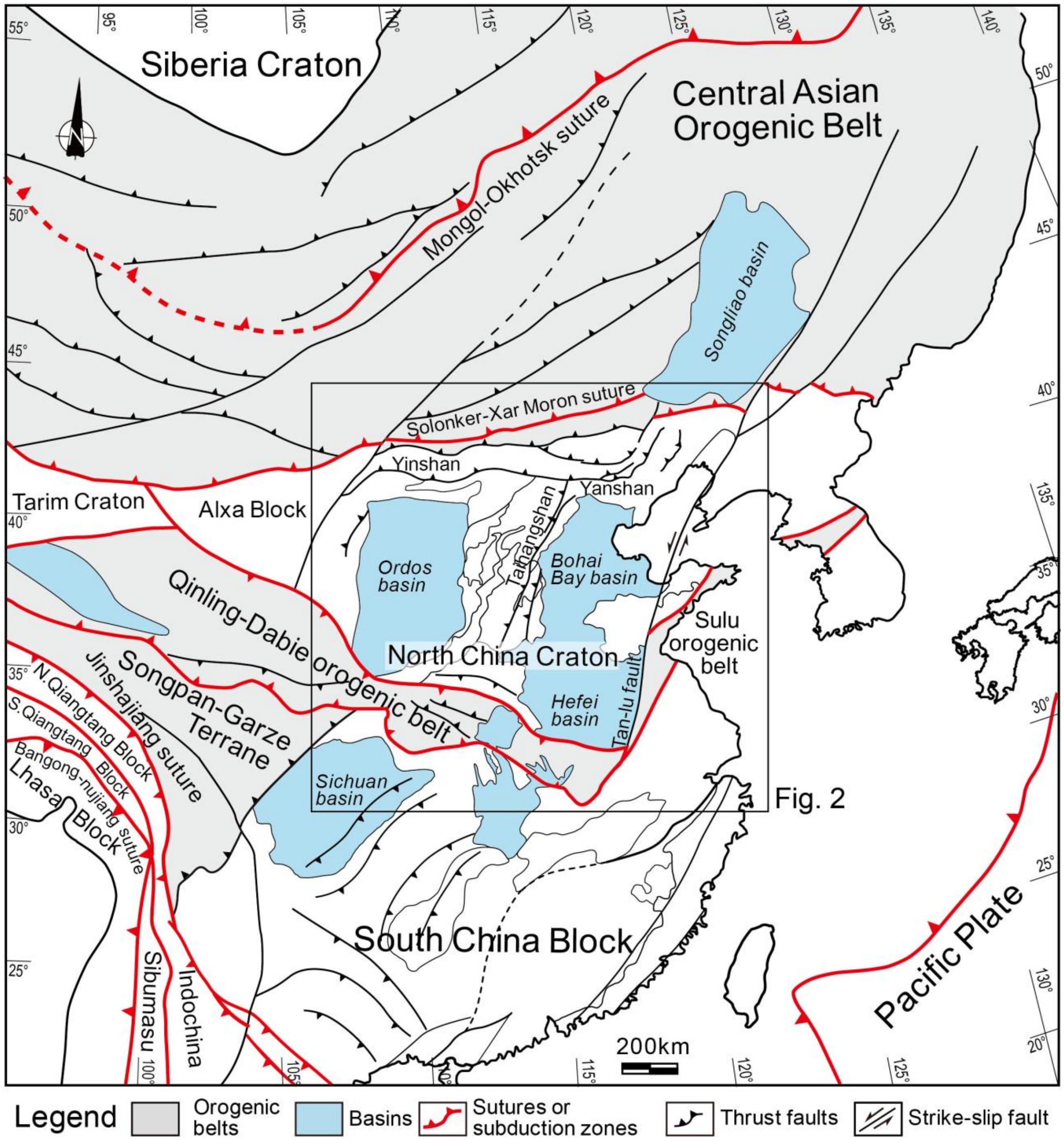

Fig. 1. Simplified geological sketch map of the East Asian continent.

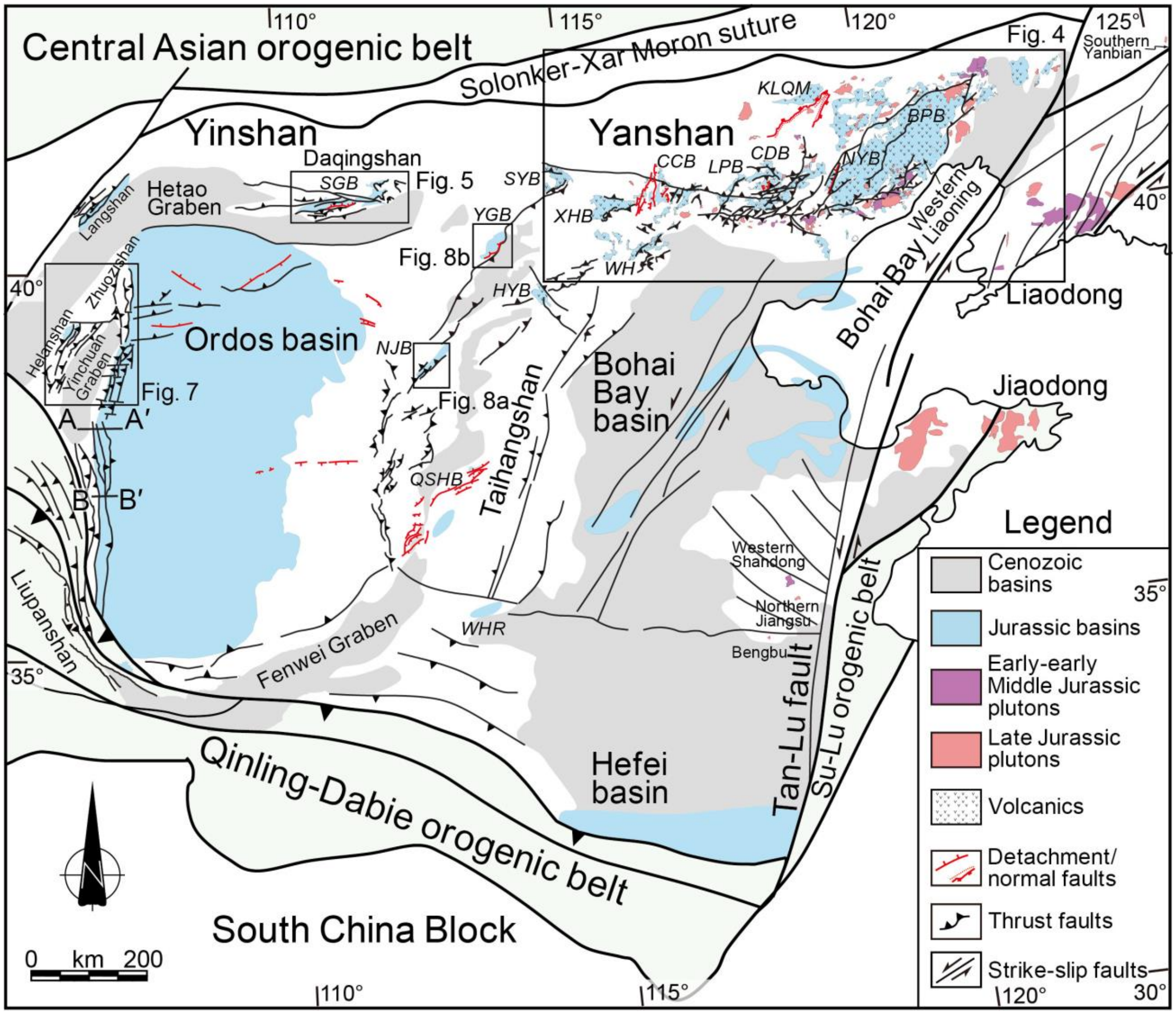

Fig. 2. Simplified geological map showing the Jurassic–earliest Cretaceous structures and magmatic rocks in the NCC (Modified from Zhang et al., 2011). SGB: Shiguai basin; YGB: Yungang basin; HYB: Hunyuan basin; NJB: Ningwu-Jingle basin; QSHB: Qinshuihe basin; WHR: West Henan region; SYB: Shangyi basin; XHB: Xuanhua basin; WH: Western Hill; CCB: Chicheng basin; CDB: Chengde basin; NYB: Niuyingzi basin; LPB: Luanping basin; BPB: Beipiao basin; KLQM: Kalaqin metamorphic core complex (MCC). See Fig. 1 for locations.

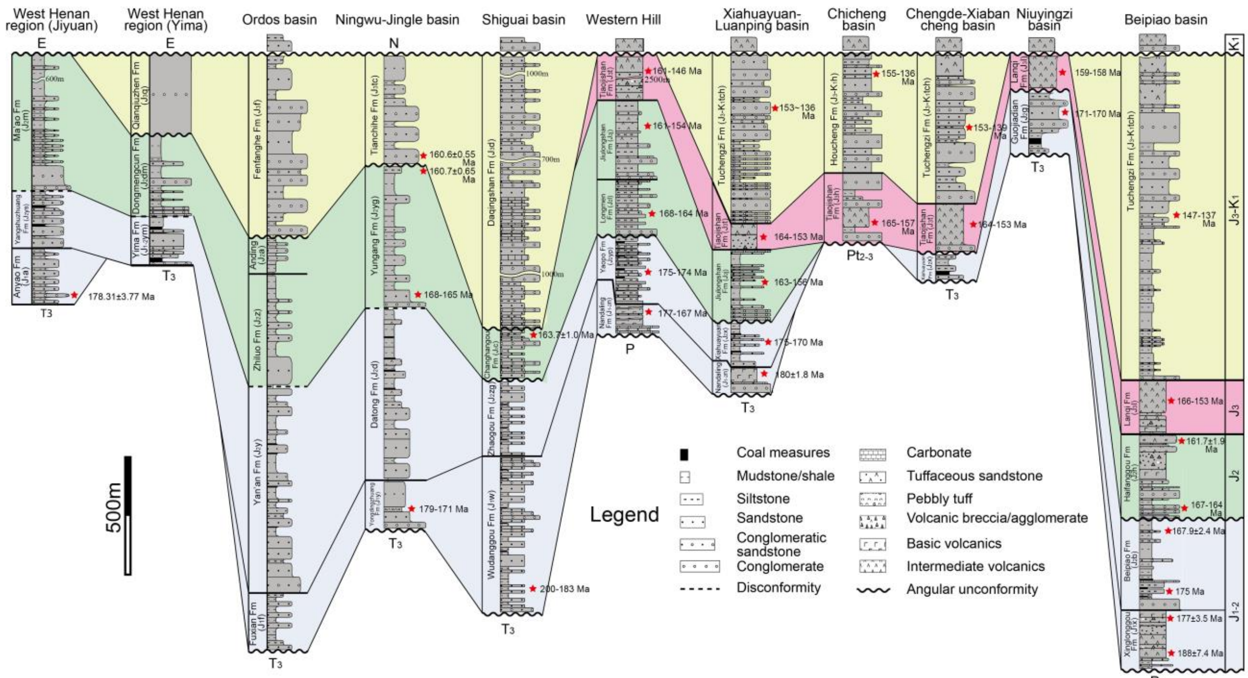

Fig. 3. Stratigraphic correlation and chronostratigraphic framework of the Jurassic–lowest Cretaceous strata (Data from BGMNM, 1983; BGMH, 1989; BGML, 1989). The red stars indicate the sampling sites of the zircon U-Pb and ^{40}Ar-^{39}Ar data, which are summarized in Table S1. See Fig. 2 for locations of the basins.

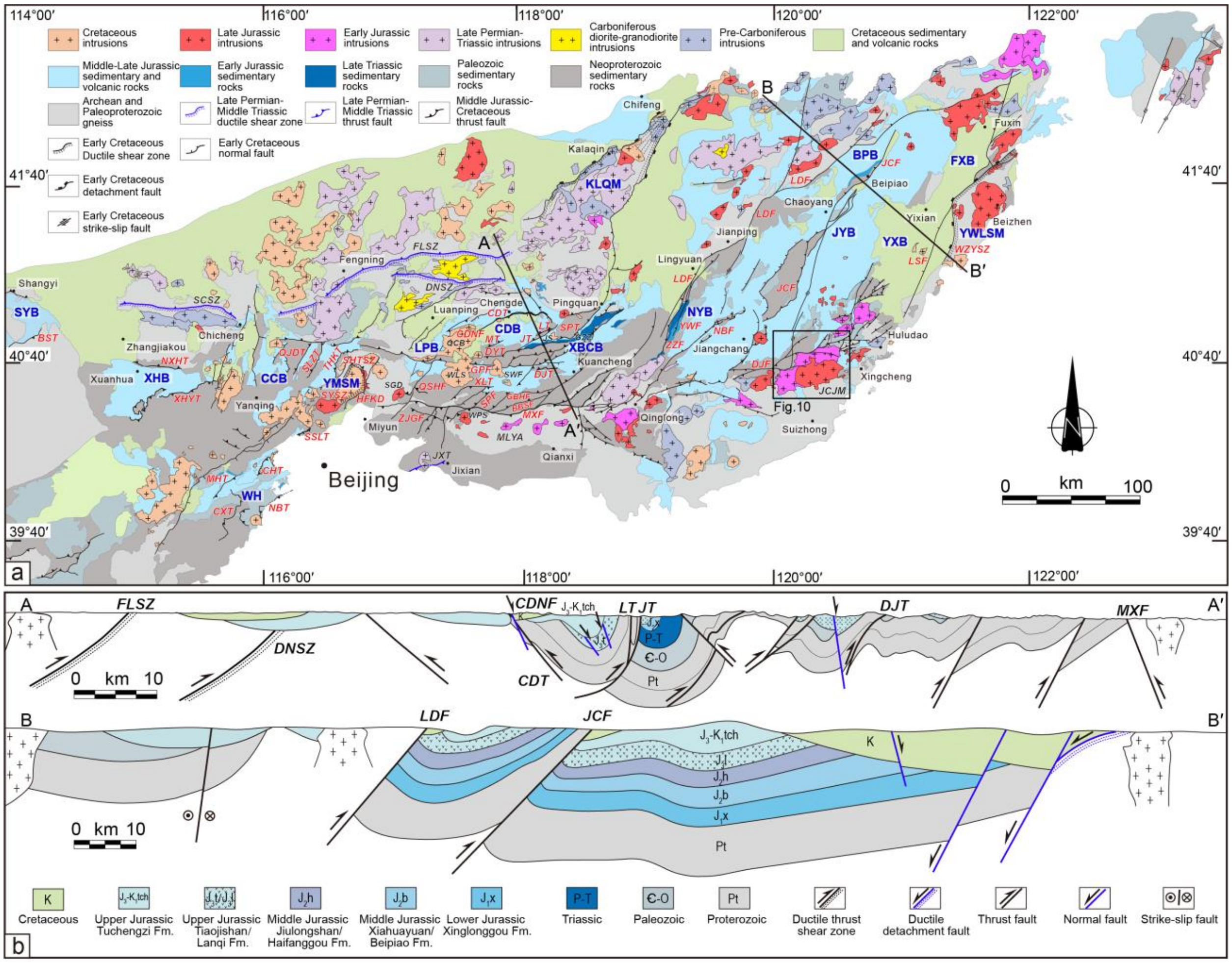

Fig. 4. Overview map of the Yanshan belt. (a) Simplified tectonic map of the Yanshan belt (modified from BGMH, 1989; BGML, 1989; Qiu et al. 2020, 2021; See Fig. 2 for location). (b) Geological cross-sections across the Yanshan belt (modified from Davis et al., 2001; Li et al., 2016a; Su et al. 2021). SYB: Shangyi basin; XHB: Xuanhua basin; WH: Western Hill; CCB: Chicheng basin; LPB: Luanping basin; CDB: Chengde basin; XBCB: Xiabancheng basin; NYB: Niuyingzi basin; JYB: Jinyang basin; YXB: Yixian basin; BPB: Beipiao basin; FXB: Fuxian basin; KLQM: Kalaqin MCC; YMSM: Yunmengshan MCC; YWLSM: Yiwulüshan MCC. See Table 2 for the abbreviations of the structures.

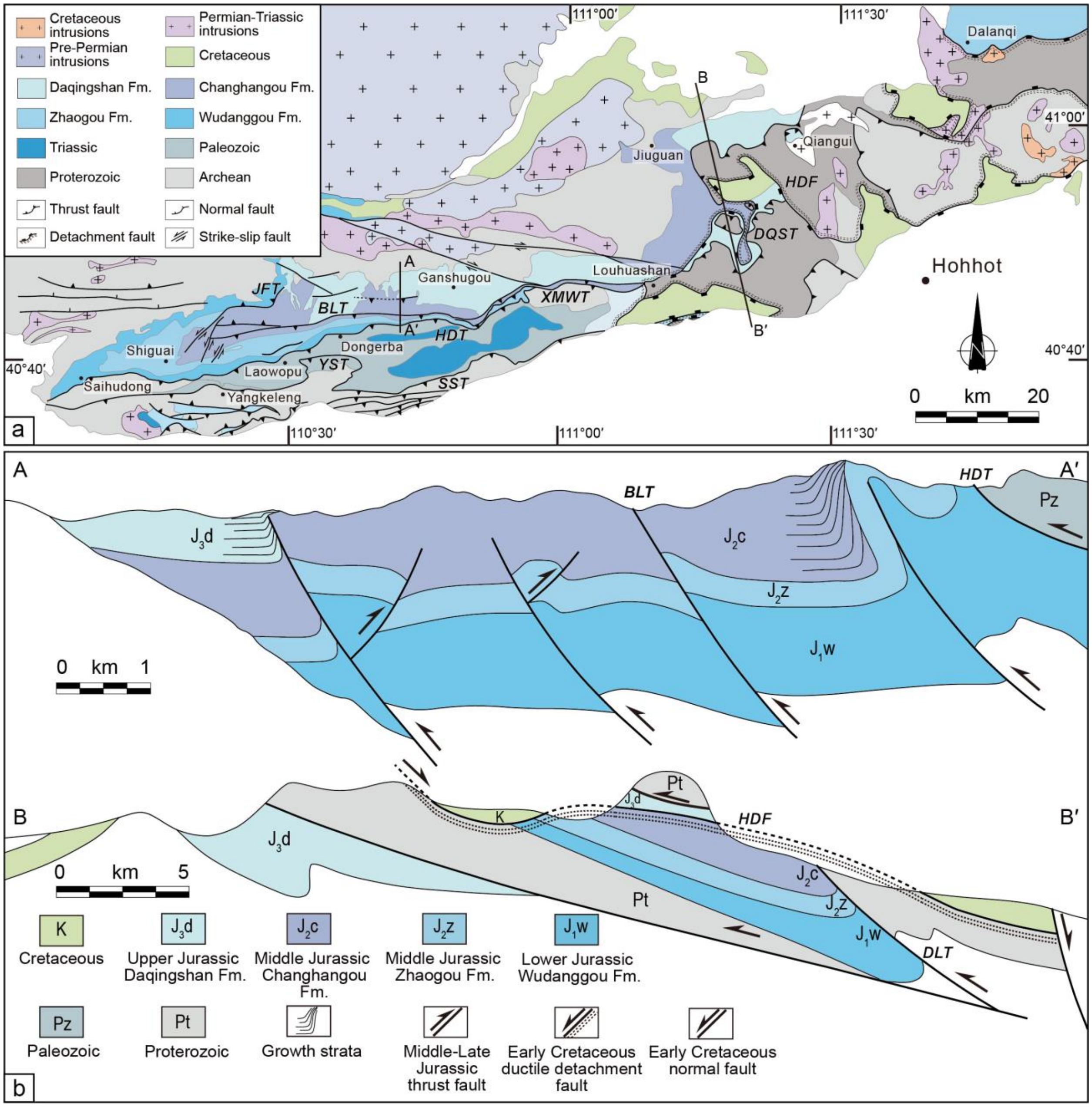

Fig. 5. Overview map of Daqingshan in the Yinshan belt (modified from BGMNM, 1983; Gong et al., 2017; Wang et al., 2017). (a) Simplified tectonic map of Daqingshan. See Fig. 2 for location. (b) Geological cross-sections across Daqingshan. See Table 2 for the abbreviations of structures.

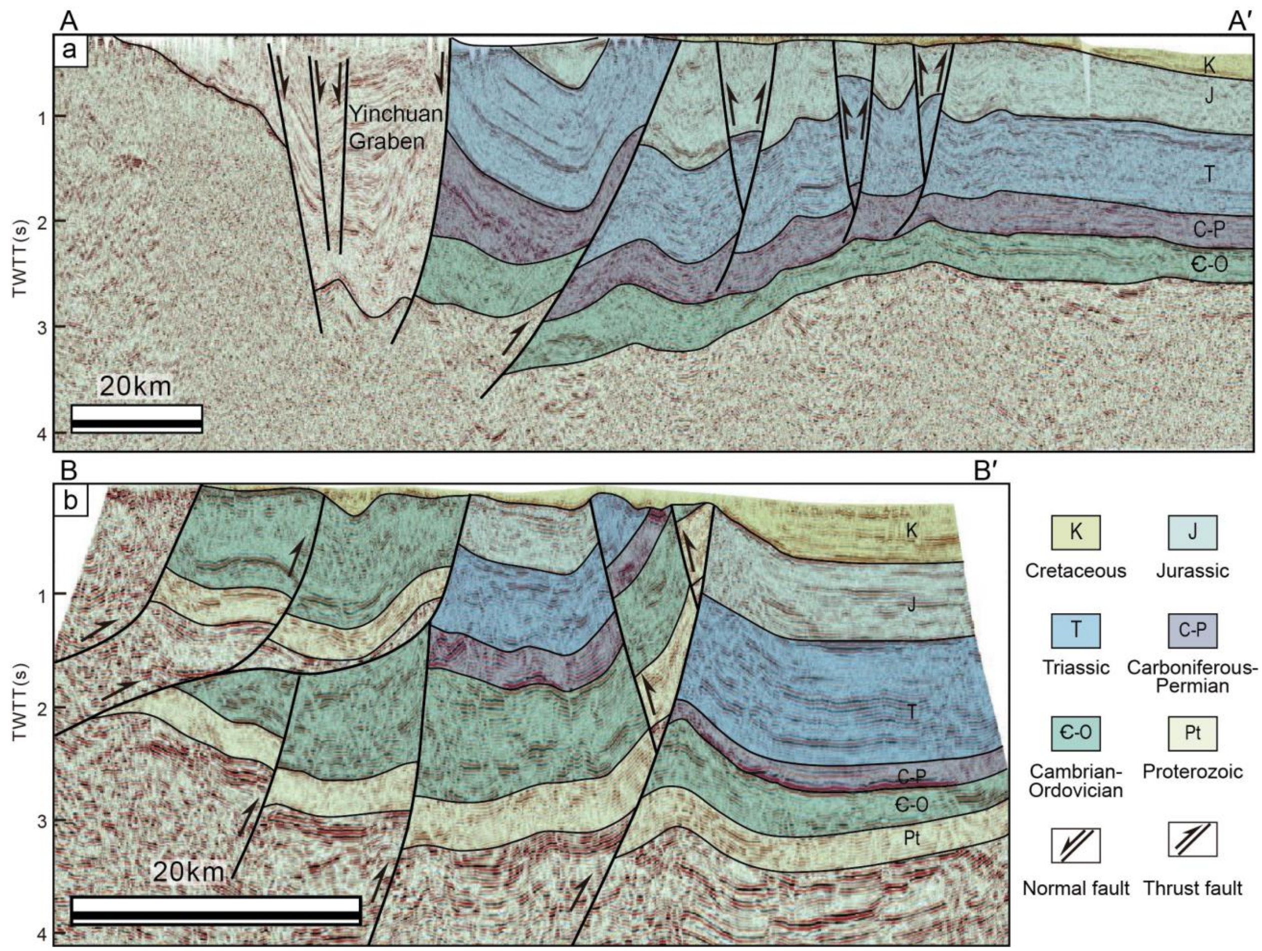

Fig. 6. Seismic reflection profiles across the Western Ordos fold-thrust belt (modified from Feng, 2021; See Fig. 2 for locations).

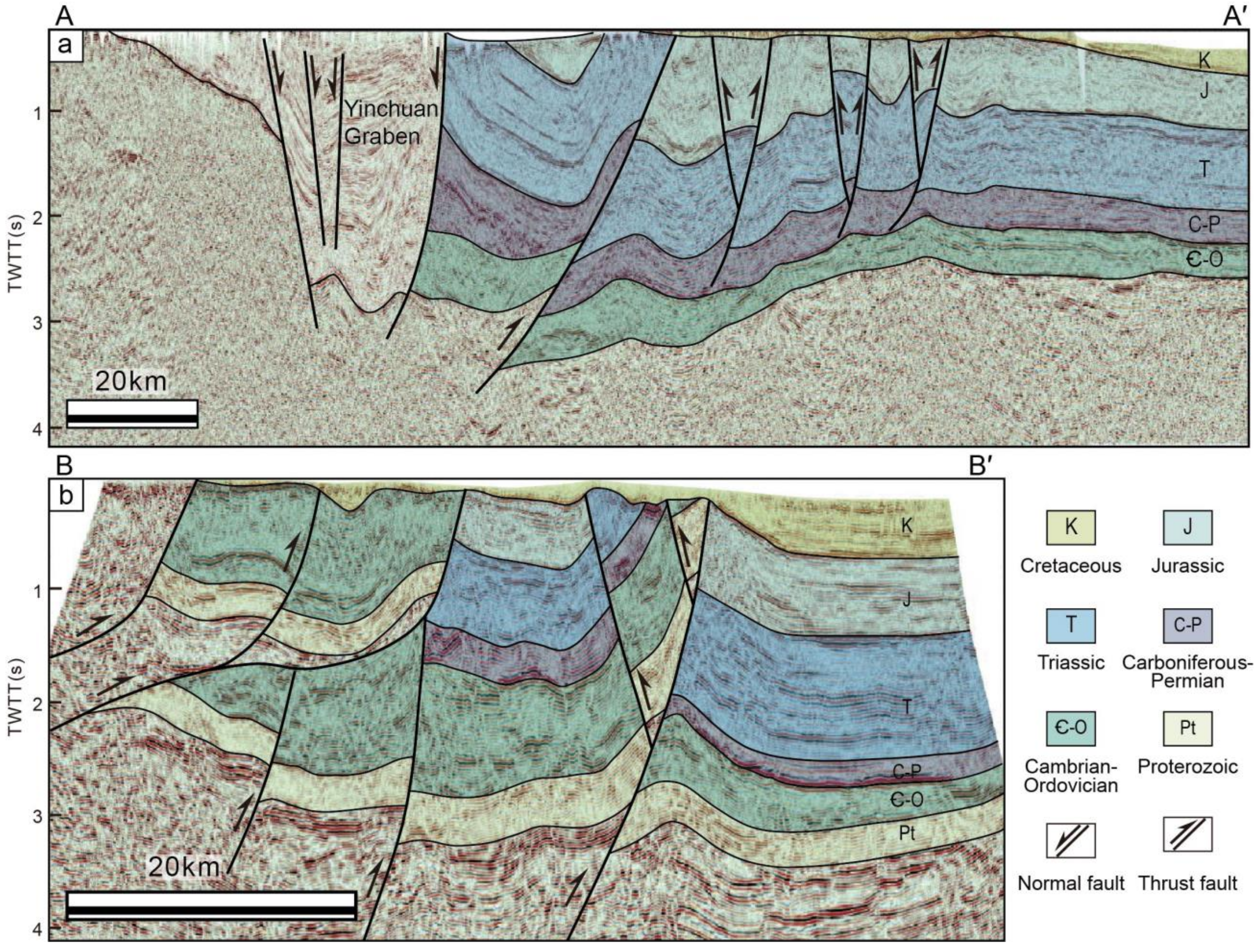

Fig. 7. Overview map of Helanshan-Zhuozishan in the west of the Ordos basin (modified from Darby and Ritts, 2002; Yang and Dong, 2018; Li et al., 2022; Cheng et al., 2022). (a) Simplified tectonic map of Helanshan-Zhuozishan. See Fig. 2 for locations. (b)–(e) Geological cross-sections across Helanshan-Zhuozishan. See Table 2 for the abbreviations of the structures.

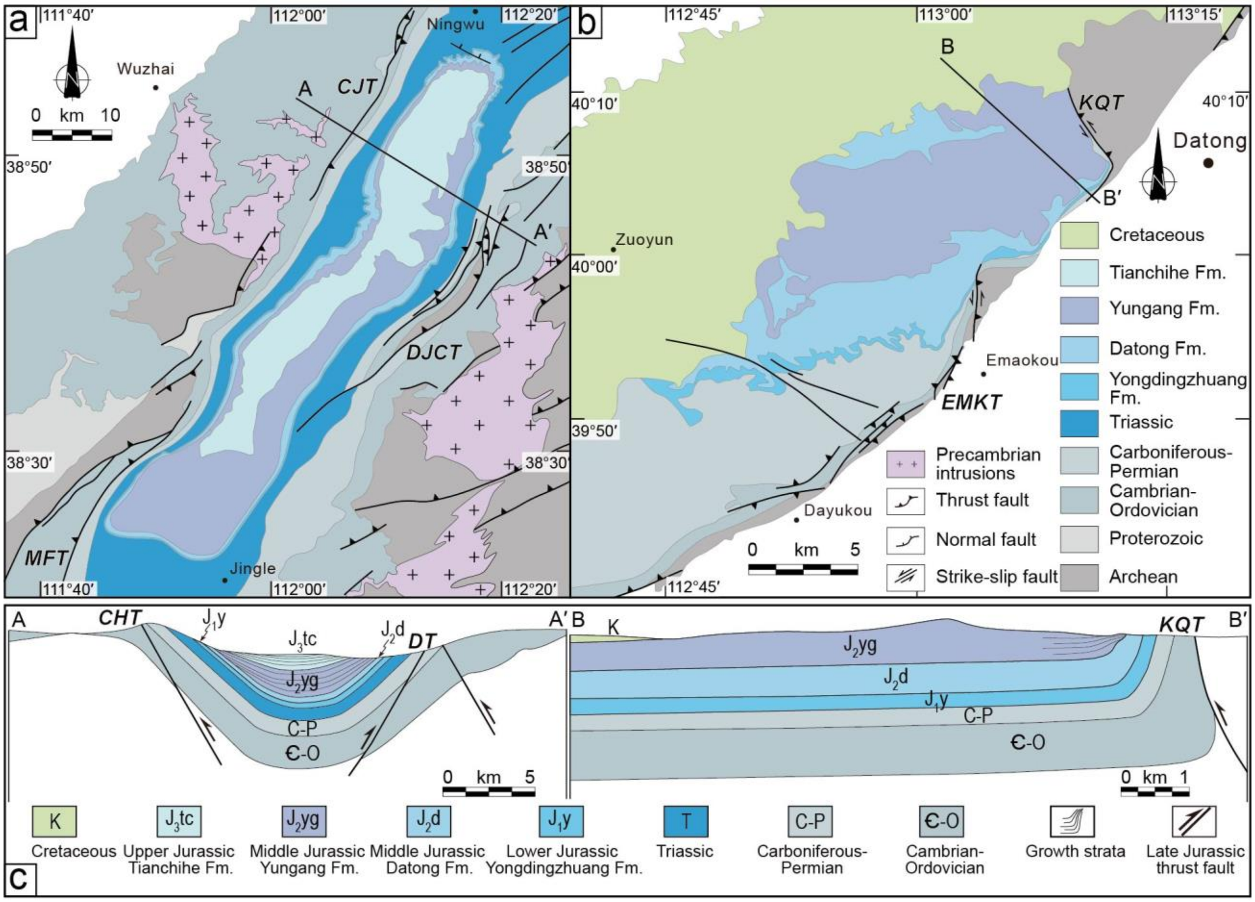

Fig. 8. Overview map of the Ningwu-Jingle and Yungang basins in the east of the Ordos basin (modified from Chen et al., 2019; Zhang et al., 2020). (a) Simplified tectonic map of the Ningwu-Jingle basin. See Fig. 2 for location. (b) Simplified tectonic map of the Yungang basin. See Fig. 2 for location. (c) Geological cross-sections across the Ningwu-Jingle and Yungang basins. See Table 2 for the abbreviations of the structures.

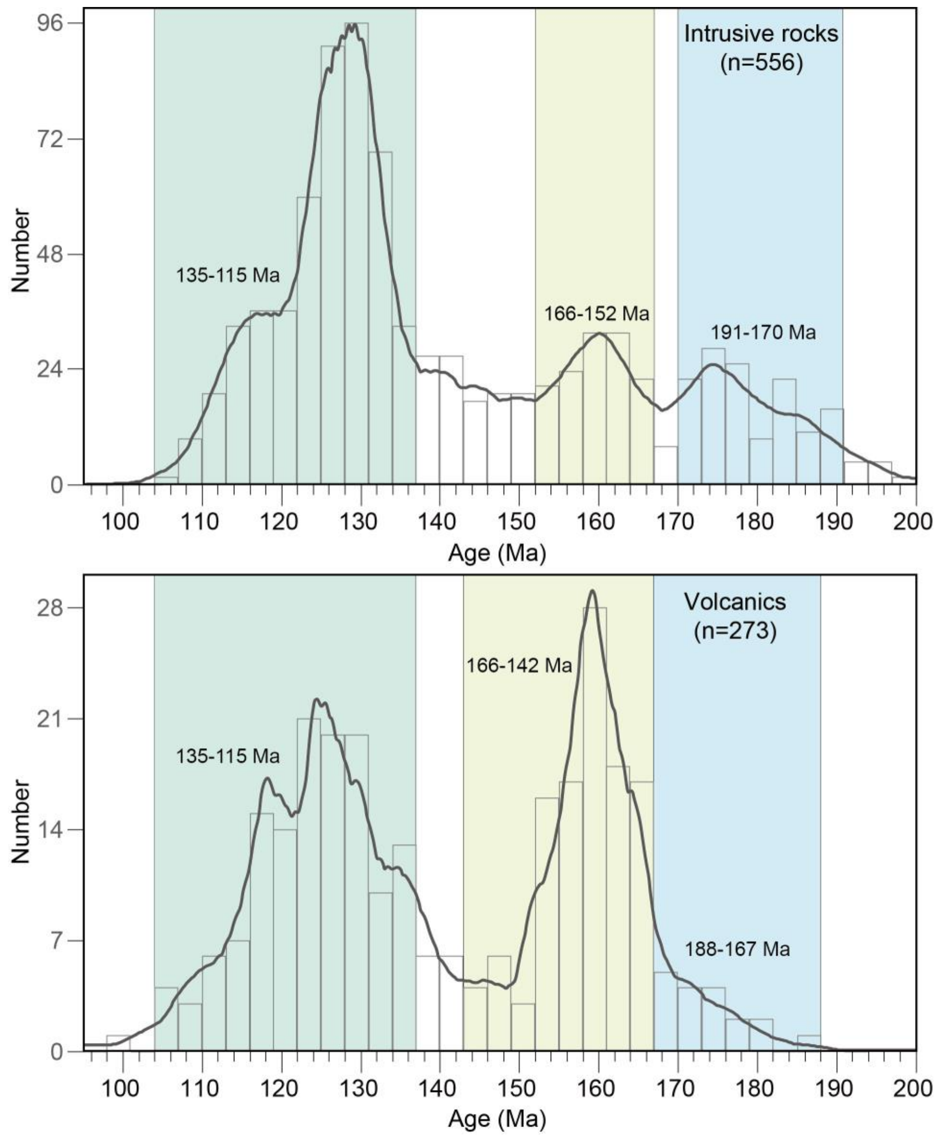

Fig. 9. The U-Pb or ^{39}Ar-^{40}Ar age probability of Jurassic–Early Cretaceous magmatism in NCC. Data are from Chen et al. (1997, 2014), Davis et al. (2001), Li et al. (2001, 2014b, 2014c, 2015, 2016a), Ritts et al. (2001), Swisher et al. (2002), Zhao et al. (2002, 2004, 2006b), Cope (2003, 2017), Niu et al. (2003, 2004), Shao et al. (2003), Lu et al. (2004), Yuan et al. (2005), Zhang et al. (2005), Yang et al. (2006), Liu et al. (2006, 2018b), Cope, et al. (2007), Yang and Li (2008), Zhang et al. (2008a, 2009), Davis and Darby (2010), Liu et al. (2012), Xu et al. (2012), Wang et al. (2013b, 2017), Chang et al. (2014), Zhang et al. (2014, 2019, 2020), Qi et al. (2015), Jiao et al. (2016), Yu et al. (2016), He et al. (2017), Fu et al. (2018), Gao et al. (2018), Lin et al. (2018, 2019), Chen et al. (2019), Hao et al. (2019, 2020), Huang (2019), Meng et al. (2019), Su et al. (2021), Wu et al. (2021), Guo et al. (2022), and references therein.

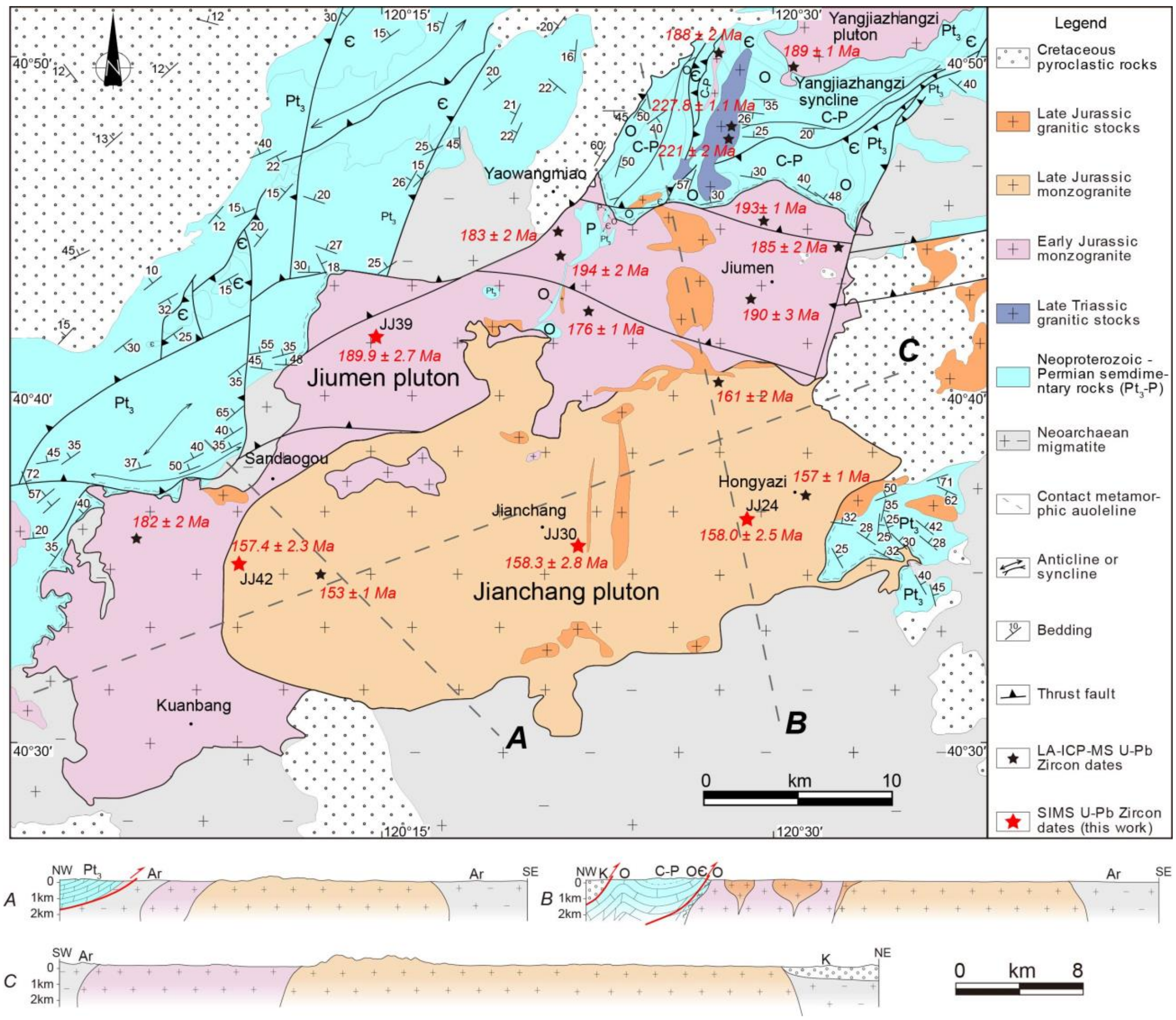

Fig. 10. Structural geological map of the Jianchang-Jiumen plutons and adjacent areas. U–Pb zircon data are from Wu et al. (2006) and Cui (2015). See Fig. 4 for location.

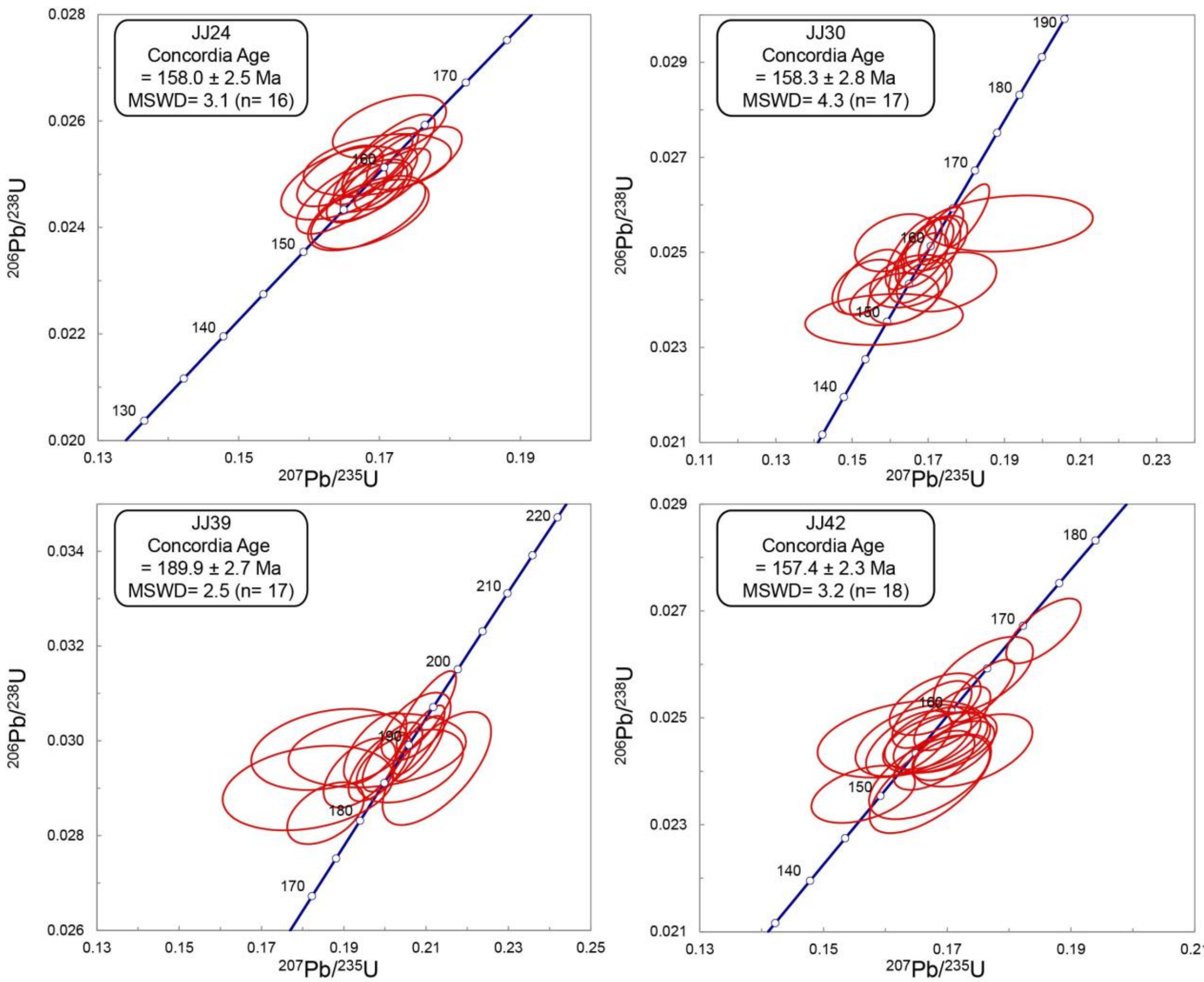

Fig. 11. U-Pb diagrams of Concordia age of representative zircons from collected samples in the Jianchang-Jiumen plutons. MSWD: mean square of weighted deviates.

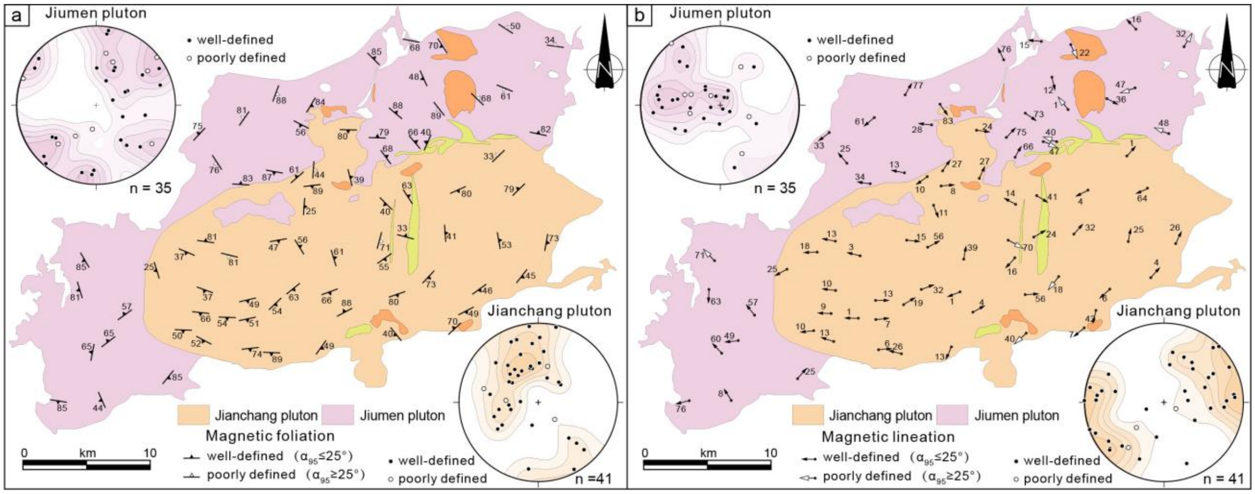

Fig. 12. Magnetic fabric patterns and orientation diagrams of K_3 and K_1 in the Jianchang-Jiumen plutons. (a) Foliations. (b) Lineations.

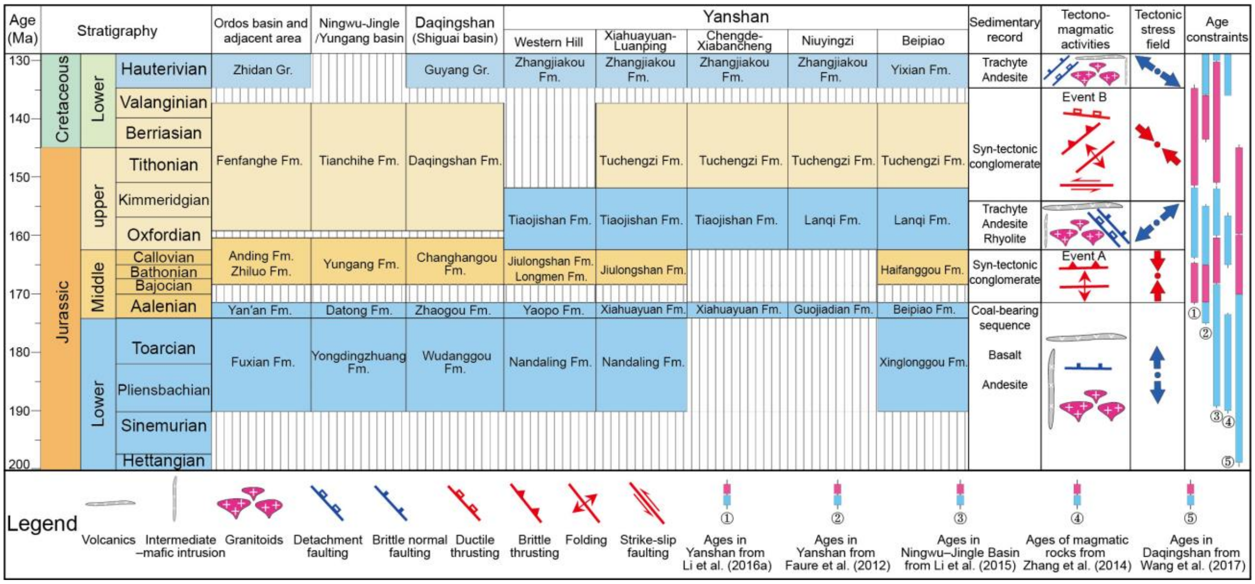

Fig. 13. Synthetic Jurassic–Early Cretaceous tectonostratigraphic framework of the NCC.

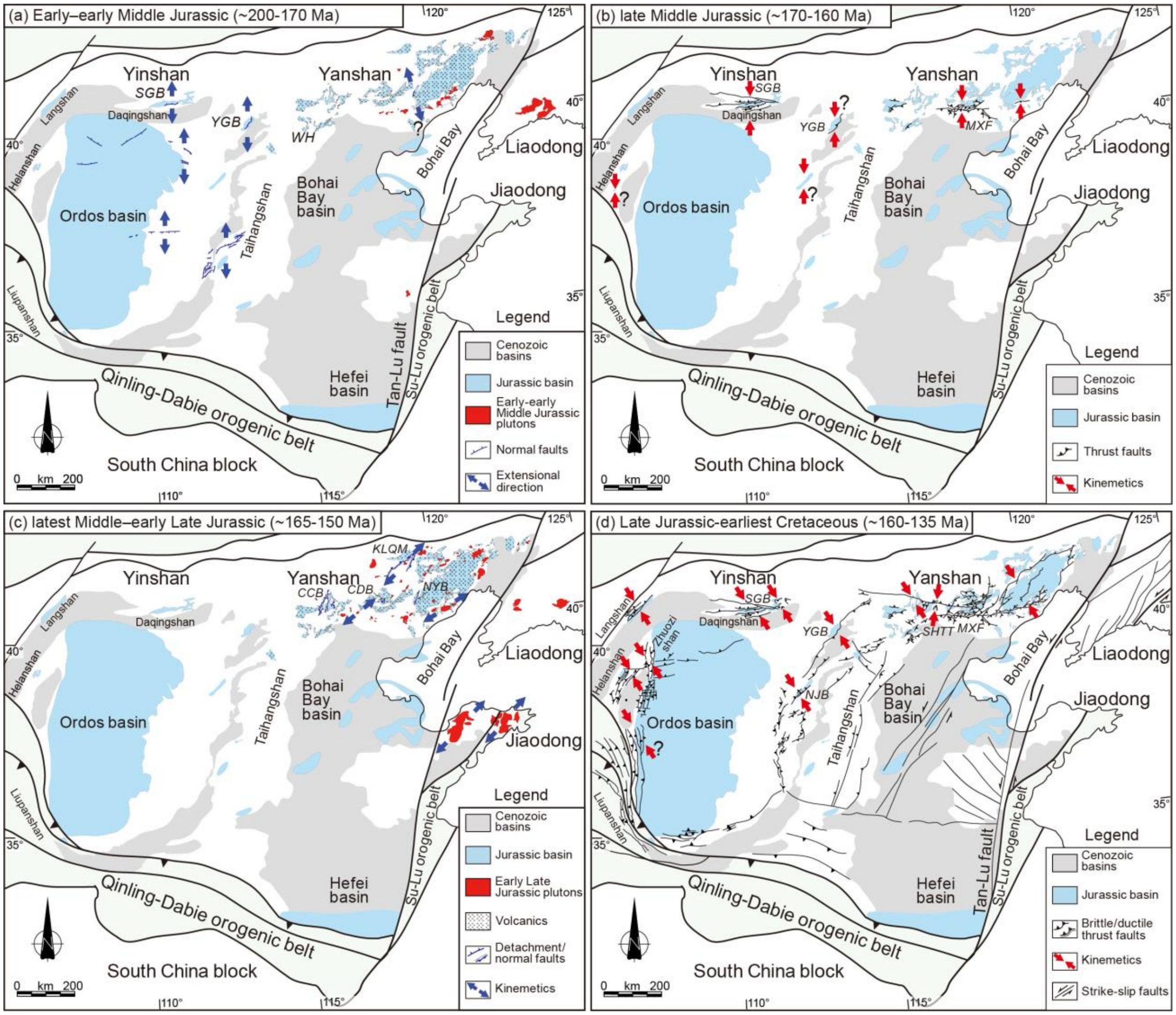

Fig. 14. Jurassic–earliest Cretaceous regional tectonics of the NCC. (a) Early–early Middle Jurassic (~200–170 Ma) extensional structures and magmatism in the NCC. (b) late Middle Jurassic (~170–160 Ma) compressional structures in the NCC. (c) latest Middle–early Late Jurassic (~165–150 Ma) local extensional structures and magmatism in the NCC. (d) Late Jurassic–earliest Cretaceous (~160–135 Ma) compressional structures in the NCC. See Fig. 2 for the abbreviations of the basins and structures.

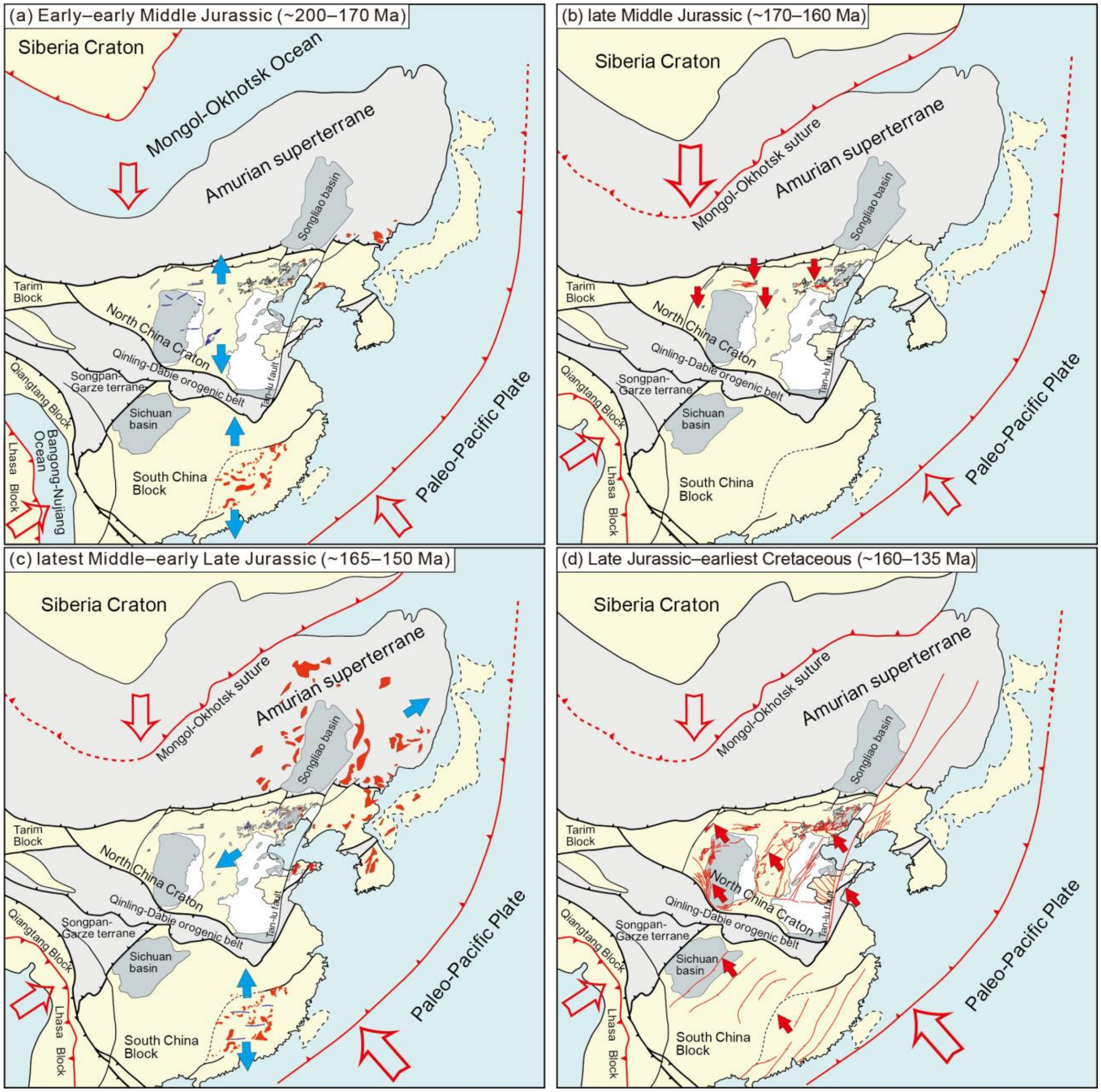

Fig. 15. Simplified geological maps showing Jurassic–earliest Cretaceous tectonic evolution in North China, and geodynamics. (a) Early–early Middle Jurassic (~200–170 Ma). (b) late Middle Jurassic (~170–160 Ma). (c) latest Middle–early Late Jurassic (~165–150 Ma). (d) Late Jurassic–earliest Cretaceous (~160–135 Ma).

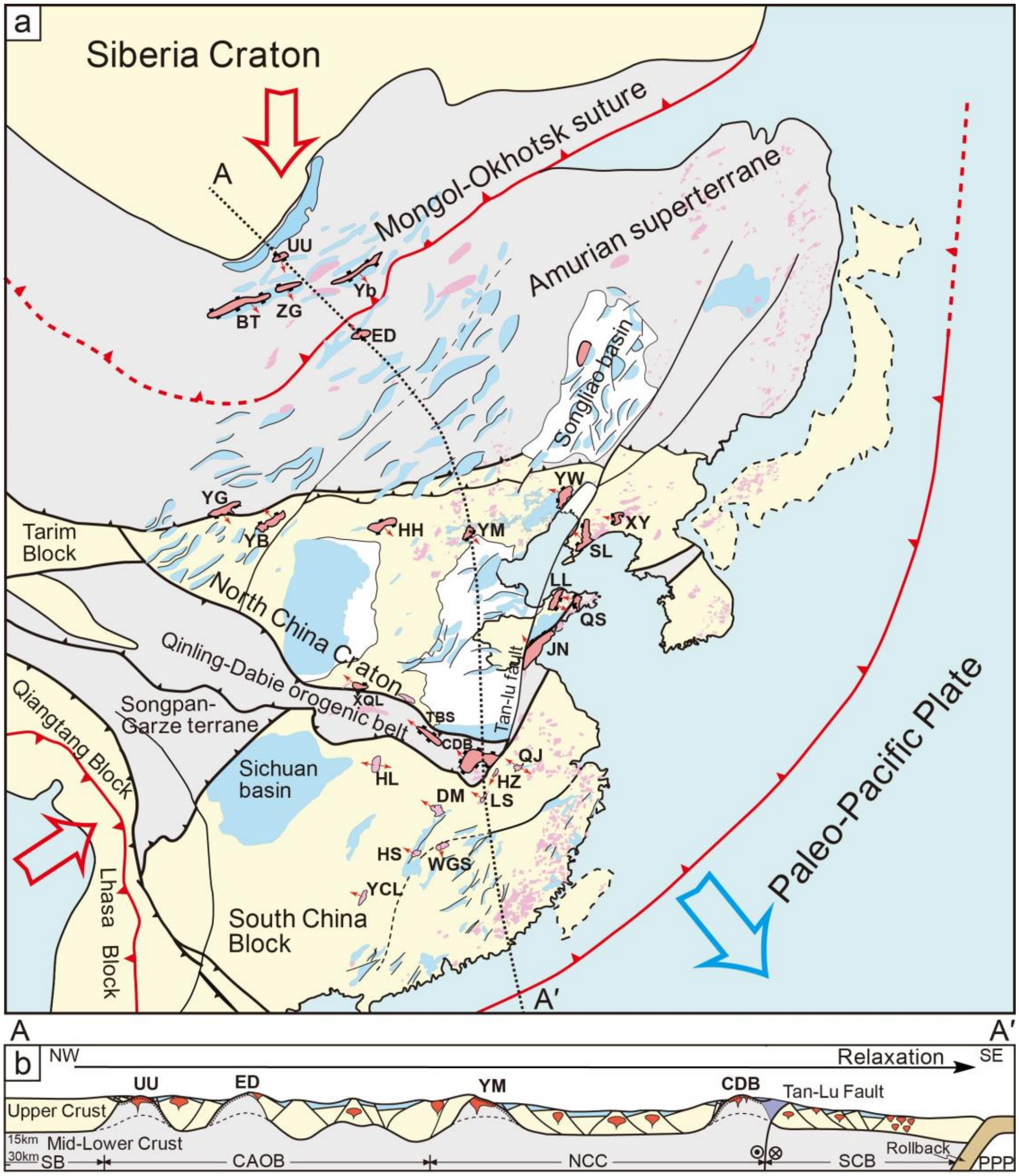

Fig. 16. Early Cretaceous regional tectonics of the NCC, showing the Early Cretaceous (~135–115 Ma) extensional structures and magmatism, and dynamics. The MCCs and syn-tectonic magmatic domes in East Asia (Wang et al., 2011; Ji et al., 2018; Lin and Wei, 2018 and references therein): UU: Ulan Ude, BT: Buteel, ZG: Zagan, Yb: Yablonovy, ED: Ereendavaa, YG: Yagan, YB: Yingba, HH: Hohhot, YM: Yunmengshan, YW: Yiwulüshan, SL: South Liaoning, XY: Xiuyan, LL: Linglong, QS: Queshan, JN: Jiaonan, XQL: Xiaoqinling, TBS: Tongbaishan; CDB: Central Dabieshan; HL: Huangling; QJ: Qingyang-Jiuhua; HZ: Hongzhen; LS: Lushan; WGS: Wugongshan; DM: Dayunshan-Mufushan; HS: Hengshan; and YCL: Yuechengling.

Table 1. Summary of distribution and characteristics of the Jurassic–Early Cretaceous strata in the NCC (Dating data for age constraints were detailedly compiled in Table S1).

Sequence	Tectonic unit	Formation	Basin	lithology	Sedimentary facies	Age constraints (Ma)	Thickness (m)
Lower Jurassic sequence	Yanshan belt	Nandaling Fm.	Western Hill	Conglomerates, sandstones, volcanics, and lahar	Fuvial facies	177–167	0–676
		Nandaling Fm.	Xiahuayuan and Luanping	Basalt interlayered with andesite and pyroclastic rocks	/	180 ± 1.8	0–330
		Xinglonggou Fm.	Beipiao	Andesite, dacites, pyroclastic rocks, and tuff	Fuvial facies	188–176	0–400
	Yinshan belt	Wudanggou Fm.	Shiguai	Cobble–boulder conglomerates, shales and lenticular sandstones	Alluvial, shallow lacustrine and deltaic facies	200–183	0–500
	Ordos basin and adjacent areas	Fuxian Fm.	Ordos	Conglomerates and sandstones	Alluvial and braided fluvial facies	/	0–195
		Yongdingzhuang Fm.	Ningwu-Jingle and Yungang	Conglomerates and sandstones	Alluvial and fluvial facies	188–171	0–220
		Lower Yima Fm.	Yima district	Conglomerates and coarse-grained sandstones	Alluvial and braided fluvial facies	/	/
		Anyao Fm.	Jiyuan region	Sandstones, mudstones and turbidites	Fan deltaic facies	178.31 ± 3.77	/
lower Middle Jurassic sequence	Yanshan belt	Yaopo Fm.	Western Hill	Sandstones and mudstones intercalated with thick coal measures	Meandering fluvial, swamp, and shallow-lacustrine facies	175–174	0–676
		Xiahuayuan Fm.	Xiahuayuan and Luanping	Basal conglomerates, sandstones, siltstones, mudstones, and coal measures	Lacustrine and swamp facies	175–170	0–430
		Beipiao Fm.	Beipiao	Sandstones and mudstones intercalated with thick swamp coal measures	Lacustrine and swamp facies	175–168	0–820
		Xiahuayuan Fm.	Xiabancheng	Coal-bearing conglomerates and sandstones	Lacustrine and swamp facies	/	0–279
		Guojiadian Fm.	Niuyingzi	Coal-bearing conglomerates, sandstones, and mudstones	Fuvial and swamp facies	171–163	/
	Yinshan belt	Zhaogou Fm.	Shiguai basin	Pebbly conglomerates, sandstones, siltstones, black shales, and coal measures	Fluvial, lacustrine, and swamp facies	The early Middle Jurassic palynoflora	0–750
	Ordos basin and adjacent areas	Yan'an Fm.	Ordos basin	Lag gravels, sandstones, coal-bearing deposits	Meandering fluvial, shallow-lacustrine and swamp facies	/	0–326
		Datong Fm.	Ningwu-Jingle and Yungang	Fine-grained sandstones, mudstones, and coal beds	Lacustrine facies	/	0–400
		Upper Yima Fm.	Yima district	Sandstones, mudstones, coal beds	Meandering fluvial, shallow-lacustrine and swamp facies	/	/
		Yangshuzhuang Fm.	Jiyuan region	Sandstones, mudstones, coal beds	Meandering fluvial, shallow-lacustrine and swamp facies	/	/
upper Middle Jurassic sequence	Yanshan belt	Longmen Fm.	Western Hill	Conglomerates intercalated with thin-bedded sandstones	Fuvial to alluvial facies	168–164	0–395
		Jiulongshan Fm.	Western Hill	Conglomerates, pebbly sandstones, and tuffaceous sandstones and siltstones	Deltaic to lacustrine facies	161–154	0–1536
		Jiulongshan Fm.	Xiahuayuan and Luanping	Conglomerates, sandstones, and mudstones	Fuvial, alluvial, lacustrine, and deltaic facies	163–156	0–1670
		Haifanggou Fm.	Beipiao	Conglomerates, sandstones, siltstones, mudstones, and pyroclastic interlayers	Alluvial to lacustrine facies	167-161	0–400
	Yinshan belt	Changhangou Fm.	Shiguai	Conglomerates, sandstones, and mudstones, tuff and gypsum	Fluvial and lacustrine facies	163.7±1.0	0–420
	Ordos basin and adjacent areas	Zhiluo Fm.	Ordos	Sandstones, siltstones, marlston, mudstones, and shales	Fluvial and lacustrine facies	/	0–268
		Anding Fm.	Ordos	Sandstones, siltstones, marlston, mudstones, and shales	Fluvial and lacustrine facies	/	0–148
		Yungang Fm.	Ningwu-Jingle and Yungang	Basal conglomerates, sandstones and sandy shales	Fluvial and lacustrine facies	168–161	0–462
		Dongmengcun Fm.	Yima district	Basal conglomerates, sandstones, mudstones and shales	Fluvial and lacustrine facies	/	/
		Ma'ao Fm.	Jiyuan region	Basal conglomerates, sandstones, mudstones and shales	Fluvial and lacustrine facies	/	/
lower Upper Jurassic sequence	Yanshan belt	Tiaojishan Fm.	Western Hill	Intermediate andesitic lavas, volcanic breccia, andesitic tuff, pyroclastics, and interbedded clastic rocks	/	161–146	0–2952
		Tiaojishan Fm.	Xiahuayuan and Luanping	Andesitic lavas, basalt lavas, volcanic breccia, tuffaceous clastic rocks	/	164–153	
		Tiaojishan Fm.	Xiabancheng	Andesite, pyroclastics, tuffaceous sandstones, with mudstone interbeds	/	164–153	
		Tiaojishan Fm.	Chicheng	Breccia, andesitic tuff, pyroclastic rocks, and interbedded sedimentary rocks	/	165-157	
		Tiaojishan Fm.	Hunyuan	Andesite interlayers and conglomerates interbedded sandstones, or mudstones	/	152.77± 0.6	
		Lanqi Fm.	Niuyingzi	Andesite, basaltic andesite, and pyroclastic rocks	/	159–158	0–1360
		Lanqi Fm.	Beipiao	Andesite, basaltic andesite, and pyroclastic rocks	/	166–153	
Upper Jurassic sequence	Yanshan belt	Tuchengzi/Houcheng Fm.	/	Conglomerates, sandstones, and mudstones	Fuvial, alluvial to lacustrine facies	155–135	0–2760
	Yinshan belt	Daqingshan Fm.	Shiguai	Cobble-pebble conglomerates, sandstones, and siltstones	Alluvial and fluvial facies	/	0–3900
	Ordos basin and adjacent areas	Fengfanghe Fm.	Ordos	Conglomerates and sandstones	Alluvial and braided fluvial facies	/	0–1174
		Tianchihe Fm.	Ningwu-Jingle and Yungang	Conglomerates, sandstones, and mudstones	Alluvial, fan delta facies	160.6 ± 0.55	0–900
Lower Cretaceous sequence	Yanshan belt	Zhangjiakou Fm.	Beipiao	Andesite and pyroclastics with a basal conglomerate	Fluvial facies	136–127	0–3867
		Donglingtai	Western Hill	Rhyolite and volcanic breccias	/		
		Zhangjiakou Fm.	The rest of yanshan belt	Rhyolitic tuff, rhyolite, andesite and quartz trachyte with sedimentary rocks	Fluvial facies		
	Yinshan belt	Guyang Gr.	Daqingshan	Conglomerates and sandstones with volcanic rocks	Fluvial and lacustrine facies		/
	Ordos basin and adjacent areas	Zhidan Gr.	Ordos	Conglomerates, sandstones	Fluvial facies	/	0–213
		Zuoyun Fm.	Ningwu-Jingle and Yungang	Conglomerates, sandstones, and mudstones	Fluvial and lacustrine facies	130.1 ± 0.8	/

Table 2. Summary of geometry and kinematics of the Jurassic–Early Cretaceous contractional structures in the NCC.

Tectonic units	Thrusts	Strikes	Fault-slip data	Involved strata	Time constraints			References
						Event A of the Yanshanian orogeny	Event B of the Yanshanian orogeny	
Central Yanshan belt	Mengjiazhuang thrust (MT)	ENE	/	Ar-Pt, J_{1-2}n: tight fold; J_3t: open fold	Pre-J_{1-2}n	Post-J_{1-2}n, pre-J_3t	Post-J_3t, pre-K_1zh	Li et al., 2016a
	Jiyuqing thrust (JT)	ENE	/	Ar-Pt, Є-O, T, J_2x: tight fold; J_3t-J_3-K_1tch: open fold	Pre-J_{1-2}n	Post-J_2x, pre-J_3t	Post-J_3t, pre-K_1zh	Li et al., 2016a
	Liudaohe thrust (LT)	ENE	/	Ar-Pt, Є-O, T, J_2x: tight fold; J_3t-J_3-K_1tch: open fold	Pre-J_{1-2}n	Post-J_2x, pre-J_3t	Post-J_3t, pre-K_1zh	Li et al., 2016a
	Duanshuwa-Jianbaoshan thrust (DJT)	E	/	Ar-Pt, Є, J_2x		Post-J_2x, pre-J_3t		Li et al., 2016a
	Qingshuihu fault (QSHF)	E	/	Ar-Pt		Pre-Siganding pluton (160-157 Ma)		Chen, 1998; Zeng et al., 2021
	Zhujiagou fault (ZJGF)	E	/	Ar-Pt		Pre-Wangping-shi pluton (162.3±1.3 Ma)		Chen, 1998
	Xinglong thrust (XLT)	E	/	Ar-Pt, Є-O		Pre-J_3t		Chen, 1998; Davis et al., 2001
	Miyun-Xifengkou fault (MXF)	E	/	Ar-Pt		Pre-mafic dyke (160 Ma)		Chen, 1998
	Gaobanhe/Sanpo/Banbishan faults (GBHF /SPF/BBSF)	NE	/	Ar-Pt		Pre-J_3t		Chen, 1998
	Gubeikou-Pingquan thrust (GPT)	E	NW-SE direction	Ar-Pt, Є-O, J_1x/J_3t-J_3-K_1tch			Post-J_3t, pre-Wulingshan and Shouwangfen plutons (132-130Ma)	Li et al., 2016a
	Dayingzi thrust (DYT)	ENE	/	Ar-Pt, Є-O, J_3t- J_3-K_1tch			Post-J_3t, pre-K_1zh	Li et al., 2016a
	Sihetang ductile shear zone (SHTSZ)	E	/	Ar			Coeval with Yunmeng-shan pluton (145 Ma)	Davis et al., 2001
	Chengde thrust (CDT)	ENE	/	Ar-Pt, J_3t-J_3-K_1tch			Post-J_3t, pre-K_1zh	Davis et al., 2001
	Shanggu-Pingquan thrust (SPT)	NE	/	Ar-Pt, Є-O, T, J_2x, J_3t-J_3-K_1tch			Post-J_3t, pre-Guozhangzi and Jiashan plutons (113-111 Ma)	Li et al., 2016a
Western Yanshan belt	Nandazhai-Babaoshan thrust (NBT)	NE	/	Ar-Pt, Є-O, C-P, J_{1-2}n-J_3t			Post-J_3t, pre-K_1d	Zhang et al., 2006
	Changcao-Xiayunling thrust (CXT)	NE	/	Ar-Pt, Є-O, C-P, J_{1-2}n-J_3t			Post-J_3t, pre-K_1d	Zhang et al., 2006
	Caojiapu-Huangtuliang thrust (CHT)	NE	/	Ar-Pt, Є-O, C-P, J_{1-2}n-J_3t			Post-J_3t, pre-K_1d	Zhang et al., 2006
	Malan-Hulin thrust (MHT)	NE	/	Ar-Pt, Є-O, C-P, J_{1-2}n-J_3t			Post-J_3t, pre-K_1d	Zhang et al., 2006
	Shisanling thrust (SSL)	NE	/	Ar-Pt, Є-O, J_{1-2}n-J_3t			Post-J_3t, pre-127.0±1.5 Ma pluton	Davis et al., 2001
	Xiahuayuan thrust (XHYT)	NE	/	Ar-Pt, Є-O, J_{1-2}n-J_3-K_1tch			Post-J_3t, pre-K_1zh	Zhang et al., 2006; Lin et al., 2019
	Qianjiadian thrust (QJDT)	NE	NW-SE direction	Ar-Pt, J_3t-J_3-K_1h			Post-J_3t, pre-K_1zh	Zhang et al., 2006; Lin et al., 2019
	Shaliangzi thrust (SLZT)	NE	NW-SE direction	Ar-Pt, J_3t-J_3-K_1h			Post-J_3t, pre-K_1zh	Zhang et al., 2006; Lin et al., 2019
	Tanghekou thrust (THKT)	NE	NW-SE direction	Ar-Pt, J_3t-J_3-K_1h			Post-J_3t, pre-K_1zh	Zhang et al., 2006; Lin et al., 2019
	Banshen-Shuiquangou thrust (BST)	NE	NW-SE direction	Ar-Pt, J_1x-J_3-K_1tch			Post-J_3t, pre-K_1zh	Yang et al., 2021
Eastern Yanshan belt	Yangzhangzi-Wafangdian fault (YWF)	NE	/	Ar-Pt, Є-O, C-P, J_2g, J_3l		Post-J_2g, pre-160.2 Ma rhyolitic porphyry		Davis et al., 2001; Zhang et al., 2002
	Nangongyingzi-Beipiao fault (NBF)	NE	/	Ar-Pt, Є-O, C-P, J_3l-J_3-K_1tch		Pre-J_3l	Post-J_3l, pre-K_1y	Zhang et al., 2002
	Jianchang-Chaoyang fault (JCF)	NE	/	Ar-Pt, Є-O, C-P, J_1x-J_3-K_1tch			Post-J_3l, pre-K_1y and post-K_1y	Zhang et al., 2002
	Datun-Jinzhou fault (NEF)	NE	/	Ar-Pt, Є-O, C-P, J_3l-J_3-K_1tch			Post-J_3l, pre-K_1y	Zhang et al., 2002
	Lingyuan-Dongguanyingzi fault (LDF)	NE	/	Ar-Pt, Є-O, C-P, J_3l-J_3-K_1tch			Post-J_3l, pre-K_1y	Zhang et al., 2002
Yinshan belt	Hetangou-Dongerba thrust (HDT)	E	N-S direction/ NW-SE direction	Ar, Є-O, C-P, J_1w-J_3d		Post-J_2zg, pre-J_3d	Post-J_2c, pre-K_1g	Wang et al., 2017
	Beilinshan thrust (BLT)	E	NW-SE direction	Ar, Є-O, C-P, J_1w-J_3d			Post-J_2c, pre-K_1g	Wang et al., 2017
	Daqingshan thrust (DQST)	/	NW-SE direction	Ar-Pt, J_1w-J_3d			Post-J_2c, pre-K_1g	Gong et al., 2015
	Thrusts in Langshan	NE	/	Ar,J			J_3 to K_1	Darby and Ritts, 2007
Ordos basin and adjacent areas	Chunjing thrust (CJT)	NE	/	Ar-Pt, Є-O, C-P, J_1y-J_3tc			Post-J_2yg, pre-K_1zy	Zhang et al., 2020
	Mafangzhen thrust (MFT)	NE	/	Ar-Pt, Є-O, C-P, J_1y-J_3tc			Post-J_2yg, pre-K_1zy	Zhang et al., 2020
	Dujiacun thrust (DJCT)	NE	/	Ar-Pt, Є-O, C-P, J_1y-J_3tc			Post-J_2yg, pre-K_1zy	Zhang et al., 2020
	Kouquan thrust (KQT)	NE-NNW	NW-SE direction	Ar-Pt, Є-O, C-P, J_1y-J_2yg			Post-J_2yg, pre-K_1zy	Chen et al., 2019
	Emaokou fault (EMKF)	NNE	NW-SE direction	Ar-Pt, Є-O, C-P, J_1y-J_2yg			Post-J_2yg, pre-K_1zy	Chen et al., 2019
	Thrusts in western Ordos basin	N	/	Ar-Pt, Є-O, C-P, T, J			post-J, pre-K	Feng et al., 2021
	Thrusts in Zhuozishan	N	NW-SE direction	Ar-Pt, Є-O, C-P, T, J_1f-J_3f			Post-J_2a, pre-K_1z	Li et al., 2022
	Xiaosongshan thrust (XST)	NE	NW-SE direction	Ar-Pt, Є-O, C-P, T, J_1f-J_2a			Post-J_2a, pre-K_1z	Huang, et al., 2015; Yang and Dong, 2018, 2020; Li et al., 2022
	Chaqigou-Tatagou fault (CTF)	NE	NW-SE direction	Ar-Pt, Є-O, C-P, T			Post-J_2a, pre-K_1z	Huang, et al., 2015; Yang and Dong, 2018, 2020; Li et al., 2022
	Dashuigoumen-Dawukou fault (DDF)	NE	NW-SE direction	Ar-Pt, Є-O, C-P, T			Post-J_2a, pre-K_1z	Huang, et al., 2015; Yang and Dong, 2018, 2020; Li et al., 2022
	Dazhanchang fault (DZF)	NNE	NW-SE direction	Ar-Pt, Є-O, D-P, T, J_2z, J_3f			Post-J_2a, pre-K_1z	Yang and Dong, 2020

Table 3. Summary of syn-emplacement fabrics of the Jurassic–Early Cretaceous granitic plutons in the NCC (compiled from Lin et al., 2021 and references therein).

Period	No.	Pluton	Location	Lithology	Age	Syn-emplacement foliation	Syn-emplacement lineation
Early Jurassic	1	Jiumen	Eastern Yanshan	Monzogranite	189.9±2.7 Ma	Highly scattered with variable dips	Highly scattered with variable dips
Late Jurassic	1	Yiwulüshan	Eastern Yanshan	Biotite granodiorite	162–153 Ma	Overprint by the Wangziyu detachment fault	Overprint by the Wangziyu detachment fault
	2	Jianchang	Eastern Yanshan	Monzogranite	158−157 Ma	Margin-parallel with moderate to high dips	Gentle to moderate NE-SW plunging
	3	Siganding	Central Yanshan	Monzogranite and diorite	160−159 Ma	Margin-parallel with moderate to high dips	Gentle to moderate NE-SW plunging
	4	Kunyushan	Jiaodong peninsula	Biotite monzogranite	160−153 Ma	Concentric patterns with moderate to low dips	Predominately (E)NE-(W)SW plunging
	5	Queshan	Jiaodong peninsula	Biotite monzogranite	162−156 Ma	NW−SE striking with variable dips	Highly scattered with variable dips
	6	Linglong	Jiaodong peninsula	Biotite monzogranite	163−152 Ma	Concentric patterns	Dominantly (E)NE-(W)SW plunging
	7	Luanjiahe	Jiaodong peninsula	Biotite monzogranite	157−152 Ma	SE- or NW-dipping with high angles	NE-SW plunging with gentle dips
	8	Wendeng	Jiaodong peninsula	Biotite monzogranite	160−151 Ma	Margin-parallel with moderate to high dips	Highly scattered with gentle dips
Early Cretaceous	1	Yunmengshan	Western Yanshan	Granodiorite	145-141 Ma	Overprint by the Shuiyu detachment fault	Overprint by the Shuiyu detachment fault
	2	Gudaoling	Liaodong peninsula	Biotite monzogranite	127−118 Ma	W- or WSW- dipping with moderate to low angles	Sub-horizontal NW-SE plunging
	3	Yinmawanshan	Liaodong peninsula	Porphyritic granite	129−120 Ma	Margin-parallel with moderate to gentle dips	Various plunges and dips in the west and E-W plunging in the
	4	Guojialing	Jiaodong peninsula	Porphyritic granodiorite	130−128 Ma	NW-dipping with moderate-low angles in the west and NNW- or NE- dipping with low angles in the east	NW-SE plunging with moderate to low dips
	5	Congjia	Jiaodong peninsula	Porphyritic granodiorite	130−128 Ma	NE- or SE- dipping	Sub-horizontal NW-SE plunging
	6	Wang'anzhen	Taihangshan	Granodiorite and monzogranite	130−128 Ma	Concentric pattern with a NE-SW long axis	Predominantly NW-SE or E-W trending with moderate to high dips
	7	Fengjiayu-Xibailianyu	Central Yanshan	Monzogranite and diorite	131−127 Ma	Concentric patterns with high and moderate to gentle dips, respectively	Scattered with moderate to gentle dips
	8	Gubeikou (Qiancengbei)	Central Yanshan	Granite	129−128 Ma	Roughly margin-parallel with moderate to low dips	Highly scattered with moderate to low dips
	9	Dahaituo	Western Yanshan	Quartz monzonite and monzogranite	119±2 Ma	Concentric pattern with a NE-SW long axis	Highly scattered with moderate to low dips
	10	Haiyang	Jiaodong peninsula	Porphyritic granodiorite	118−114 Ma	Concentric pattern with mainly sub-horizontal dips	Scattered with sub-horizontal dips
	11	Aishan	Jiaodong peninsula	Porphyritic granodiorite	118−115 Ma	Margin-parallel with moderate to low dips	Sub-horizontal NW-SE plunging